

Dissertation zur Erlangung des Doktorgrades

der Fakultät für Biologie

der Ludwig-Maximilians-Universität München

**A structural analysis of the TOB complex,
the insertase for β -barrel proteins of the
mitochondrial outer membrane**

Astrid Klein

aus

Gießen

München

2011

Ehrenwörtliche Versicherung

Diese Dissertation wurde selbständig, ohne unerlaubte Hilfe erarbeitet.

München, den 12.09.2011

Dissertation eingereicht am: 12.09.2011

Sondergutachter: Herr Prof. Dr. Dr. Walter Neupert

1. Gutachter: Frau Prof. Dr. Angelika Böttger
2. Gutachter: Frau Prof. Dr. Ute Vothknecht

Mündliche Prüfung am: 18.10.2011

Für meine Eltern

1	INTRODUCTION	1
1.1	MITOCHONDRIA	1
1.2	PROTEIN TRANSLOCATION INTO MITOCHONDRIA	4
1.2.1	<i>The TOM complex</i>	6
1.2.2	<i>Import of proteins into the matrix</i>	7
1.2.3	<i>Import of proteins into the inner mitochondrial membrane</i>	9
1.2.4	<i>Import of proteins into the intermembrane space</i>	12
1.2.5	<i>Import of proteins into the outer mitochondrial membrane</i>	12
1.3	THE TOB COMPLEX	15
1.3.1	<i>Introduction</i>	15
1.3.2	<i>Composition of the TOB complex</i>	15
1.3.3	<i>Topogenesis of mitochondrial β-barrel proteins</i>	17
1.4	AIM OF THE PRESENT STUDY	19
2	RESULTS	20
2.1	TOB55 IS EXPRESSED IN THREE DIFFERENT ISOFORMS DUE TO ALTERNATIVE SPLICING	20
2.2	ISOLATION OF THE TOB COMPLEX	23
2.3	COMPOSITION OF THE TOB COMPLEX	26
2.4	TOB55, TOB38 AND TOB37 ARE PRESENT IN THE TOB COMPLEX IN A 1:1:1 STOICHIOMETRY	38
2.5	RECONSTRUCTION OF THE ISOLATED TOB COMPLEX BY CRYO-ELECTRON MICROSCOPY	42
2.6	THE SUBUNITS OF THE TOB COMPLEX ARE TIGHTLY ASSOCIATED WITH THE OUTER MITOCHONDRIAL MEMBRANE	52
2.7	THE ISOLATED TOB COMPLEX SHOWS SPECIFIC SUBSTRATE BINDING BEHAVIOR	54
3	DISCUSSION	61
3.1	COMPOSITION OF THE TOB COMPLEX	61
3.2	STRUCTURE OF THE TOB COMPLEX	66
3.3	THE FUNCTIONAL MECHANISM OF THE TOB COMPLEX	69
3.4	ALTERNATIVE SPLICING OF TOB55	74
3.5	A-HELICAL SUBSTRATES OF THE TOB COMPLEX	75
4	SUMMARY	76
5	ZUSAMMENFASSUNG	77
6	MATERIAL AND METHODS	78
6.1	MATERIALS	78
6.1.1	<i>Equipment</i>	78
6.1.2	<i>Chemicals</i>	81
6.1.3	<i>Preparation Kits</i>	84
6.1.4	<i>Medias and buffers</i>	84
6.1.5	<i>Neurospora crassa strains</i>	89
6.1.6	<i>Saccharomyces cerevisiae strain</i>	91
6.1.7	<i>Peptides</i>	91
6.1.8	<i>Whitehead codes and molecular masses of selected proteins from Neurospora crassa</i>	94
6.1.9	<i>Antibodies</i>	94
6.1.10	<i>Plasmids</i>	95
6.2	METHODS	96
6.2.1	<i>Cell biology</i>	96
6.2.2	<i>Molecular biology</i>	100
6.2.3	<i>Protein biochemistry</i>	103
6.2.4	<i>Immunology</i>	112
6.2.5	<i>Cryo-electron microscopy</i>	115
7	ABBREVIATIONS	117
8	REFERENCES	122

1 Introduction

1.1 Mitochondria

Mitochondria are cell organelles which are found in virtually all eukaryotic cells (1). The number of mitochondria in a cell varies widely by organism and tissue type, from only a single mitochondrion to several thousand mitochondria (2, 3). These organelles have many features in common with prokaryotes. As a result, they are believed to be originally derived from endosymbiotic prokaryotes (4-7).

Mitochondria are bounded by two membranes, the outer and the inner membrane, which are separating the organelle into two aqueous subcompartments. There are the intermembrane space (IMS) and the innermost mitochondrial matrix (Figure 1) (8). In the matrix, mitochondria have their own independent genome. One mitochondrion contains around two to ten copies of its desoxyribonucleic acid (DNA) (9). In animals, the mitochondrial genome is typically a single circular chromosome of about 16 kDa coding for protein subunits of respiratory complexes I, III, IV and V, as well as for some ribonucleic acids (RNAs) of mitochondrial ribosomes and the 22 transfer ribonucleic acids (tRNAs) necessary for the translation of mitochondrial desoxyribonucleic acid (mtDNA) transcripts (10, 11). A circular DNA structure is also found in prokaryotes and the similarity to the prokaryotic genome is extended by the fact that mtDNA is organized with a variant genetic code similar to that of proteobacteria (11). Interestingly, mitochondria have far fewer genes than the bacteria from which they are thought to be descended. While most of the genes have been transferred to the host nucleus, for example genes encoding the protein subunits of the respiratory complex II, others have been lost entirely (10). However, not all nuclear genes encoding mitochondrial proteins are of eubacterial origin. Some were already present in the ancestral eukaryotic host (12).

In contrast to the inheritance of nuclear genes, where the egg and sperm nuclei each contribute equally to the genetic makeup of the zygote nucleus, mitochondria, and thereby the mtDNA, are transmitted almost exclusively from the ovum. Mitochondria are therefore in most cases inherited down the female line, known as maternal inheritance (10). Due to this maternal inheritance, diseases caused by mitochondrial dysfunction, are, in general, passed on by a female to her children (13).

Introduction

Mitochondria are not synthesized *de novo* but derived from binary fission of pre-existing organelles similar to bacterial cell division. Mitochondrial inheritance therefore depends on mitochondrial fission during cytokinesis (14). Unlike bacteria however, mitochondria can also fuse with other mitochondria (10). Fusion of several mitochondria results in extended interconnected mitochondrial networks and serves to mix and unify the mitochondrial compartment. In case of an accumulation of different somatic mutations in the mtDNA of individual mitochondria this fusion can, for example, counteract the manifestation of respiratory deficiencies by allowing the complementation of mtDNA gene products in the heteroplasmic cells. Furthermore, the connectivity of the mitochondrial network is an important factor in the cell's calcium signaling response, embryonic development and spermatogenesis (14).

The most prominent role of mitochondria is the production of adenosine triphosphate (ATP), a source of chemical energy (15), through respiration. This is also reflected by the large number of proteins involved in ATP synthesis in the inner membrane (3). The central set of reactions involved in ATP production is collectively known as the citric acid cycle, or Krebs Cycle, followed by the electron transport chain in the mitochondrial inner membrane. The electrochemical gradient established across the inner mitochondrial membrane by the electron transport chain is used by ATP-synthase to synthesize ATP from adenosine diphosphate (ADP) and inorganic phosphate (Pi). This process is known as oxidative phosphorylation (3). As mentioned above, mitochondria have many others functions in addition to the production of ATP. They play a central role in calcium signaling (16), apoptosis (17), regulations of membrane potential (3), cellular proliferation (18), and heme synthesis or the formation and export of iron-sulfur (Fe/S) clusters (12).

Given the critical role mitochondria play in cell metabolism, damage and the resultant dysfunction of these organelles are key components in a wide range of human diseases. Classic mitochondrial disorders typically appear to affect brain and skeletal muscle functions, often referred to as mitochondrial encephalomyopathies, but can also result in diabetes, multiple endocrinopathy or a variety of other systemic manifestations (10, 13).

Mitochondrial encephalomyopathy with lactic acidosis and stroke-like episodes (MELAS) syndrome, Kearns-Sayre syndrome, cardiomyopathy, and Leber's hereditary optic neuropathy (LHON) are diseases caused by mutations in the mtDNA (12, 19). Additionally, in early tumors of the bladder, prostate, liver or head and neck, mtDNA alterations could be observed (12). Dysfunctions of mitochondrial proteins caused by defects in nuclear genes evoke clinical observations such as Friedreich's ataxia, hereditary spastic paraplegia and

Wilson's disease (20). Moreover, cardiovascular disease, stroke, dementia, Alzheimer's disease, epilepsy, Parkinson's disease and diabetes mellitus are examples of diseases associated with defective mitochondrial functionality (21, 22). How exactly mitochondrial dysfunction fits into the etiology of these pathologies has yet to be elucidated.

Taken together, mitochondria are associated with a variety of essential functions in the cell, which, in the vast majority of the cases, are only poorly understood and whose disturbance leads again to a variety of diseases. Therefore, the investigation of these organelles presents an important field in cell biology.

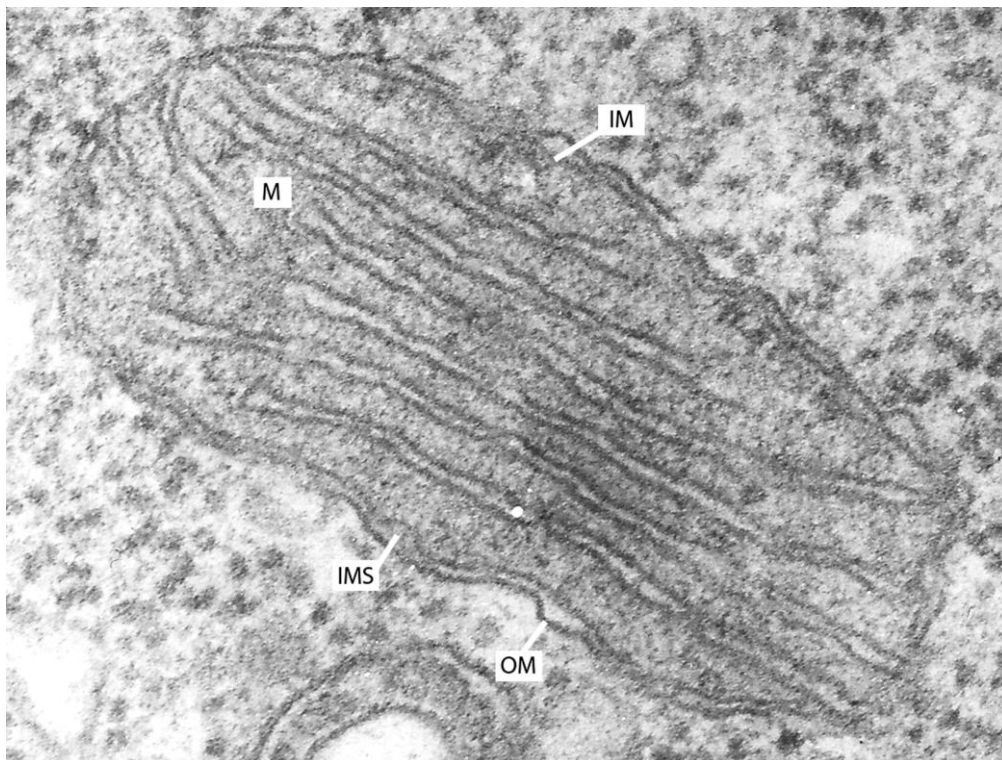


Figure 1

The general organisation of a mitochondrion

OM: outer mitochondrial membrane, IMS: intermembrane space, IM: inner mitochondrial membrane, M: matrix

(N. crassa, courtesy of F. Miller, LMU München, GER)

1.2 Protein translocation into mitochondria

As already mentioned, the mitochondrial genome encodes only a rather small number of proteins. Therefore, about 99% of the mitochondrial proteins are encoded in the nucleus of the host (8) and synthesized in the cytosol as precursor proteins. These preproteins have to be transported into the mitochondria and be targeted to their final submitochondrial destination, the outer or inner mitochondrial membrane, the IMS or the matrix. The process of protein sorting and export or transport to intracellular membranes or compartments is termed “protein topogenesis” (23).

In contrast to the inner mitochondrial membrane, the outer mitochondrial membrane contains porin protein channels. These channels allow the passage of molecules smaller than 5000 Daltons (2), whereas the inner membrane is impermeable to virtually all molecules (24). Consequently, transport of larger proteins into the mitochondrial subcompartments is a selective and controlled process, performed by a variety of complex molecular machineries known collectively as mitochondrial protein translocases (Figure 2). Mitochondrial protein translocases are able to recognize so called targeting signals or topogenic sequences (23) of the precursor proteins. These targeting signals are present either as amino-terminal extensions, which are usually proteolytically removed after import into mitochondria, or they are non-cleavable internal elements which remain part of the mature protein. Targeting signals facilitate recognition of the precursor proteins by receptors on the mitochondrial surface. Thereafter, they are sorted to their appropriate destination within the mitochondria (8, 25).

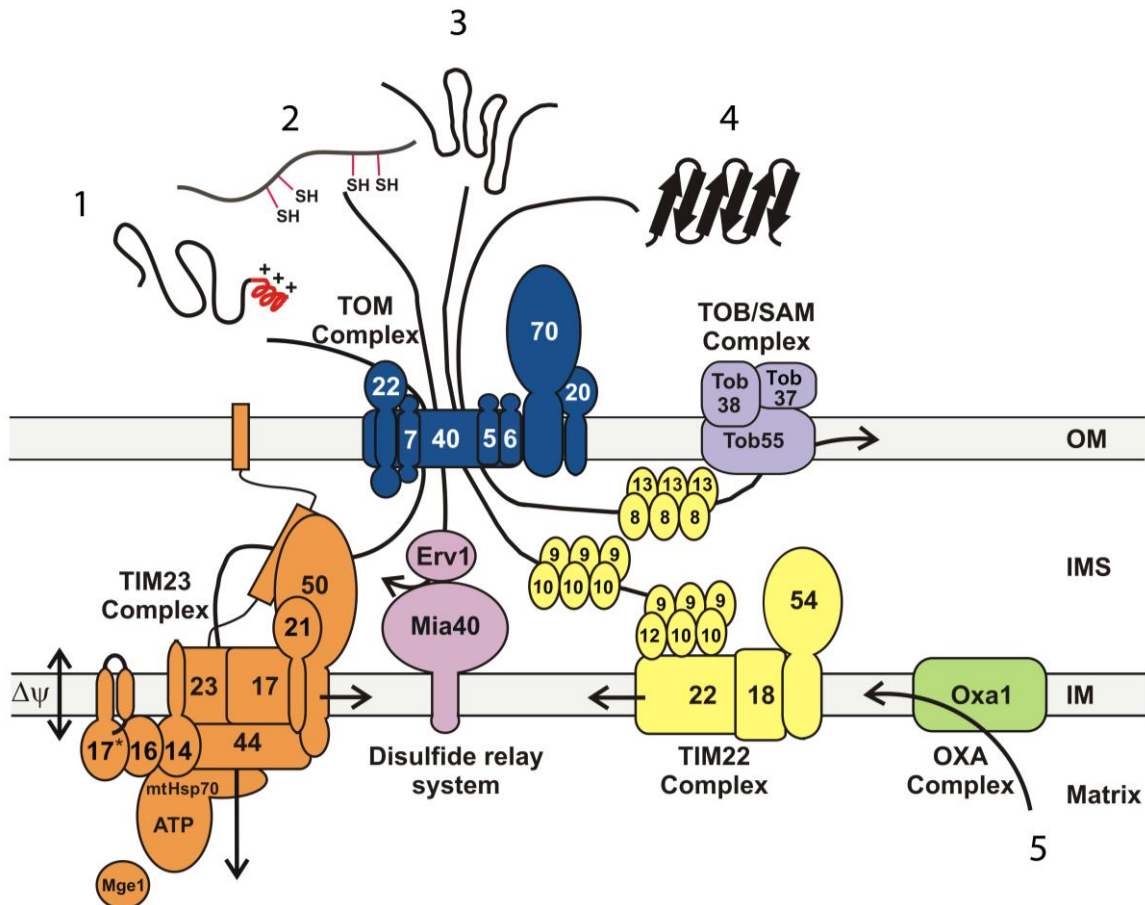


Figure 2

Protein translocases in the outer and inner mitochondrial membrane

Precursor proteins are imported into mitochondria via the TOM complex, some are further transported into the matrix, or integrated into the inner membrane by the TIM23 complex (1), directed to the IMS (2), inserted into the inner membrane by the TIM22 complex (3) or embedded into the outer membrane via the TOB complex (4). The Oxa1 complex facilitates the insertion into the inner mitochondrial membrane of a subset of preproteins approaching it from the matrix (5).

IM: inner mitochondrial membrane, IMS: intermembrane space, OM: outer mitochondrial membrane

The figure was adapted from Mokranjac et al., 2008 (26).

1.2.1 The TOM complex

The first transport machinery that mitochondrial preproteins are encountering in the outer mitochondrial membrane is the translocase of the outer membrane (TOM) complex (Figure 2). This major entry gate of the mitochondria is used by all preproteins analyzed to date for transport across the outer membrane. The TOM complex consists of the general insertion pore (GIP), made up by Tom40, Tom22, Tom5, Tom6 and Tom7. The receptors Tom20 and Tom70 are loosely attached to the GIP (8, 27). Tom40 is the major and only essential subunit of the GIP. It presumably forms a membrane-embedded β -barrel. Tom5, Tom6 and Tom7 are small subunits with a length ranging from 50 – 70 amino acids and seem to be involved in the stability of the complex. Since isolated Tom40 forms pores in artificial membranes and demonstrates characteristics comparable to those of the entire TOM complex (28-31), Tom40 is believed to be the central, pore forming subunit of the complex. However, it is still unclear whether this translocation channel comprises a single or multiple Tom40 molecules.

Receptors of the TOM complex are the proteins Tom20, Tom70 and Tom22. Tom20 and Tom70 are signal-anchored proteins which are integrated with an N-terminal α -helix into the outer membrane exposing their C-terminus to the cytosol. Tom22 is bearing a predicted α -helical transmembrane domain in the middle of its sequence and exposes its C-terminus to the IMS. The preproteins interact with the receptors at the so-called *cis*-binding site of the TOM complex, made up by the cytosolic components of Tom20, Tom22 and Tom70. Tom20 and Tom70 are the major recognition sites for the precursor proteins, while Tom22 mainly contributes to the integrity of the TOM complex (32, 33). After the interaction of targeting sequences with receptors, the preproteins are relayed to the GIP and pass the outer mitochondrial membrane. Arriving in the IMS, the precursor proteins interact with the *trans*-binding site, formed by domains of Tom22, Tom40 and Tom7 (34-36). An increased affinity at the *trans*-binding side presumably fuels the vectorial translocation of the targeting signals to the IMS side of the TOM complex (37).

Then, the precursor proteins use different pathways to reach the mitochondrial subcompartments - a topogenetic process which is coordinated by the cooperation between the TOM complex and other mitochondrial translocases in accordance to the type of targeting signal of the preproteins (8, 27).

1.2.2 Import of proteins into the matrix

Mitochondrial matrix proteins make up the majority of all mitochondrial proteins. Their precursor forms are transported across both mitochondrial membranes by the concerted interaction of two protein translocases, the aforementioned TOM complex in the outer mitochondrial membrane and the TIM23 (translocase of the inner membrane) complex in the inner mitochondrial membrane (27).

The TIM23 complex can be subdivided into the membrane component, comprising those proteins which are forming the protein-conducting channel, and the import motor, which drives the translocation of the precursor proteins into the matrix. The membrane component consists of three essential proteins namely Tim23, Tim17 and Tim50. They, together with the non-essential Tim21, are highly conserved throughout the eukaryotic kingdom. Tim50 forms the receptor subunit of the membrane component, exposing a large C-terminal domain to the IMS. The N-terminus is anchored to the inner membrane with a single transmembrane domain. Tim50 is the first component of the inner membrane interacting with incoming precursor proteins as they emerge from the trans-binding site at the TOM complex (38, 39). Afterwards, the precursor proteins are presumably transferred to Tim23 (25, 27). Tim50 has been proposed to block the protein-conducting channel of the TIM23 complex in the absence of any precursor protein and thereby prevent the collapse of the membrane potential ($\Delta\psi$) by ion leakage (25, 40). Tim23 and its associated Tim17 form the translocation channel of the TIM23 complex. The C-terminus of Tim23 is embedded by four transmembrane helices into the inner mitochondrial membrane. Surprisingly, Tim23 can span the IMS and the outer mitochondrial membrane, indicated by the accessibility of the N-terminus to proteases added to intact mitochondria (41). It has been suggested that the N-terminus of Tim23 brings the TIM23 translocase in proximity to the outer mitochondrial membrane to facilitate its interplay with the TOM complex (41). Interestingly, a comparable function has been suggested for Tim21, bringing together the TOM and the TIM23 complex due to its binding to the IMS-exposed part of Tom22 (27, 42, 43). The segment of Tim23 spanning the IMS interacts with Tim50 and serves as an additional presequence receptor of the TIM23 complex (44). Comparable to Tim23, Tim17 has four C-terminal transmembrane helices anchoring it in the inner mitochondrial membrane. Although these helices have sequence similarity to those of Tim23, they seem to have diverse functions, as they are not interchangeable (8). The N-terminal segment of Tim17 exposed to the IMS is rather short and contains several conserved

negatively charged residues which play a crucial role in preprotein import and gating of the translocation channel (45, 46).

The import motor is also called presequence translocase-associated motor (PAM) and sits at the matrix site of the inner mitochondrial membrane. It is made up of the proteins Tim44, Tim14 (Pam18), Tim16 (Pam16), mtHsp70 (matrix 70 kDa heat shock protein), and Mge1. Tim44 is a peripherally attached membrane protein forming the interface of the membrane component with the import motor unit of the TIM23 complex. The C-terminus of Tim44 is embedded in the inner mitochondrial membrane. On the one side, Tim44 binds to the Tim23-Tim17 core of the membrane embedded translocation channel, while the other side interacts with mtHsp70 and its associated DnaJ-like proteins, Tim14 and Tim16 (8, 27). Tim14 is anchored with its N-terminus in the inner membrane and forms a tight complex with Tim16 which is lacking a transmembrane segment (47). mtHsp70 is an exchangeable subunit of the import motor, fluctuating between a bound and a released state. As found in all Hsp70 (heat shock protein) chaperones, mtHsp70 contains an N-terminal nucleotide (ATP) binding domain (NBD) and a C-terminal substrate or peptide binding domain (PBD) (48, 49). ATP bound mtHsp70 is recruited by Tim44 and thereby enables the interaction of the incoming polypeptide with the mtHsp70. The alternation between the binding to and release of the translocating polypeptide by mtHsp70 is an ATP-dependent process which results in the vectorial movement of the unfolded polypeptide chain into the matrix. The hydrolysis of ATP to ADP as well as substrate binding to the mtHsp70 is regulated by the DnaJ-like proteins. Upon binding of the polypeptide to mtHsp70, Tim14 stimulates ATP hydrolysis and thereby triggers the release of the mtHsp70-precursor protein complex from Tim44. The mtHsp70-precursor protein complex dissociates from the membrane and enables the binding of the next ATP bound mtHsp70. After ATP hydrolysis, ADP is exchanged for ATP by the nucleotide exchange factor Mge1. This leads to a release of the substrate (8, 27, 50, 51). Tim16 is not a functional DnaJ-like protein, as it is missing the HPD (His-Pro-Asp) motif which is crucial for the stimulation of mtHsp70. Rather it functions as a negative regulator of the import motor by blocking the contact between Tim14 and mtHsp70 (52-54).

Roughly half of the mitochondrial proteins are synthesized with an N-terminal extension as a targeting signal. This signal is also called the presequence, prepeptide or matrix targeting sequence (MTS), since it directs the N-terminus across the inner mitochondrial membrane. To date the DNA helicase Hmi1 is the only exception known, where the MTS is positioned at the C-terminus (55). The MTSs do not share a conserved primary sequence but they all have the propensity to form an amphipathic helix presenting one hydrophobic and one positively

charged face. Tom20 possesses a binding groove for the hydrophobic site of those N-terminal presequences (MTSs), where Tom22 recognizes the positively charged surface (8, 25). After passing the TOM complex, the precursor proteins are transferred to the TIM23 complex. The membrane component of the TIM23 complex only transports the MTS through the inner mitochondrial membrane, a process driven by the membrane potential $\Delta\psi$. The translocation into the mitochondrial matrix of the polypeptide chain C-terminal to the MTS is performed by the import motor unit of the TIM23 complex and fuelled by a second energy source, ATP. As already mentioned above, this ATP is used by mtHsp70 to pull the polypeptide in a stepwise manner into the matrix. In the absence of further sorting information, MTS-containing precursor proteins are fully transferred into the matrix. The MTS is sufficient to direct a preprotein into the matrix and is therefore referred to as the default mode of the TIM23 complex (56, 57). Currently this is under debate (8, 25). Once the precursor proteins have reached the mitochondrial matrix, the MTS is removed by the matrix processing peptidase (MPP).

1.2.3 Import of proteins into the inner mitochondrial membrane

For those nuclear encoded mitochondrial proteins which have the inner mitochondrial membrane as their final destination there are three different pathways for their translocation from the cytosol into the mitochondria: (1) the stop-transfer pathway, (2) the TIM22 pathway, and (3) the conservative sorting pathway.

The stop-transfer pathway includes the already described protein translocases TOM and TIM23. TIM23 is not only capable of transporting precursor proteins into the matrix (translocation mode), but can also switch to a second mode, for the stop-transfer pathway, in which the preproteins are stopped during the translocation and are laterally inserted into the inner mitochondrial membrane (lateral insertion mode). In contrast to the preproteins directed to the matrix, which only possess an MTS at the N-terminus, preproteins designated for lateral insertion have an additional signal, a stop-transfer signal, in some distance C-terminal to the MTS. This stop-transfer signal is a transmembrane domain which causes the arrest of the precursor protein inside the TIM23 complex (27).

Depending on the type of targeting signal the TIM23 complex encounters, the complex changes its internal conformation to set up either for the translocation mode or the lateral insertion mode (58, 59).

Another pathway for proteins to be transported from the cytosol to the inner mitochondrial membrane is the TIM22 pathway. This pathway requires the concerted action of three different consecutive mitochondrial protein translocases: (1) the TOM complex in the outer membrane, (2) the complexes of the small Tim proteins in the IMS, and (3) the TIM22 translocase in the inner mitochondrial membrane.

The small Tim protein complexes Tim9-Tim10 and Tim8-Tim13 reside in the IMS and are composed of polypeptides with a molecular weight between 8 and 12 kDa. They are characterized by twin C_X3C motifs. The cysteine residues of these motifs form pairs of intramolecular disulfide bridges which are crucial for the structure of the small Tim proteins. Small Tim proteins oligomerize as tightly bound hexamers with a “jellyfish-like structure”. The tentacles of this jellyfish-like structure might be able to bind to the hydrophobic regions of incoming proteins from the TOM complex (60) and therefore are supposed to fulfill a chaperone like function while transferring the precursor proteins in the IMS from the TOM to the TIM22 complex (61, 62), although this is still hypothetical.

The TIM22 complex is made up of the membrane proteins Tim22, Tim54 and Tim18 and has a combined molecular weight of around 300 kDa. Tim22 is the core subunit of the complex and is embedded in the inner mitochondrial membrane with four transmembrane helices which presumably form the translocation pore of the complex (63). Tim54 and Tim18 are associated with Tim22 and seem to be important but non-essential components of the TIM22 complex, since preproteins are inserted even in the absence of Tim54 and Tim18, although at strongly reduced levels (63). Tim54 exposes a large domain in the IMS and might serve as a docking site for a small Tim protein complex consisting of Tim9, Tim10, and Tim12, which is permanently bound to the TIM22 complex (63, 64). The essential small Tim protein Tim12 is exclusively found in the TIM22 associated complex but not in the soluble chaperone complexes of the IMS and might be involved in substrate recognition at the TIM22 complex. Tim18 is supposed to play a role in the assembly of the TIM22 complex (25, 27).

The TIM22 pathway is responsible for the insertion of members of the solute carrier family, such as the ATP/ADP or the phosphate carrier as well as the membrane embedded subunits of TIM complexes such as Tim17, Tim22 and Tim23. All these proteins are lacking cleavable presequences but contain internal non-cleavable targeting signals (8, 27). After their synthesis in the cytosol, the carrier precursor proteins are bound by the chaperones Hsp70 and Hsp90 and guided to the Tom70 receptor at the TOM complex. Here, the chaperones dock to the tetratricopeptide repeat (TPR) domain of the receptor (65). Following the ATP-dependent release and transfer from the chaperones to the TOM complex, the precursor proteins are

transferred through the Tom40 translocation channel. In contrast to the MTS bearing precursor proteins, carrier precursor proteins are not transported as linear polypeptide chains through the TOM complex but pass it in a loop structure (66). Subsequently, with the help of the small Tim protein complex Tim9-Tim10, the preproteins are transferred to the Tim9-Tim10-Tim12 chaperone complex at the surface of the TIM22 translocase. Finally, substrates of the TIM22 complex are laterally inserted into the membrane in a membrane potential-dependent process and result in an even-numbered transmembrane segment in the inner mitochondrial membrane exposing both their N- and C-termini into the IMS. The import process of the TIM subunits Tim17, Tim22, and Tim23 is comparable to that of the carrier proteins, however, not well characterized. Instead of utilizing the Tim9-Tim10 complex, the precursor proteins of the TIM subunits are interacting with an alternative Tim complex made up by Tim8 and Tim13 (8, 27).

In the conservative sorting pathway, proteins destined for the inner mitochondrial membrane are first transported from the cytosol into the matrix and from there inserted into the inner membrane. Due to the resemblance of the export-like transport of the proteins from the matrix side into the inner membrane to that of protein transport in prokaryotes, this pathway is termed the 'conservative sorting pathway'. Precursor proteins following this pathway are for example Oxa1 (67) and subunit 9 of the F_0F_1 -ATPase of *Neurospora crassa* (*N. crassa*, *N.c.*), (68). They are synthesized with an N-terminal cleavable presequence and consist of more than one transmembrane domain. As they reach the matrix, they are bound by mtHsp70 to prevent them from aggregating. Thereafter, the MTS is removed by the MPP. The molecular mechanism by which these precursor proteins are integrated into the inner mitochondrial membrane is still ill defined. In general, protein segments which are transported from the matrix across the inner membrane are enriched in negatively charged amino acid residues. Since the membrane insertion from the matrix strongly depends on the membrane potential, it is likely that the negative charged regions are pulled to the IMS in an electrophoretic manner (67-69). The Oxa1 (oxidase assembly) complex of the inner membrane facilitates the insertion of at least some of these inner membrane proteins (69, 70). Oxa1 is also involved in the co-translational insertion of proteins encoded in the mtDNA (70-72).

1.2.4 Import of proteins into the intermembrane space

The biogenesis of proteins which reside in the IMS is diverse. Three different import mechanisms are known: (1) the bipartite presequence coordinated pathway, (2) the folding trap mechanism, and (3) the localization of proteins in the IMS due to affinity interactions.

Some of the proteins which are directed to the IMS have bipartite presequences or sorting signals, consisting of an N-terminal MTS as well as a hydrophobic sorting sequence. The precursor proteins follow the translocation path provided by the TOM and the TIM23 complex. In general, following the arrest of the incoming proteins in the inner mitochondrial membrane, peptidases remove those targeting signals by proteolytic cleavage and thereby release the proteins into the IMS. Proteins located in the IMS which are using this pathway are for example the cytochrome *c* peroxidase (CCPO) or cytochrome *b*₂ (27).

Another import pathway by which proteins are directed into the IMS is the folding trap mechanism. Here, after passing the outer mitochondrial membrane, the proteins are stabilized by cofactors or disulfide bridges in their folded state and are thereby trapped in the IMS. Prominent examples are the folding of small Tim proteins mediated by the MIA (mitochondrial intermembrane space import and assembly) machinery (73-76) or the covalent addition of heme to apocytochrome *c* catalyzed by the cytochrome *c* heme lyase (CCHL) in the IMS (77). The MIA machinery comprises the disulfide carrier Mia40, which is anchored in the inner mitochondrial membrane, and the soluble sulfhydryl oxidase Erv1 (essential for respiration and viability), and promotes the formation of intramolecular disulfide bonds in, for example, the imported small Tim proteins.

Finally, the import of proteins such as cytochrome *c* heme lyase or the creatine kinase seems to be driven by their high affinity to certain components in the IMS to which they are permanently associated after they have reached the IMS (27). The mechanism of this import pathway is largely obscure.

1.2.5 Import of proteins into the outer mitochondrial membrane

All proteins of the outer mitochondrial membrane known to date are nuclear encoded. They are missing canonical cleavable N-terminal prepeptides, but contain non-cleavable targeting and sorting signals within the protein sequence itself. The membrane-integrated proteins of the outer mitochondrial membrane can be subdivided into two groups: α -helical proteins and β -barrel proteins. β -barrel proteins can only be found in the outer membranes of Gram-

negative bacteria, chloroplasts and mitochondria while all other membranes harbour α -helical membrane proteins (78).

1.2.5.1 Insertion of α -helical proteins into the outer mitochondrial membrane

According to their topology, different classes of α -helical proteins can be distinguished in the outer mitochondrial membrane. Characteristically, these proteins are anchored with one or more α -helical transmembrane segments into the membrane. Signal anchored proteins carry one α -helical transmembrane domain at the N-terminus. This group includes the primary import receptors of the TOM complex, Tom20 and Tom70. When the transmembrane segment is located at the C-terminus, such as in Tom5, Tom6, Tom7 or Fis1, the proteins are referred to as tail-anchored proteins. Proteins of both categories expose their main part into the cytosol and only a short segment into the IMS. Tom22 and mitochondrial import protein 1 (Mim1) have one central embedded transmembrane domain and are orientated with the N-terminus to the cytosol and the C-terminus to the IMS. The peripheral benzodiazepine receptor (PBR), Fzo1 and Ugo1 are examples of proteins which contain multiple α -helices in the membrane, spanning the outer mitochondrial membrane five, two and three times, respectively (79-82).

In all these proteins, the hydrophobic segments do not only serve as anchors within the membrane, but also typically function as targeting signals of the proteins. However, no sequence similarities could be found among those targeting sequences. The targeting information is apparently encoded in structural elements such as the hydrophobicity and charge of the transmembrane α -helix and its flanking regions (83). The mechanism by which the different α -helical membrane proteins are inserted into the outer mitochondrial membrane seems to differ between the individual members and is still ill defined. The insertion of the signal-anchored proteins Tom20, Tom70 or Mcr1, for example, was shown to be independent of the presence of import receptors while unaffected by the blocking of the translocation pore of the TOM complex (84-87). However, in contrast to Mcr1, Tom20 seems to be dependent on Tom40 for acquiring its correct topology. It has been suggested that the TOM translocase can facilitate protein insertion at its protein-lipid interface (86-88). Moreover, both Tom20 and Tom70 were described to use a further outer membrane protein for membrane insertion, namely the mitochondrial import protein 1 (Mim1) (89-91). Mim1 was also found to be important for the insertion of the small TOM proteins (92). Other tail-anchored proteins do not require any of the known outer membrane machineries and seem to be dependent on the lipid composition of the membrane for their insertion (93, 94). The precursor of Tom22 needs

the TOM receptors to be directed to the mitochondrial surface and seems to use the TOB complex for its insertion into the outer mitochondrial membrane (95). Multiple spanning membrane proteins were reported to use components of the IMS, Tom70, but no other TOM complex proteins for efficient insertion into the outer mitochondrial membrane (96).

Taken together, the TOM complex was found to have two distinct functions: (1) the aforementioned translocation of virtually all preproteins from the cytosol across the outer mitochondrial membrane and (2) the direct integration of α -helical outer membrane proteins. Our knowledge of how those α -helical transmembrane proteins are inserted into the outer envelope of mitochondria is still elusive. Since the pore of the TOM complex seems not to be needed for that process, at least in some cases, those proteins may not follow the canonical route through the import channel, but are following a second pathway which awaits further analysis.

1.2.5.2 Insertion of β -barrel proteins into the outer mitochondrial membrane

β -barrel proteins are embedded in the outer mitochondrial membrane by multiple antiparallel β -strands. The topogenesis of the mitochondrial outer membrane β -barrel proteins (TOB) complex (97), also termed the sorting and assembly machinery (SAM) (98), is specialized in the insertion of the β -barrel precursor proteins into the outer membrane and requires a coordinated interaction with the TOM complex and small Tim protein complexes to fulfill its task. Composition and function of the TOB complex are discussed in detail below.

1.3 The TOB complex

1.3.1 Introduction

In eukaryotes, β -barrel proteins are exclusively found in the outer membrane of organelles of endosymbiotic origin, namely chloroplast and mitochondria (99, 100). Furthermore, β -barrel proteins can only be found in the outer membrane of Gram-negative bacteria (101), which supports the idea that these organelles are derived from a bacterial ancestor (5, 102). Membrane-embedded β -barrel proteins are referred to as outer membrane proteins (OMPs) (103). The TOB complex in the outer mitochondrial membrane is responsible for the correct insertion of β -barrel proteins and cooperates with the TOM complex, which is also sitting in the outer mitochondrial membrane and with the small Tim protein complexes in the IMS.

1.3.2 Composition of the TOB complex

TOB is a hetero-oligomeric protein complex which comprises the proteins Tob55 (Sam50, Tom50), Tob38 (Sam35, Tom38) and Tob37 (Mas37, Sam37, Tom37) (97, 98, 104-108). Tob55 is the main component of this complex and was found in a proteomic screening of outer mitochondrial membrane proteins from *N. crassa* by mass spectrometry analysis (97). It was also found in copurification experiments with Tob37 (98), a known subunit of the TOB complex (104). Sequence analysis revealed homologues of Tob55 not only in the genomes of virtually all eukaryotes, but significant sequence similarity was also detected with the outer membrane protein 85 (Omp85) from Gram-negative bacteria (97, 109). Omp85 (YaeT, BamA) is the main subunit of the bacterial β -barrel assembly machinery (BAM) and was determined to be a β -barrel protein itself (25, 110-113).

It is assumed that Tob55 is also a β -barrel protein. This is mainly based on sequence analysis and secondary structure prediction, since, to date, no high resolution structure of Tob55 and its homologues could be solved (97, 98, 109, 113-116). Therefore, Tob55 is supposedly both a substrate and subunit of the TOB complex. Besides Tob55, porin (also termed as voltage-dependent anion-selective channel (VDAC)), Tom40, Mdm10 and Mmm2 are assigned to the family of outer mitochondrial β -barrel membrane proteins and thereby putative substrates of the TOB complex (27). The membrane-embedded β -barrel of Tob55 is predicted to be formed by the C-terminus, whereas the hydrophilic amino acids at the N-terminus are facing the IMS and fold into a characteristic structure, the polypeptide transport associated (POTRA) domain (112, 113, 117). These POTRA domains were described to have receptor functions and were not only found in Tob55 but also in other OMPs such as Omp85/YaeT (114, 118), although

the amount of POTRA domains could vary between one (Tob55), two (FhaC (filamentous haemagglutinin adhesin)), and even up to five (Omp85) (103, 117, 118).

Several experiments indicated a specific role of the TOB complex in the biogenesis of β -barrel precursor proteins in the outer membrane. The Tob55 gene was found to be essential for cell viability (109, 119, 120) and downregulation of Tob55 (Tob55 \downarrow) resulted in low levels of β -barrel proteins such as Tom40, porin and Mdm10 in the outer mitochondrial membrane. In contrast, the levels of α -helical proteins in the outer mitochondrial membrane, the IMS, the inner mitochondrial membrane and the matrix remained unaffected (97, 120). There is only one exception, the α -helical protein Tom22, which was decreased in Tob55 \downarrow mitochondria in *N. crassa* (120). In accordance with that, import of the pre-proteins Tom40 and Tob55 itself in Tob55 \downarrow mitochondria was also strongly reduced, whereas α -helical outer mitochondrial membrane proteins or proteins designated to the IMS, the inner mitochondrial membrane or the matrix were imported at roughly wild-type levels (97, 120). Studies on the assembly process of the β -barrel proteins Tom40 and porin also revealed that the biogenesis of these proteins is severely impaired by the depletion of Tob55. Antibody supershift assays presented direct evidence for the interaction of the TOB complex with β -barrel precursor proteins (98, 109, 120).

Consisting of a POTRA domain and a β -barrel, having a high sequence similarity to Omp85, and functioning as a transporter of β -barrel precursor proteins makes it tempting to assign the TOB complex to the Omp85-TpsB transporter superfamily (Tps – Two-Partner Secretion), and there to the Omp85 subfamily (109, 115, 121-124).

The Omp85 family is a conserved family of protein transporters and includes Toc75 (translocon at the outer envelope membrane of chloroplasts) of chloroplasts, D15 of *Haemophilus influenzae*, Omp85 from *Neisseria meningitides* and YaeT from *Escherichia coli*. So far, Tob55 is the only known mitochondrial β -barrel protein with clear homologues outside the kingdom of eukaryotes (78).

To date only one member of the Omp85-TpsB transporter superfamily could be crystallized, FhaC (115, 121). FhaC belongs to the second subfamily of the Omp85-TpsB transporter superfamily, the TpsB-transporter family. TpsB transporter can be found in a subset of Gram-negative bacteria and are responsible for the secretion of their dedicated TpsA substrates (124). Whereas Tob55 was primarily predicted to have 12 β -strands (112, 113), recent alignments with the FhaC sequence in combination with the resolved β -barrel structure of FhaC suggest a 16-stranded β -barrel for members of the Omp85 transporter family (115, 121).

Despite these similarities between Tob55 and the prokaryotic members of this transporter family, the insertion mechanism of β -barrel precursor proteins in prokaryotes and mitochondria are expected to diverge due to the different additional components of the transporter complexes (8).

The additional components to Tob55 of the TOB complex, Tob38 and Tob37, are located at the cytosolic surface of the outer mitochondrial membrane (104-107). So far, a high homology of both proteins could only be found among fungi (27). Only a moderate sequence homology to the mammalian metaxin-1 was reported for Tob37 (125-127). Furthermore, Tob38 was proposed to be a homologue of the mammalian metaxin-2. Convincing evidence for homology of metaxin proteins with Tob38 and Tob37 is still lacking (105, 107, 126). Tob38 is an essential component of the TOB complex in yeast and depletion of Tob38 results in impaired β -barrel import comparable to a loss of Tob55 (105-107). In contrast to Tob55 and Tob38, yeast Tob37 is not an essential protein, but the deletion of Tob37 compromises the insertion of β -barrel precursor proteins and results in growth defects (104). Similarly, metaxin-1 and metaxin-2 were also indicated to play important roles in β -barrel biogenesis (126). Electron microscopy images of negative stained native and recombinant Tob55 revealed ring-shaped structures with a fivefold symmetry which displayed an inner pore size of 4-5 nm and an outer diameter of 15 nm (97). To date, high resolution structures for Tob38 as well as Tob37 are still elusive.

1.3.3 Topogenesis of mitochondrial β -barrel proteins

After their synthesis in the cytosol, β -barrel precursor proteins interact with the receptors of the TOM complex (83, 128) and subsequently pass through the TOM pore into the IMS (97, 104). There, they are transferred from the TOM pore to the TOB complex with the help of the small Tim protein complexes Tim8-Tim13 and Tim9-Tim10. These complexes presumably prevent backsliding of the β -barrel precursor proteins and have a chaperone-like function analogous to the bacterial chaperone Skp (129-131). As the β -barrel precursors reach the TOB complex, they are supposedly bound by the POTRA domain of Tob55 (114, 118) and inserted into the outer mitochondrial membrane from the IMS side (97, 104). Interestingly, the translocation across the TOM pore seems to be coupled to the membrane insertion of the β -barrel precursor proteins by the TOB complex, as a depletion of Tob55 leads to an accumulation of preproteins within the TOM complex and prevents them from reaching the IMS (27, 97). Interaction of the β -barrel precursor proteins with the POTRA domain and their

membrane insertion from the IMS side are corresponding to the insertion mechanism in prokaryotes, where the preproteins are inserted into the outer envelope from the periplasm. This reflects the evolutionary origin of mitochondria from bacteria.

The mechanism by which the β -barrels are inserted into the outer-mitochondrial membrane by the TOB complex is still ill defined. Tob38 and Tob37 are both contributing to the stability of the TOB complex (105, 129, 132). Recently, Tob38 was reported to have a receptor-like function for β -barrel precursor proteins by binding to a conserved β -signal peptide at the most C-terminal β -strand and thereby initiating their membrane-insertion (132, 133). Tob37 was described to be responsible for the release of precursors into the lipid phase of the membrane and thereby act downstream of Tob38 in β -barrel assembly (129, 132). Moreover, recent findings assigned diverse proteins a role in the membrane insertion of β -barrel precursor proteins. Mdm10, Mdm12 and Mmm1, constituents of the MDM (mitochondrial distribution and morphology) complex, were determined to act downstream of the TOB complex in the assembly pathway. Depletion of these proteins reduced the assembly of Tom40 and porin in the outer mitochondrial membrane (108, 134, 135). Mdm10 was also suggested to be a constituent of the TOB complex (134, 136, 137). Mim1 was found to associate with Tob55 and is essential in the late steps of the assembly pathway of Tom40 (91, 106, 138). In addition to its role in the topogenesis of mitochondrial outer membrane β -barrel proteins, TOB was shown to participate in the insertion of α -helical subunits of the TOM complex such as Tom6 and Tom22 (92, 95).

1.4 Aim of the present study

The TOB complex was proven to be responsible for the insertion of β -barrel precursor proteins into the outer membrane of mitochondria, a process which is crucial for the functionality of these organelles and consequently the host cell. During the last years, remarkable progress was made in the identification of proteins involved in the biogenesis of β -barrel proteins. However, our knowledge about their structures, mechanism of membrane insertion and interplay is still fragmentary. The filamentous fungi *N. crassa* turned out to be an excellent organism for studying the biogenesis of mitochondrial proteins, due to its simple cultivation conditions and genetic manipulation procedures, and the fact that relatively large amounts of functionally and structurally intact mitochondria can be easily obtained (139). The aim of this study was to establish an isolation procedure of the TOB complex from *N. crassa*, with a view to carefully identify its composition and biochemical characteristics and thereby elucidating its functional mechanism.

2 Results

2.1 *Tob55* is expressed in three different isoforms due to alternative splicing

For the isolation of the TOB complex of *N. crassa*, it was planned to start with a Ni-NTA (nickel-nitriloacetic acid) affinity purification from a strain expressing a His-tagged form (bearing a stretch of attached histidinyl residues) of the *Tob55* protein. Surprisingly, *Tob55* appeared in two bands upon sodiumdodecylsulfate polyacrylamide gel electrophoresis (SDS-PAGE) and Western blotting using antibodies directed against *Tob55*. Both bands were absent when the mitochondria were isolated from a strain in which *Tob55* was downregulated (*Tob55*↓, *Tob55KO-3*) indicating two forms of *Tob55* (Figure 3A).

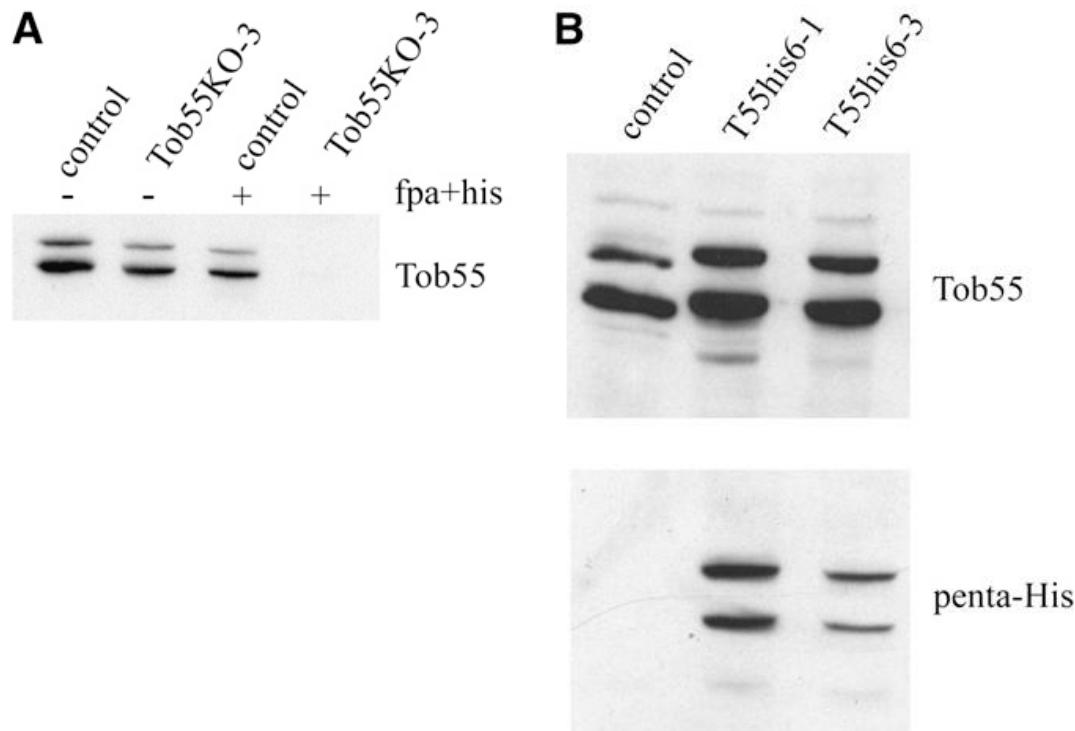


Figure 3

N. crassa *Tob55* appears in two bands upon SDS-PAGE

A: The control strain HP1 and the *Tob55KO-3* strain were cultivated on non-selective medium (-) or selective medium (+) with 400 mM *fpa* and histidine. *Tob55KO-3* is a *tob55* knockout sheltered heterokaryon strain. Its growth on selective medium forces the *tob55*-knockout-bearing nucleus to predominate in the heterokaryon, leading to a severe reduction of *Tob55*-levels in comparison to controls. Following SDS-PAGE, the separated proteins were analyzed by immunodecoration against *Tob55*.

B: As in “A” except mitochondria were isolated from the control strain (HP1) and two strains, *T55his6-1* and *T55his6-3*, expressing *Tob55* with an N-terminal hexahistidinyl tag. Immunodecoration was performed with *Tob55* antiserum or penta-His antiserum.

(Nargang group, University of Edmonton, Alberta, CA)

To find out whether the translation of diverse messenger ribonucleic acids (mRNAs) causes the double band of Tob55 in *N. crassa*, complementary desoxyribonucleic acid (cDNA) clones of *tob55* were sequenced in cooperation with the group of F. Nargang (University of Edmonton, Alberta, CA). Three different *tob55* cDNAs were obtained encoding Tob55 proteins of 483, 516 and 521 amino acids in length, termed long, intermediate and short Tob55, respectively (Figure 4B). Only two bands were observed by Western blot analysis. Therefore, it was assumed that the intermediate and long isoform cannot be distinguished by the electrophoretic procedure used. The variation between the cDNA clones was caused by the absence or presence of the exons 2 and 2a due to alternative splicing at three possible 5'- and two possible 3'-splice sites (Figure 4A). Sequence analysis of 20 randomly selected cloned cDNAs showed that the short form represents 50%, the intermediate form 35% and the long form 15% of total Tob55 cDNA.

Immunodecoration with a Tob55 antibody suggested that the short Tob55 isoform is more abundant than the intermediate and the long isoform together (Figure 4A). On the other hand, immunodecoration with penta-His antibody yielded roughly equal signal intensities of the two Tob55 bands (Figure 4B). This can be explained by the fact that the Tob55 antibody was produced against the N-terminal 108 residues of the short form. Therefore, the short Tob55 isoform presumably has a stronger interaction with the Tob55 antibody compared to the long and intermediate form due to more available epitopes.

To obtain evidence for the existence of the different Tob55 forms at the protein level, outer mitochondrial membrane vesicles (OMVs) were purified from the strain T55His6-1. T55His6-1 contains an N-terminal hexahistidinylyl-tagged genomic *tob55* gene. Following SDS-PAGE, the separated proteins from the OMVs were stained with Coomassie Brilliant Blue and bands of the size predicted for the Tob55 isoforms were excised. They were then analyzed by matrix-assisted laser desorption ionization time of flight (MALDI-TOF) mass spectrometry. Signature peptides unique for the long and intermediate Tob55 isoform could be detected in the higher molecular weight Tob55 band, while the signature peptide identifying the short Tob55 isoform was found in the lower molecular weight Tob55 band (Figure 4C). Taken together, these data demonstrate that in *N. crassa* Tob55 is expressed in three different isoforms due to alternative splicing, as there are the long form with 521 amino acids (54.7 kDa), the intermediate form with 516 amino acids (54.1 kDa) and the short form with 483 amino acids (50.7 kDa).

Results

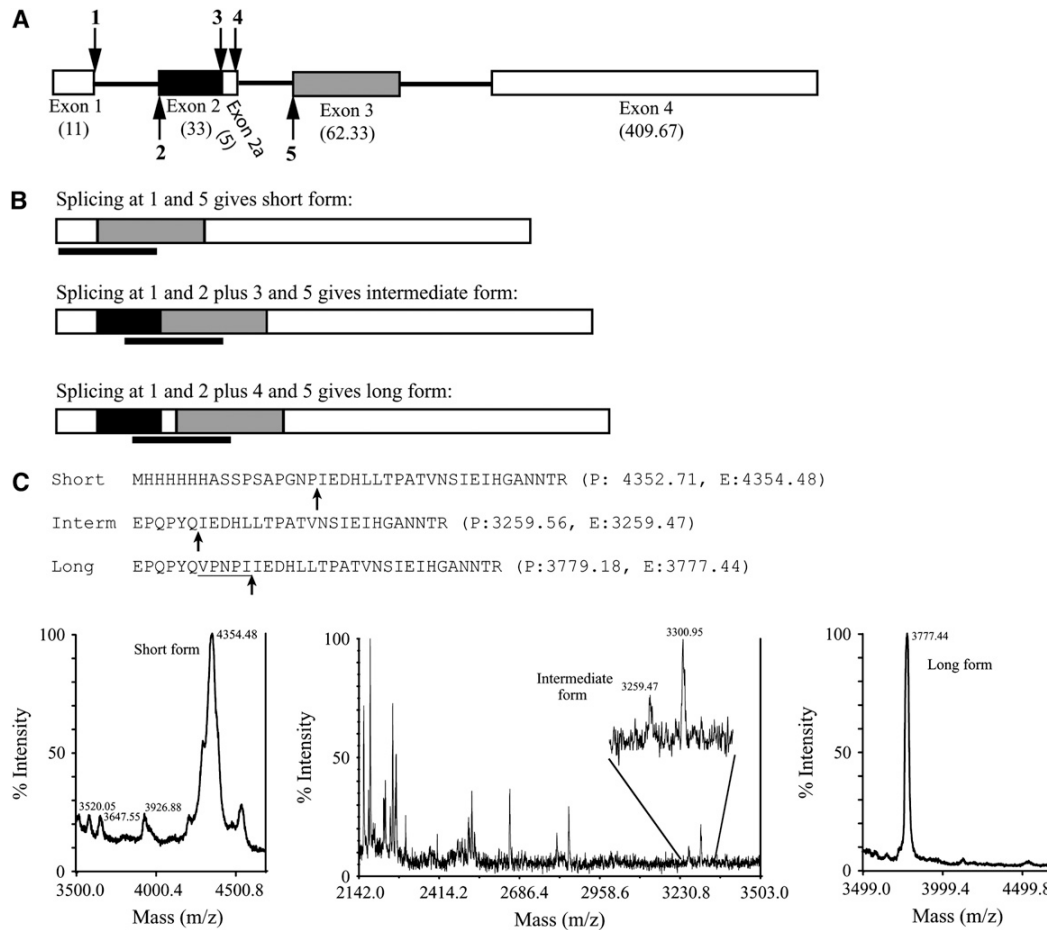


Figure 4

Three isoforms of Tob55 arise from alternative splicing

A: Overview of the intron/exon structure of the *tob55* gene

Exons are sketched as rectangular boxes, introns as solid lines. The amount of codons comprised by each exon is given in parentheses. Possible 5'- and 3'-splice sites are indicated by numbered arrows above and below the line.

B: The three different Tob55 isoforms resulting from alternative splicing

The exons are shaded as in "A". Predicted tryptic peptide fragments which are unique for each isoform (signature peptides) are underlined by solid bars.

C: The signature peptides that are predicted to arise from the tryptic digestion

The initial methionine is followed by six histidiny residues, since the analysis was performed with the short Tob55 isoform bearing an N-terminal hexahistidiny tag. Splice points between exon 1 and 3 for the short form, between exon 2 and 3 for the intermediate ("interm") form, and between exon 2a and 3 for the long form of Tob55 are marked by arrows below the peptide sequence. The underlined residues in the long Tob55 isoform represent exon 2a.

Coomassie blue-stained Tob55 bands were excised from a gel and analyzed by MALDI-TOF. For each signature peptide the predicted ("P") mass and the mass that was determined experimentally ("E") by mass spectrometry is given. The experimentally determined mass of the signature peptide of the short Tob55 isoform indicates an oxidation, which presumably took place at the N-terminal Met residue. For each signature peptide the tracings from the appropriate region of the mass spectra are shown.

2.2 Isolation of the TOB complex

An isolation procedure of the TOB complex from the filamentous fungus *N. crassa* was established using His-tagged variants of components of the TOB complex. The first step was the purification of OMVs to enrich the amount of TOB complex in the starting material for Ni-NTA affinity. The TOB complex is present at very low levels in mitochondria and separation of the outer membrane leads to a strong enrichment as well as removal of potential contaminating proteins.

A strain expressing the short Tob55 isoform with an N-terminal hexahistidinyl tag was chosen to be used for Ni-NTA affinity purification. The tag had to be extended from six to nine histidinyl residues to obtain efficient purification. Lysis of the OMVs was performed with the detergents TX-100 (Figure 5) or digitonin (Figure 6). The lysates were passed over Ni-NTA columns for affinity purification. The specifically bound proteins were eluted and subjected to SDS-PAGE. They were identified by Western blotting and immunodecoration (Figure 5B, Figure 6B) or Coomassie blue staining (Figure 5C, Figure 6C). Coomassie blue-stained bands were excised and proteins identified by LS-MS/MS. With both detergents, Tob55, Tob38 (37.3 kDa) and Tob37 (48.6 kDa) were the only proteins, which were detectable in the eluate (Figure 5, B and C, Figure 6, B and C). Very minor amounts of Mdm10 (52.7 kDa) were detected by immunodecoration (Figure 5B, Figure 6B). The amounts of this protein were not high enough to show up upon LC-MS/MS. In the preparations obtained with digitonin sometimes traces of the very abundant outer membrane protein porin were present.

The same isolation procedure was carried out with OMVs from the strains His9-Tob38 and His9-Tob37. These strains express Tob38 or Tob37 with an N-terminal ninefold His-tag and all three untagged Tob55 isoforms. These preparations were performed to exclude loss of TOB complex subunits caused by the absence of the intermediate and long Tob55 isoform. The only proteins recovered in the eluate were Tob55, Tob37 and Tob38, and again, very small amounts of Mdm10 (Figure 5, Figure 6). Thus, these results suggest that Tob55, Tob38 and Tob37 are the subunits of the TOB complex.

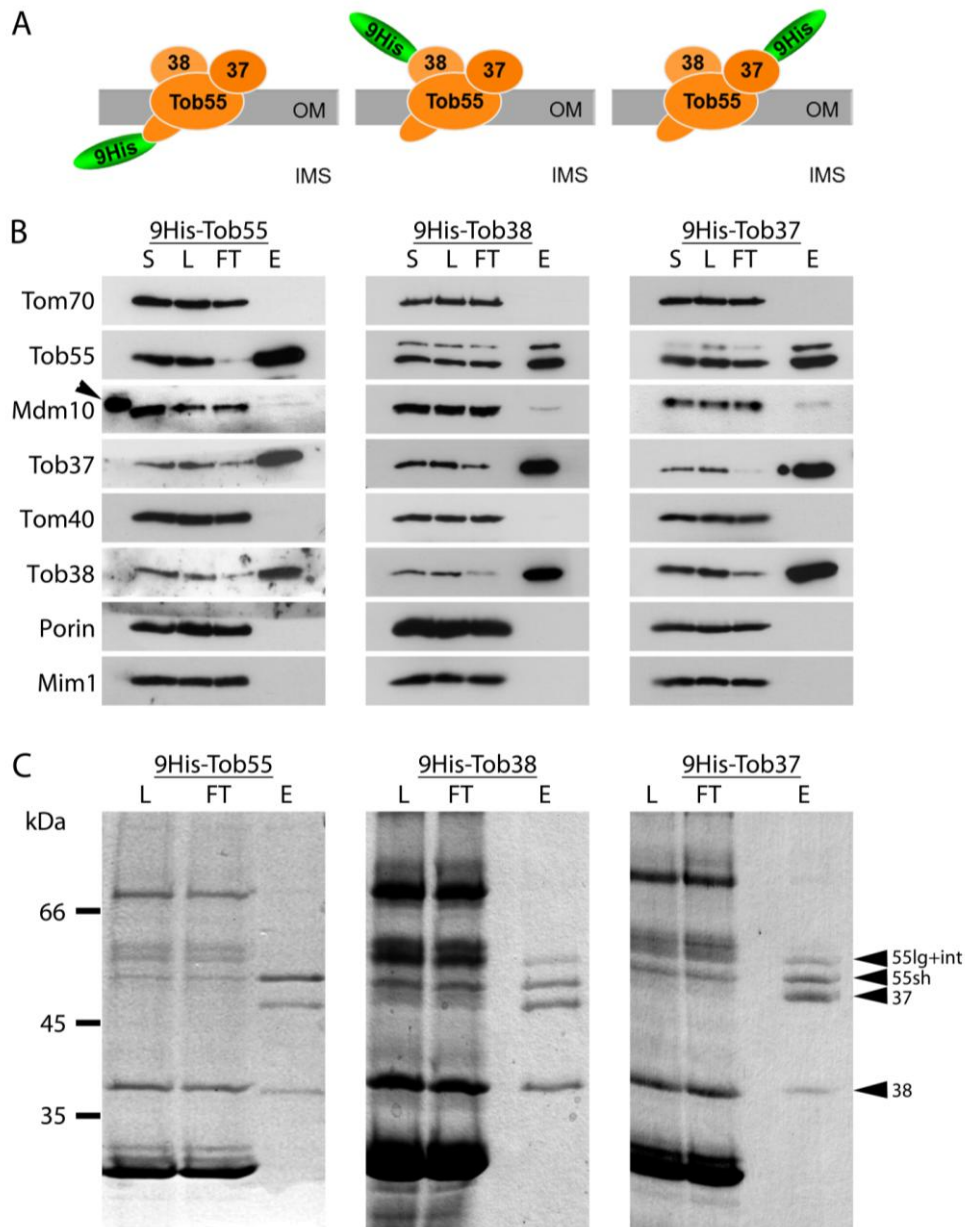


Figure 5

Tob38, Tob37 and Tob55 copurify in the presence of TX-100

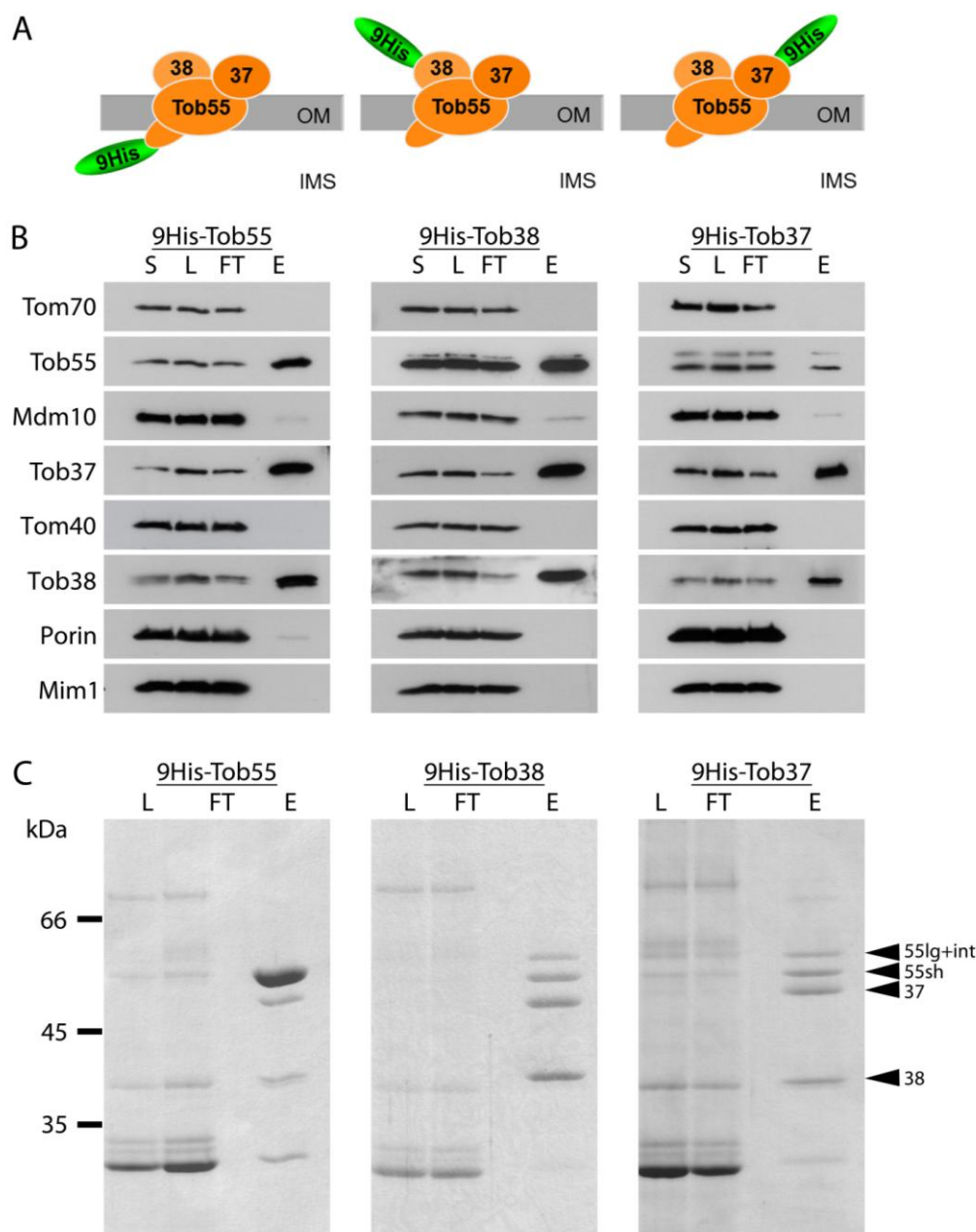
A: Schematic representation of TOB complexes with N-terminal ninefold His-tags at Tob55, Tob38 or Tob37.

OM: outer mitochondrial membrane, IMS: intermembrane space

B and C: Outer mitochondrial membrane vesicles (OMVs) from N.c. strains with the His-tagged TOB-subunit, 9His-Tob55, 9His-Tob38 or 9His-Tob37 were solubilized with TX-100; proteins were isolated by Ni-NTA affinity purification and analyzed by SDS-PAGE followed by immunodecoration (B) or Coomassie blue staining (C).

Solubilized outer mitochondrial membrane vesicles (OMVs) before (S) or after (L) clarifying spin. FT: flowthrough with unbound proteins of the Ni-NTA column, E: eluate of bound proteins, 55 lg and int: Tob55-intermediate and long isoform, 55sh: Tob55-short isoform, 37: Tob37, 38: Tob38.

The strain with His-tagged Tob55 is only expressing the short isoform; hence only one band can be seen in the immunodecorations. Note that only traces of Mdm10 can be copurified in all three approaches.

**Figure 6*****Tob38, Tob37 and Tob55 copurify in the presence of digitonin***

A: Schematic representation of TOB complexes with N-terminal ninefold His-tags at Tob55, Tob38 or Tob37. OM: outer mitochondrial membrane, IMS: intermembrane space

B and C: Outer mitochondrial membrane vesicles (OMVs) from N.c. strains with the His-tagged TOB-subunit, 9His-Tob55, 9His-Tob38 or 9His-Tob37, were solubilized with digitonin; proteins were isolated by Ni-NTA affinity purification and analyzed by SDS-PAGE followed by immunodecoration (B) or Coomassie blue staining (C).

Solubilized outer mitochondrial membrane vesicles (OMVs) before (S) or after (L) clarifying spin. FT: flowthrough with unbound proteins of the Ni-NTA column; E: eluate of bound proteins, 55 lg and int: Tob55-intermediate and long isoform, 55sh: Tob55-short isoform, 37: Tob37, 38: Tob38, Arrow head in "B" indicates a nonspecific interaction of a standard protein in the immunodecoration.

The strain with His-tagged Tob55 is only expressing the short isoform; hence only one band can be seen after immunodecoration. Note that only traces of Mdm10 can be copurified in all three approaches.

2.3 Composition of the TOB complex

To ascertain that no subunit of the TOB complex got lost during the isolation procedure of OMVs from mitochondria, proteins from mitochondria and OMVs were separated by blue native gel electrophoresis (BNGE). The TOB complex was detected by immunodecoration. In wild type *Neurospora* and strains bearing a His-tagged TOB subunit, the electrophoretic mobility of the TOB complex from OMVs and from mitochondria was comparable. Size differences which would indicate a loss of additional proteins were not observed (Figure 7).

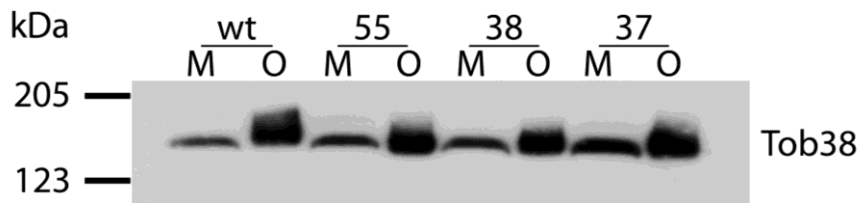


Figure 7

The TOB complex remains intact during the isolation of OMVs from mitochondria

Mitochondria (M) and outer mitochondrial membrane vesicles (O) from different N.c. strains, either wild type (wt) or strains bearing His-tagged Tob55 (55), Tob38 (38) or Tob37 (37), were solubilized with digitonin. They were then analyzed by BNGE and immunodecorated with Tob38 antiserum. Membrane protein complexes from bovine heart mitochondria were used as marker proteins.

The TOB complex is a membrane protein complex and therefore the use of membrane proteins as a standard seemed appropriate. To this end, membrane protein complexes from bovine heart mitochondria with defined molecular masses served as markers upon by BNGE analysis (140). The TOB complex of mitochondria and OMVs solubilized with digitonin was running correspondingly to an estimated molecular mass of 130-160 kDa (Figure 7). Coomassie blue staining of the TOB complex isolated by using TX-100 revealed the same electrophoretic migration behavior as when digitonin was used (Figure 8). When the TOB complex was isolated from strains expressing 9His-Tob38 and 9His-Tob37, a minor amount of the isolated protein migrated in a lower fraction. This might be due to a partial decay of the TOB complex after solubilization with the comparatively harsher detergent TX-100 (Figure 8). A small fraction of the isolated complexes seems to represent TOB complex oligomers of around 400 kDa and 1000 kDa. The preparations from OMVs bearing a His-tagged short isoform of Tob55 looked different from the former preparations. In this case, two strong bands were observed in addition to that of the TOB complex, running below the 123 kDa marker band (Figure 8).

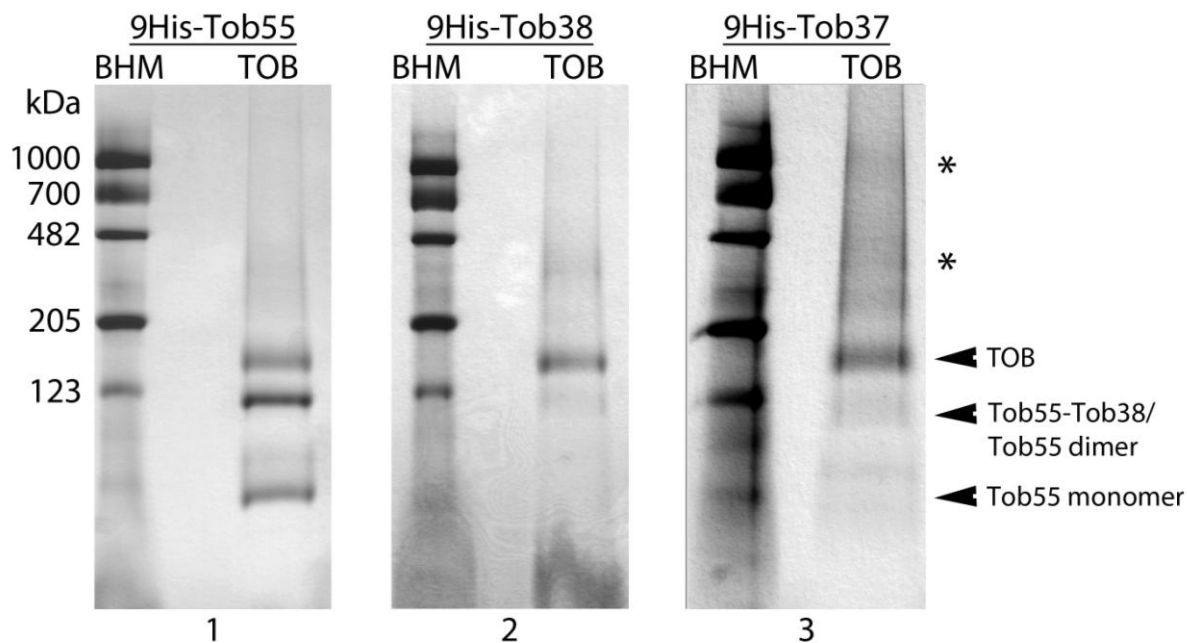


Figure 8

TOB complex purification by affinity chromatography after lysis of OMVs with TX-100

Bovine heart mitochondria (BHM) were solubilized with TX-100. The TOB complex was isolated from N.c. strains bearing His-tagged Tob55, Tob38 or Tob37 using TX-100. The samples were subjected to BN-PAGE and Coomassie blue staining. Membrane protein complexes from bovine heart mitochondria were used as markers.

Asterisks indicate possible oligomeric forms of the TOB complex.

The isolated complexes were further analyzed by immunodecoration after BN-PAGE. The dominant band of the TOB complex isolated from strains harboring 9His-Tob38 or 9His-Tob37 showed the same electrophoretic mobility as the complex from solubilized OMVs without further affinity purification (Figure 9, B and C). This form of the TOB complex contains Tob55, Tob38 and Tob37 and is therefore representing the TOB complex. Decoration with antibodies against Mdm10 identified traces of copurified Mdm10 as part of an apparent molecular mass species of around 200 kDa (Figure 9, B and C), and not as a constituent of the TOB complex. In this 200 kDa complex, Tob55, Tob38 and Tob37 were also detected. Considering the molecular weight of Mdm10 of 52.7 kDa, this complex most likely represents one Mdm10 bound to the TOB complex. It was termed TOB-Mdm10 complex.

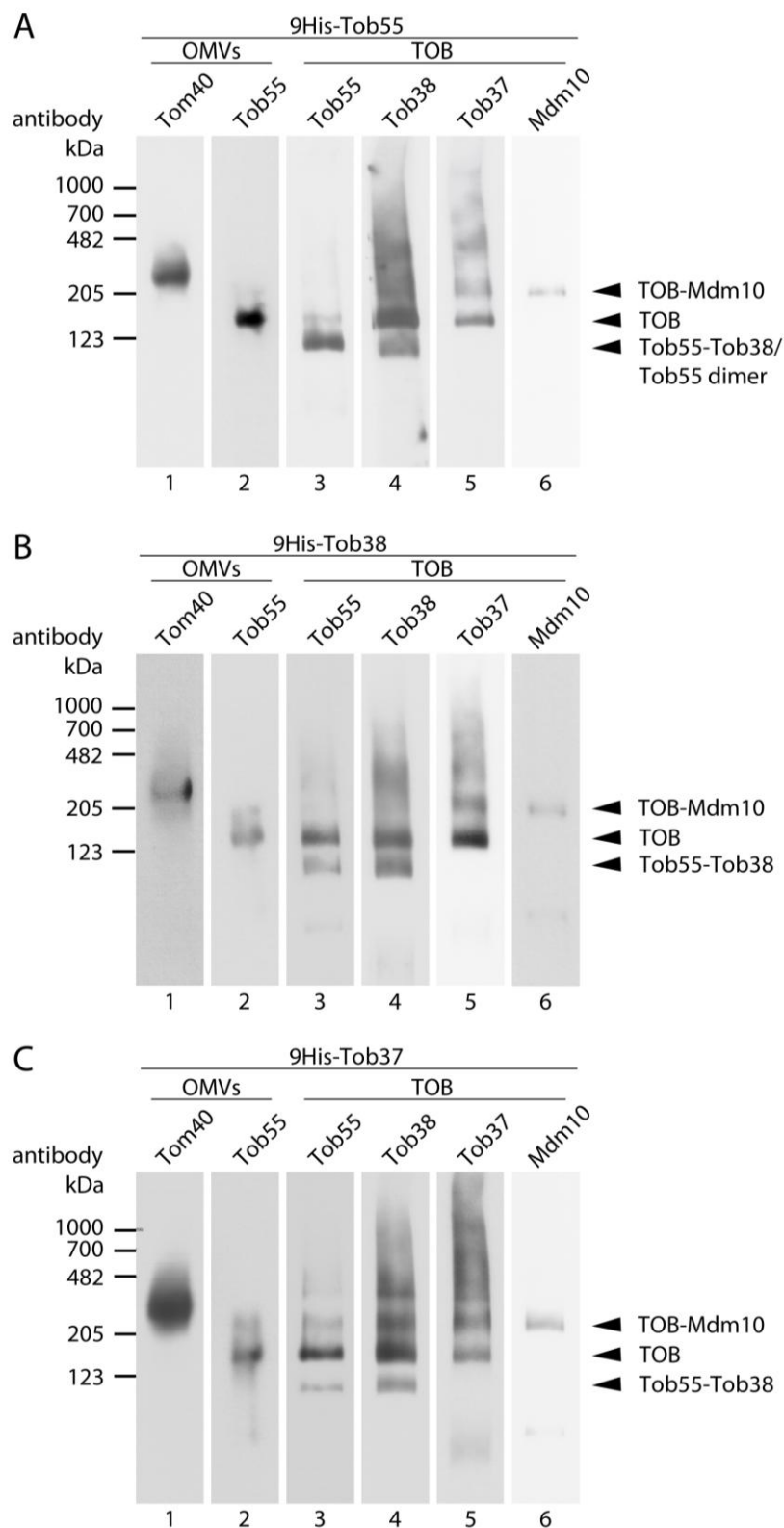


Figure 9

Tob55, Tob38 and Tob37 constitute the TOB complex isolated using TX-100 as detergent
A-C: Outer mitochondrial membrane vesicles (OMVs) and bovine heart mitochondria were solubilized with TX-100. The TOB complex was isolated from N.c. strains bearing His-tagged Tob55, Tob38 or Tob37. The samples were separated by BN-PAGE and analyzed by immunodecoration. Membrane protein complexes from bovine heart mitochondria were used as marker proteins.

The protein complex running faster than the TOB complex (apparent molecular mass around 90 kDa) contained Tob55 and Tob38 (Figure 9). Tob37 was missing and therefore seems to be a subunit which can be lost from the TOB complex during isolation. The 90 kDa complex is referred to as Tob55-Tob38 complex in the following. The Tob55-Tob38 complex makes up just a very minor species as judged by its intensity upon staining with Coomassie blue (Figure 8, panel 2 and 3).

Upon comparing immunodecorations of the TOB complex isolated with 9His-Tob55 with those in which 9His-Tob37 or 9His-Tob38 were present, most Tob55 was found at a complex running at around 100 kDa, roughly the size of Tob55-Tob38 (Figure 9A). Hence, tagging Tob55 could possibly have a destabilizing effect on the TOB complex causing a decay of the complex. Nevertheless, the amount of Tob38 was higher in the TOB complex than in the Tob55-Tob38 complex. This is inconsistent with the possibility that this 100 kDa species might have arisen from the loss of Tob37 from the TOB complex.

In addition to the preparations performed with TX-100, the TOB complex was isolated using digitonin as detergent for the solubilization of the OMVs. With strains expressing 9His-Tob38 or 9His-Tob37, the dominant TOB complex was running somewhat faster than that isolated with TX-100 (Figure 10). A second, weaker band was present above the main complex, presumably representing the TOB-Mdm10 complex. The Tob55-Tob38 complex is missing. This supports the suggestion that the complex is more prone to the loss of Tob37 when the solubilization is performed with TX-100 (Figure 10). Again, the elution pattern was very different when the complex was isolated via His-tagged Tob55 in comparison to preparations from the His9-Tob38 or His9-Tob37 strain (Figure 10, panel 1). Similar to the affinity purifications performed with TX-100, monomeric Tob55 was found in addition to the TOB and the TOB-Mdm10 complex. Moreover an enriched complex at around 100 kDa was observed.

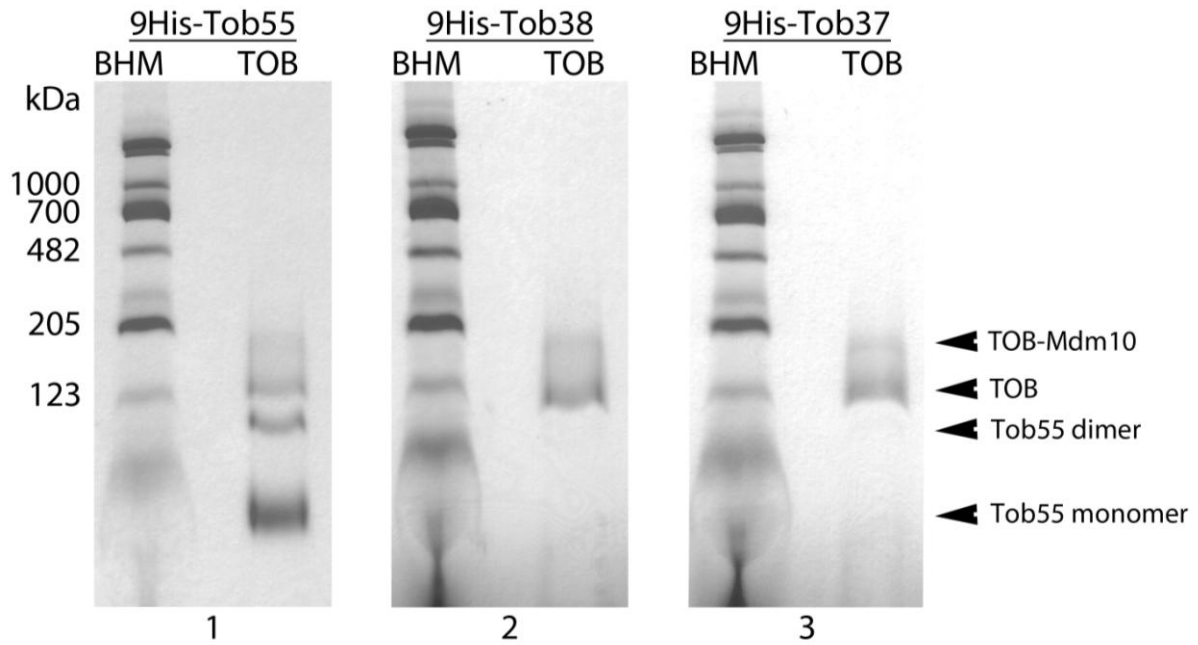
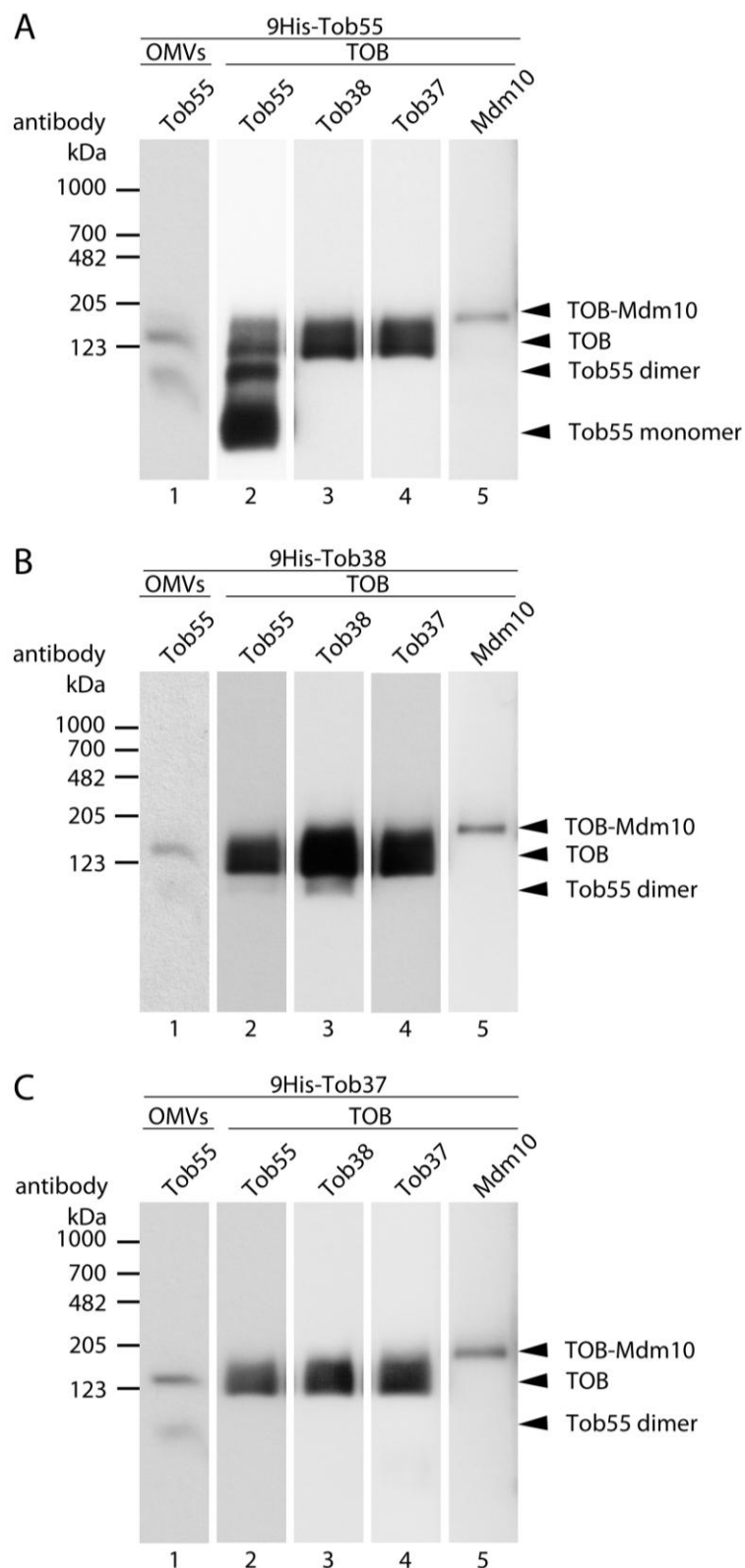


Figure 10

TOB complex purification by affinity chromatography after lysis of OMVs with digitonin

Bovine heart mitochondria (BHM) were solubilized with digitonin. The TOB complex was isolated from N.c. strains bearing His-tagged Tob55, Tob38 or Tob37 by the use of digitonin. The samples were subjected to BNGE and Coomassie blue staining. Membrane protein complexes from bovine heart mitochondria were used as markers.

**Figure 11**

Tob55, Tob38 and Tob37 constitute the TOB complex isolated using digitonin as detergent
A-C: Outer mitochondrial membrane vesicles (OMVs) and bovine heart mitochondria were solubilized with digitonin. The TOB complex was isolated from N.c. strains bearing a His-tagged Tob55, Tob38 or Tob37. The samples were separated by BNGE and analyzed by immunodecoration. Membrane protein complexes from bovine heart mitochondria were used as markers.

Results

The TOB complex isolated from OMVs solubilized with digitonin was found to be made up by the proteins Tob55, Tob38 and Tob37, only (Figure 11). No Tob55-Tob38 complex was present in the eluate. Therefore, no Tob37 is lost from the TOB complex in course of the Ni-NTA affinity purification. By the use of the strain, which expresses 9His-Tob55, an enrichment of Tob55 in a complex with an apparent molecular mass of 100 kDa was observed and in addition monomeric Tob55 (Figure 11A). This 100 kDa complex was not detected when antibodies against Tob38, Tob37 or Mdm10 were used. Therefore, Tob55 exists as a dimer. Interestingly, this Tob55 dimer was also present in solubilized OMVs from all various strains without any further isolation. This demonstrates that the Tob55 dimer is not an artefact caused in the course of the Ni-NTA purification. Mdm10 again was running in a complex with a slightly higher apparent molecular mass than the TOB complex. Thereby it most likely represents the TOB-Mdm10 complex. Taken together, the use of digitonin and TX-100 for the solubilization of OMVs resulted in the isolation of complexes of very similar composition. The only species which was only present in preparations using TX-100 was the Tob55-Tob38 complex. However, only very minor amounts of this complex were found. Therefore, both detergents are suitable for the purification of the TOB complex.

Antibody supershift assays were performed to further analyze the diverse complexes observed by BNGE after preparation of the TOB complex by affinity purification. To this end, OMVs differing in the His-tagged TOB complex subunit were solubilized with digitonin. Subsequently, penta-His antibody was added and BNGE was performed. Tob38, Tob37 and Tob55 were present in the TOB complex as well as in the far less abundant TOB-Mdm10 complex running directly above the TOB complex at around 200 kDa. Both complexes could be shifted with the penta-his antibody directed against Tob55, Tob38 or Tob37 (Figure 12). Tob55 was further detected in a second abundant complex of around 100 kDa. This band could only be shifted when the His-tag was attached to the Tob55, but not with His-tagged Tob38 and Tob37 (Figure 12). Decoration with Tob38 and Tob37 antibody showed the absence of these proteins in the 100 kDa complex. The 100 kDa complex was not the result of a decay of the TOB complex due to the modification of Tob55 by the attachment of the His-tag, since it was also present in the His9-Tob38 and His9-Tob37 strains and even in the wild type strain (Figure 12A). In addition, a control with penta-his antibody alone excluded an unspecific interaction with the Tob55 antibody during immunodecoration. When affinity purification experiments were performed with His-tagged Tob55 and digitonin, only traces of porin and Mdm10 could be found in addition to the subunits Tob55, Tob38 and Tob37

(Figure 6B). Mdm10 and porin, as well as Tom40 are β -barrels themselves. Therefore, they are substrates of the TOB complex. The distribution of these proteins was determined by immunodecoration following BNAGE and Western blotting. An interaction of porin or Tom40 with the TOB complex was not detected in the antibody supershift assays (Figure 12, D and F). Mdm10 was not detected together with Tob55 in the complex of around 100 kDa, but it was present in the complex of 200 kDa which could be shifted with His-tagged Tob55, Tob38 or Tob37 (Figure 12B).

The 100 kDa complex most likely represents a Tob55 dimer, since none of the co-isolated proteins was found to be part of it.

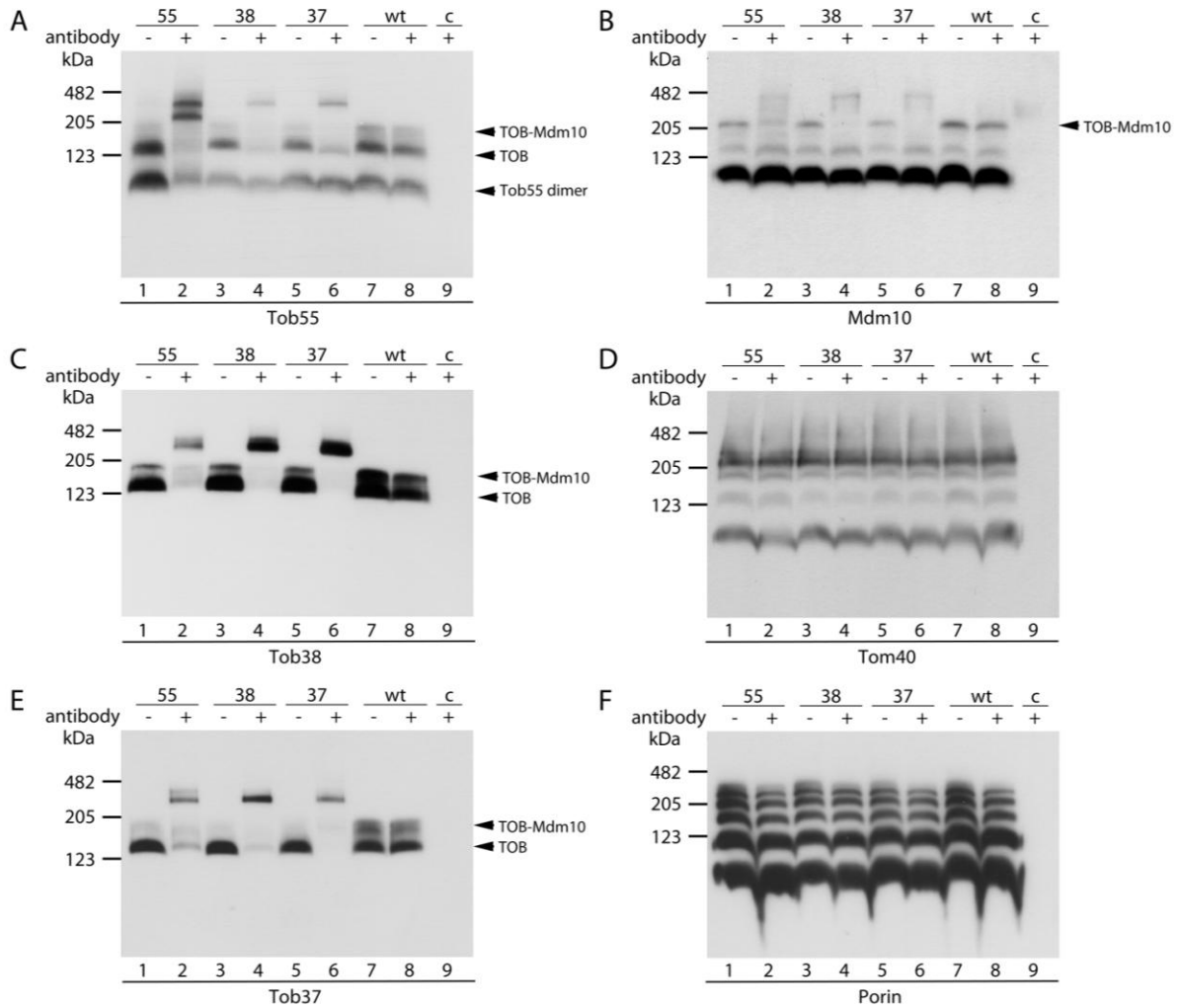


Figure 12

Tob55 is not only present in the TOB complex but in addition forms a dimer and Mdm10 is present in a 200 kDa complex.

A-F: Outer mitochondrial membrane vesicles from different N.c. strains, either wild type (wt) or strains bearing a His-tagged Tob55 (55), Tob38 (38), or Tob37 (37), were solubilized with digitonin. Where indicated, monoclonal His-antibody was added to the solubilized proteins or loaded as controls (c) before the samples were separated by BNGE. Immunodecoration was performed with antibodies as indicated. Membrane protein complexes from bovine heart mitochondria were used as markers.

When TX-100 was used only a very faint band representing a putative Tob55 dimer was observed (Figure 13A). This is in contrast to the result of solubilisation of the OMVs with digitonin (Figure 12A). Nonetheless, upon isolation of the TOB complex with His-tagged Tob55 using TX-100, a substantial amount of the very same band at around 100 kDa was present in the eluate (Figure 8, Figure 9A). This finding is comparable to preparations performed with digitonin (Figure 10, Figure 11A). The unexpected appearance of the Tob55 dimer in the eluate of TOB complex preparations performed with TX-100 suggests that TX-100 leads to disintegration of the Tob55 dimers. Ni-NTA affinity isolation of the TOB complex includes loading of solubilized OMVs in presence of high detergent concentrations. Upon elution the detergent concentration is reduced. Therefore, isolated Tob55 monomers might reform dimers upon decrease of the detergent concentration or when their concentration is increased.

The origin of the Tob55 dimers was to be analyzed in more detail. To this end, affinity purification was performed with a strain expressing the short isoform of Tob55 with a ninefold His-tag as well as the intermediate Tob55 isoform bearing a Flag-tag. Pulldowns directed against one or the other tag only eluted one kind of tag. This indicates that Tob55 is not present in dimers under the given conditions (Figure 14). However, with this result one can only exclude the presence of Tob55 dimers formed by the short and intermediate Tob55 isoform. Tob55 dimers constituted by different Tob55 isoform combinations might still exist. Monomeric Tob55 was found in addition to Tob55 dimers preparations performed with TX-100 as well as with digitonin (Figure 8, Figure 10). It remains to be elucidated where these Tob55 monomers originated from. In case of a decay of the TOB complex, there should also be an equivalent amount of monomeric Tob38 and Tob37 which should also be enriched when the TOB isolation is performed with 9His-Tob38 or 9His-Tob37. Such an enrichment of Tob38 and Tob37 in the eluate was not observed (Figure 5, Figure 6). In conclusion, the enriched Tob55 originates from an excess of Tob55 over Tob38 and Tob37 in mitochondria rather than from a decay of the TOB complex.

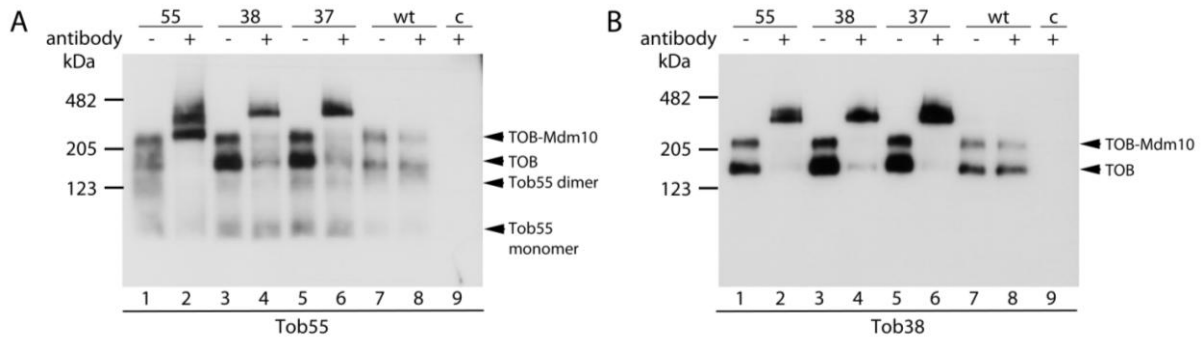


Figure 13

Analysis of the isolated TOB complex by Blue native shift experiments

Outer mitochondrial membrane vesicles from different N.c. strains, either wild type (wt) or strains bearing His-tagged Tob55 (55), Tob38 (38), or Tob37 (37), were solubilized with TX-100. Where indicated, His-antibody was added to the solubilized proteins or loaded alone as a control (c). Samples were then analyzed by BNGE. Immunodecoration was performed with diverse antibodies as indicated.

Membrane protein complexes from bovine heart mitochondria were used as marker proteins.

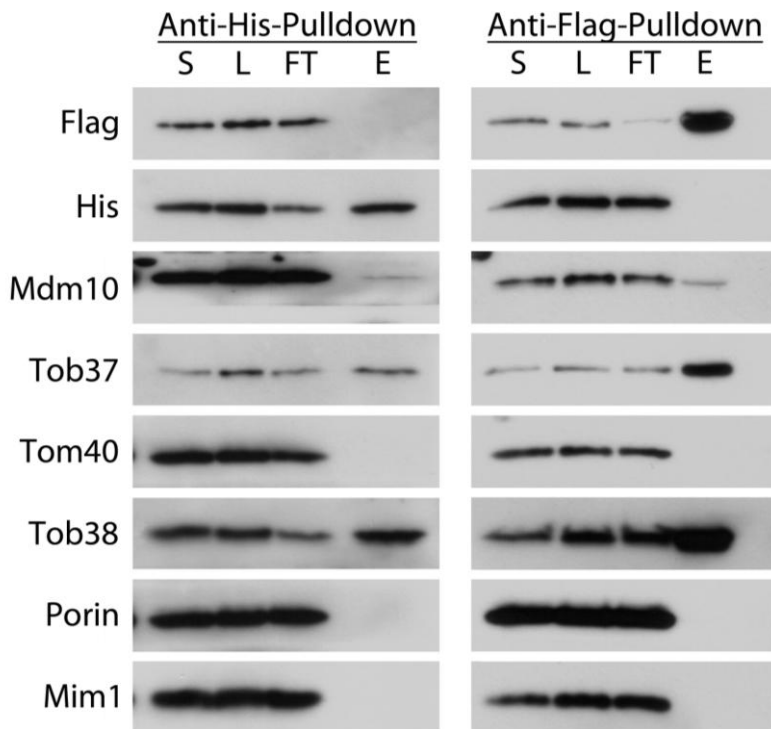


Figure 14

The TOB complex contains only one Tob55 subunit

Outer mitochondrial membrane vesicles bearing a His-tagged short isoform and a Flag-tagged intermediate isoform of Tob55 were solubilized with TX-100. Proteins were isolated by Ni-NTA or anti-Flag-tag affinity purification and analyzed by SDS-PAGE followed by immunodecoration.

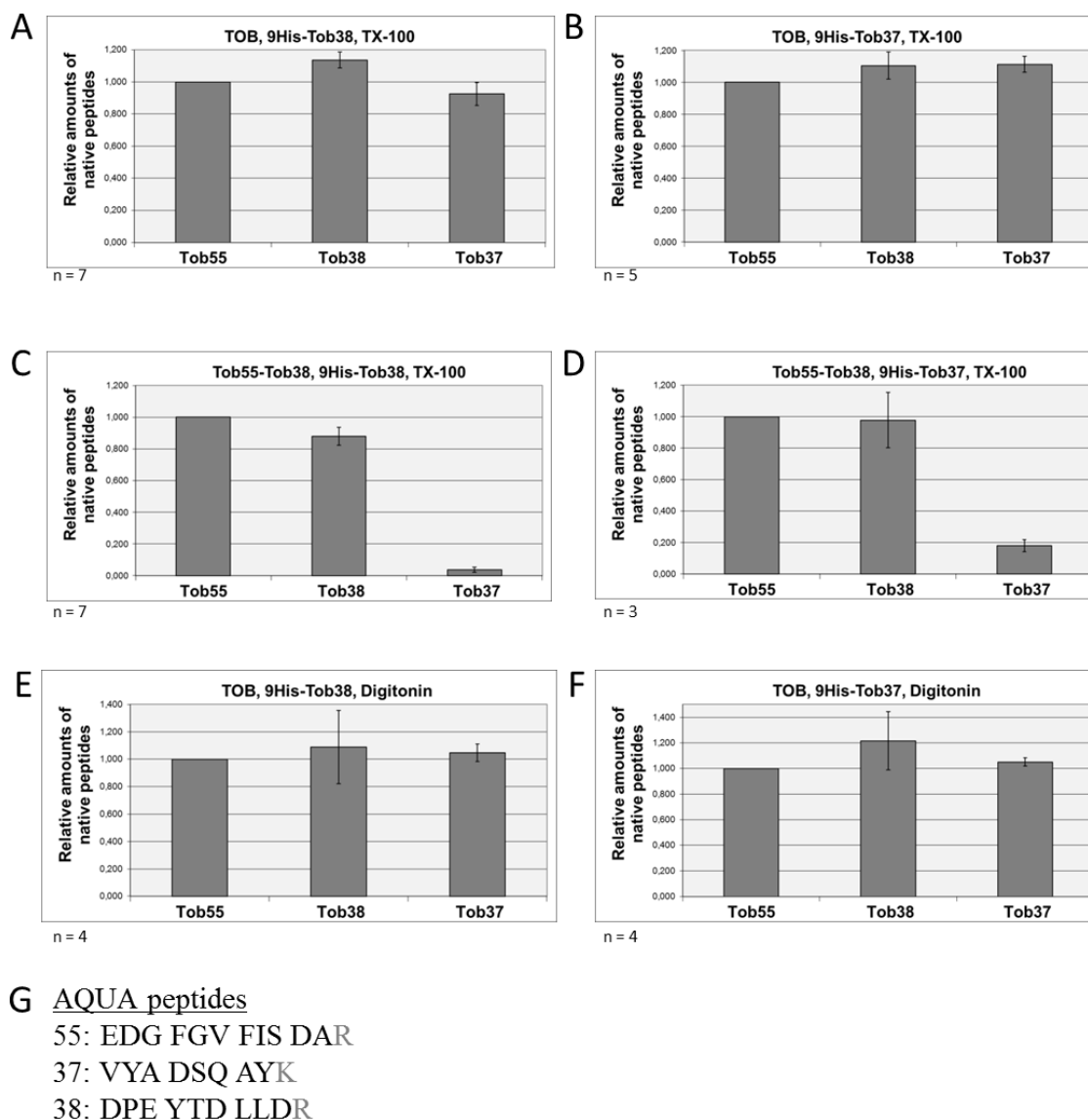
OMVs before (S) or after (L) clarifying spin. FT: flowthrough with unbound proteins of the Ni-NTA column; E: eluate of bound proteins

The antibody supershift assays demonstrated the presence of Mdm10 in a complex of around 200 kDa together with Tob55, Tob38 and Tob37. This 200 kDa complex therefore reflects the association of Mdm10 with the TOB complex. Since porin and Tom40 were not observed to bind to the TOB complex, unspecific co-purification of β -barrel precursor proteins can be excluded.

Taken together, Tob55, Tob38 and Tob37 exclusively constitute the TOB complex with an estimated molecular mass of ca 150 kDa. Mdm10 is not part of the TOB complex. Very small amounts of Mdm10 are recovered with Tob55, Tob38 and Tob37 in a complex of around 200 kDa, forming the TOB-Mdm10 complex. Furthermore, a substantial amount of Tob55 in the outer mitochondrial membrane occurs in a form that is not associated with Tob38 and Tob37.

2.4 Tob55, Tob38 and Tob37 are present in the TOB complex in a 1:1:1 stoichiometry

In order to further analyze the structure of the TOB complex it was necessary to determine the stoichiometry of the three different subunits. This could not be achieved by determination of the molecular mass of the complex since reliable methods for measuring the precise molecular mass of membrane inserted complexes do not exist. Therefore, quantitative mass spectrometry was employed to determine the stoichiometry of the subunits Tob55, Tob38 and Tob37 in the TOB complex. TOB complexes were excised from gels after BNGE (Figure 8, Figure 10). They were analyzed by isotope diluted mass spectrometry (IDMS) with quantified stable isotope ($^{13}\text{C}/^{15}\text{N}$) labeled internal peptide standards of all three subunits (Figure 15G; see also: Material and Methods, 6.1.7, “Peptides”). Figure 15 depicts representative measurements of technical replicates of the different isolated complexes to illustrate the reproducibility of the quantification by IDMS. A total of six biological replicates of the TOB complex, and four biological replicates of the Tob55-Tob38 complex, isolated using TX-100 or digitonin, from both strains, His9-Tob38 and His9-Tob37, were analyzed. The various analyses yielded the same results, as described in the following: TOB complexes isolated via 9His-Tob38 or 9His-Tob37, with either TX-100 or digitonin, had a 1:1:1 ratio between the subunits Tob55, Tob38 and Tob37 (Figure 15). Therefore, the slight difference in the electrophoretic mobility between the TOB complex isolated with TX-100 and digitonin (Figure 8, Figure 10) was caused by the use of the different detergents but not by different stoichiometries of the subunits of the complex. The absence of Tob37 in the Tob55-Tob38 complex, found in preparations performed with TX-100, could be confirmed by the IDMS measurements, resulting in a 1:1:0 ratio (Figure 15, C and D). Moreover, protein identification by LC-MS/MS could not detect any other proteins than Tob55, Tob38 and Tob37 in the TOB or Tob55-Tob38 complex. A 1:1:1 ratio of Tob55, Tob38 and Tob37 monomers results in a molecular weight of about 140 kDa. This is in accordance with the electrophoretic mobility of the complex in relation to the protein complexes from bovine heart mitochondria that served as standards (Figure 7 - Figure 13). Thus it is concluded that one Tob55 protein assembles with one Tob38 and Tob37 molecule each.

**Figure 15*****Tob55, Tob38 and Tob37 are present in the TOB complex in a 1:1:1 stoichiometry***

A, C and E: TOB complex was isolated from N.c. strains bearing a His-tagged Tob38 using TX-100 (A and C) or digitonin (E). It was subjected to BNGE and cut out after Coomassie blue staining of the native gel. The complexes were analyzed by IDMS. By comparing the two peak areas of the heavy and light peptides, the amount of each TOB complex subunit could be determined. The relative amounts of the native peptides and thereby the native proteins are depicted; Tob55 was set to 1. Representative experiments for each measured protein complex are shown. The error bars depict the standard deviation of the measurements of several diverse samples (n) originating from the very same isolated complex and illustrate the reproducibility of the quantification by IDMS.

B, D and F: Same as in “A”, “C” and “E” with N.c. strains bearing a His-tagged Tob37. TX-100 (B and D) or digitonin (F), was used for solubilization.

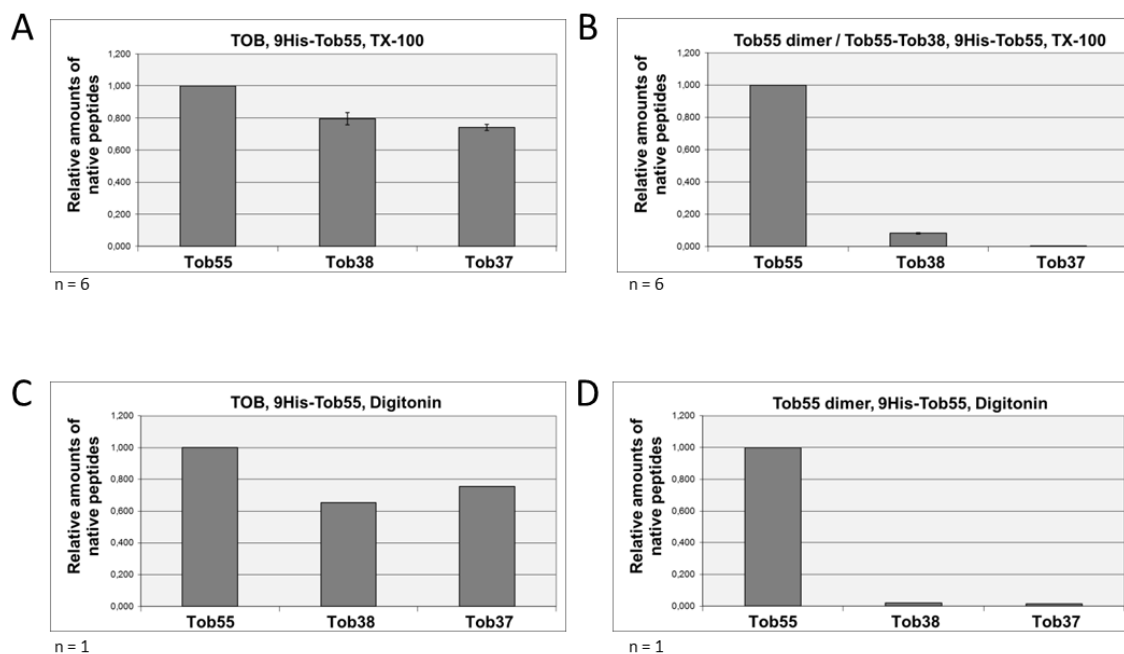
G: Quantified stable isotope ($^{13}\text{C}/^{15}\text{N}$) labeled internal peptide standards, AQUA (AbsoluteQUAntification) peptides, for the proteins Tob55 (55), Tob38 (38) and Tob37 (37) are shown; the amino acid substituted with a stable isotopic amino acid is written in gray.

Results

IDMS was also performed with the other complexes present as higher apparent molecular mass species in the BNGE than the TOB complex (Figure 8, Figure 10). However, due to the tailing of the protein bands in the upper part of the gels reproducible and therefore reliable results could not be obtained.

In addition, the TOB complex which was isolated by affinity purification using His-tagged Tob55 was mass-spectrometrically analyzed. The TOB complex was determined to have a 1:1:1 stoichiometry. Due to the high amounts of Tob55 in the isolate and the tailing of Tob55 in many replicates, the relative amounts of Tob55 were slightly higher (Figure 16, A and C). The presence of more than one Tob55 in the TOB complex isolated with His-tagged Tob55 can be excluded, since this complex has the very same running behavior as the complexes isolated via a His-tagged Tob37 or Tob38. Furthermore, the TOB complex did not show an increased Tob55 upon immunodecoration with Tob55 antiserum (Figure 9, A-C, Figure 11, A-C). The majority of Tob55 was detected in the complexes with an apparent molecular mass of ca. 100 kDa (Figure 16, B and D). Only traces of Tob38 were found in this band when TX-100 was used for the TOB complex preparation (Figure 16B). The excess of Tob55 over Tob38 in preparations of the TOB complex obtained with TX-100 indicates that Tob55 dimers apparently overlay smaller amounts of the Tob55-Tob38 complex in the native gel. When digitonin was used, no Tob55-Tob38 complex was observed and accordingly no Tob38 was detected in the 100 kDa band. The distinct bands on the BN-gels with an apparent molecular mass of ca. 60 kDa (Figure 8, Figure 10) were identified as Tob55 monomers, since only Tob55 was detected.

In summary, these studies support our findings that there is a large amount of Tob55 which is not associated with Tob38 and Tob37.

**Figure 16*****Dimer-formation of Tob55***

A and B: TOB complex was isolated from N.c. strains bearing a His-tagged Tob55 using TX-100 and was subjected to BNGE and then cut out after Coomassie blue staining of the native gel. The complexes were analyzed by IDMS. By comparing the two peak areas of the heavy and light peptides, the amount of each TOB complex subunit could be determined. The relative amounts of the native peptides and thereby the native proteins are depicted; Tob55 was set to 1. Representative experiments for each protein complex analyzed are shown. The error bars depict the standard deviation of the measurements of diverse samples originating from the very same isolated complex and illustrate the reproducibility of the quantification by IDMS.

C and D: Same as in “A” and “B”, but solubilization was performed with digitonin.

2.5 Reconstruction of the isolated TOB complex by cryo-electron microscopy

In order to obtain further insights into the structure of the TOB complex cryo-electron microscopy (cryo-EM) analysis was performed. This analysis was carried out by single particle analysis in collaboration with Dennis Thomas (Baumeister group, MPI Martinsried, GER). A 2D structure prediction of Tob55 was made since no crystal structure of a TOB complex subunit was available. The Research Collaboratory for Structural Bioinformatics Protein Data Bank (RCSB PDB) was searched for known structures with sequence homology and similar predicted secondary structure. The secondary structure prediction for Tob55 showed remarkable similarity to the known structure of the FhaC β -barrel protein. Tob55 was suggested to have 16 β -strands that form a transmembrane β -barrel like FhaC and an N-terminal region harbouring one POTRA domain, whereas FhaC has two.

Using MODELLER, a 3D model for Tob55 was constructed by essentially mapping the predicted Tob55 secondary structure onto the FhaC 3D structure (PDB I.D. 2QDZ) (121). The resulting model follows the 2D structure prediction well. The β -strands are connected by short turns or longer loops sticking out on both sides of the membrane (Figure 17A). Two long defined loops (red and blue loops) are present at the cytoplasmic side in the model predicted for Tob55 (Figure 17, Figure 18, Figure 19). Superposition of both protein structures revealed that these two loops, comprising amino acid residues 267 to 291 (blue loop) and amino acid residues 412 to 439 (red loop) of Tob55 correspond to loop 5 (L5) and loop 8 (L8), respectively, in the FhaC structure (Figure 18, Figure 19). The loops at the cytoplasmic face of the predicted Tob55 β -barrel structure are longer and more exposed than those of FhaC. However, the blue loop of FhaC in fact must be longer in reality since the published structure lacks amino acid residues 384 to 398 (Figure 19A, red boxed residues in loop 5) (121). Therefore, this loop might show higher similarity to the corresponding loop in the Tob55 structure. Another significant feature in the FhaC structure is a large loop between the extra-cellular ends of strands 11 and 12. This loop is folded back into the lumen of the barrel (L6, green loop) joining an N-terminal α -helix (pink helix) to occlude the β -barrel (Figure 17, Figure 18, Figure 19). The sequence corresponding to the N-terminal α -helix of FhaC was missing in the predicted structure of Tob55 (Figure 17A). However, a long loop stretching through the interior of the β -barrel was predicted between the Tob55 strands 11 and 12, containing amino acids 318 to 376 (green loop) (Figure 17, Figure 18, Figure 19). At the tip of the loop the VRGY/F tetrad was localized (Figure 19B, grey framing). The VRGY/F tetrad

is a highly conserved motif among members of the Omp85-TpsB transporter superfamily, including FhaC. In FhaC, it is also found at the tip of the loop which is spanning the interior of β -barrel (141) (Figure 19A, grey framing). Additionally, sequence analysis of other members of this transporter superfamily suggests that this motif is always positioned in a predicted loop between two β -strands close to the C-terminus. The localization of the VRGY/F tetrad in our predicted Tob55 structure is therefore consistent with data from other family members. Taken together, structural prediction analysis suggests a high degree of similarity between FhaC and Tob55 and results in a reasonable 3D model of Tob55.

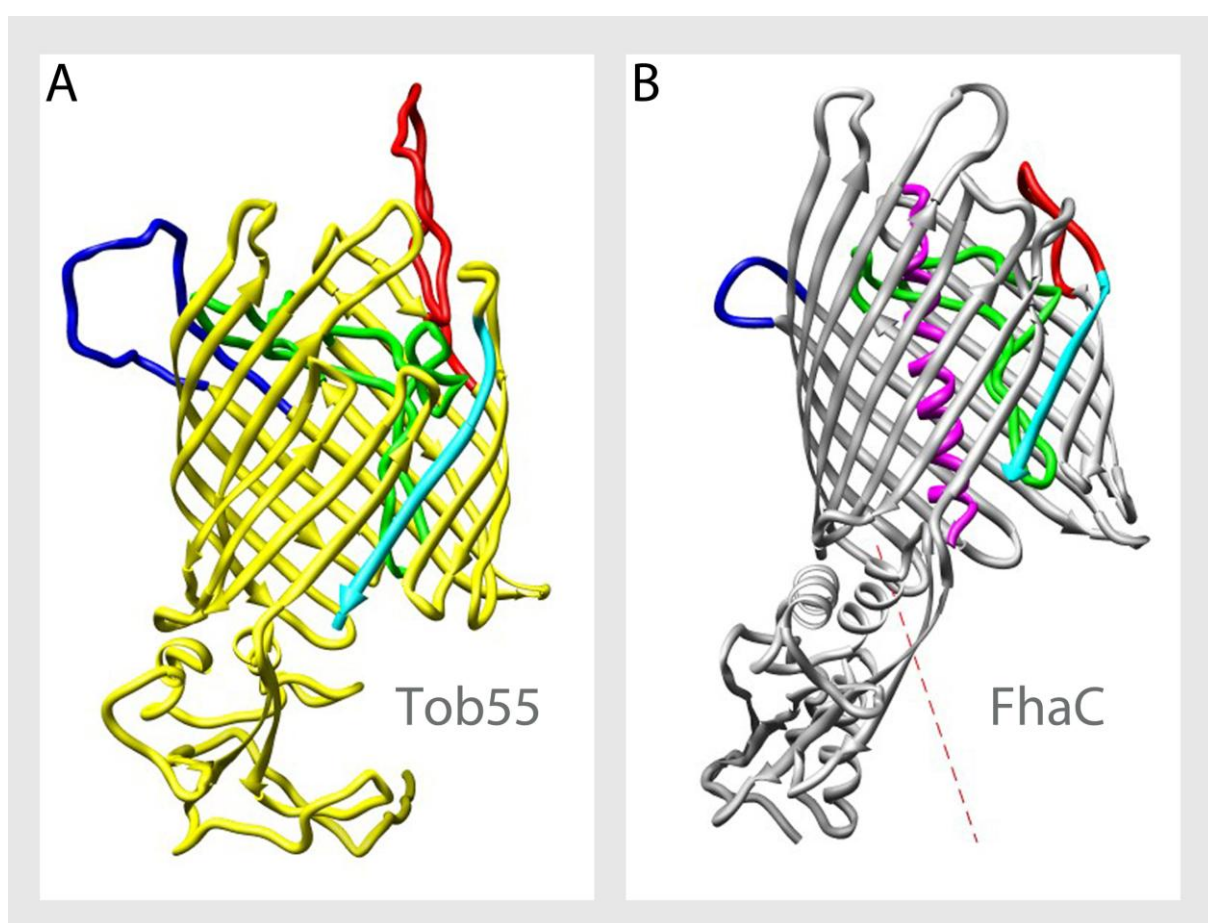


Figure 17

Modelling of the 3D structure of Tob55 suggests high similarity to the structure of FhaC

A: Ribbon representation of the predicted structure of Tob55

B: Ribbon representation of the crystal structure of FhaC

The view corresponds to the one of Tob55 in “A”. The amino acid stretch between helix 1 and the first POTRA domain had no well-defined electron density and is therefore shown as a dashed line.

The red and blue loops are located at similar sites in both structures. The C-terminus of both proteins is colored in light blue. The loops spanning the interior of the β -barrels are depicted in green. The N-terminal helix in the interior of the FhaC β -barrel is shown in pink.

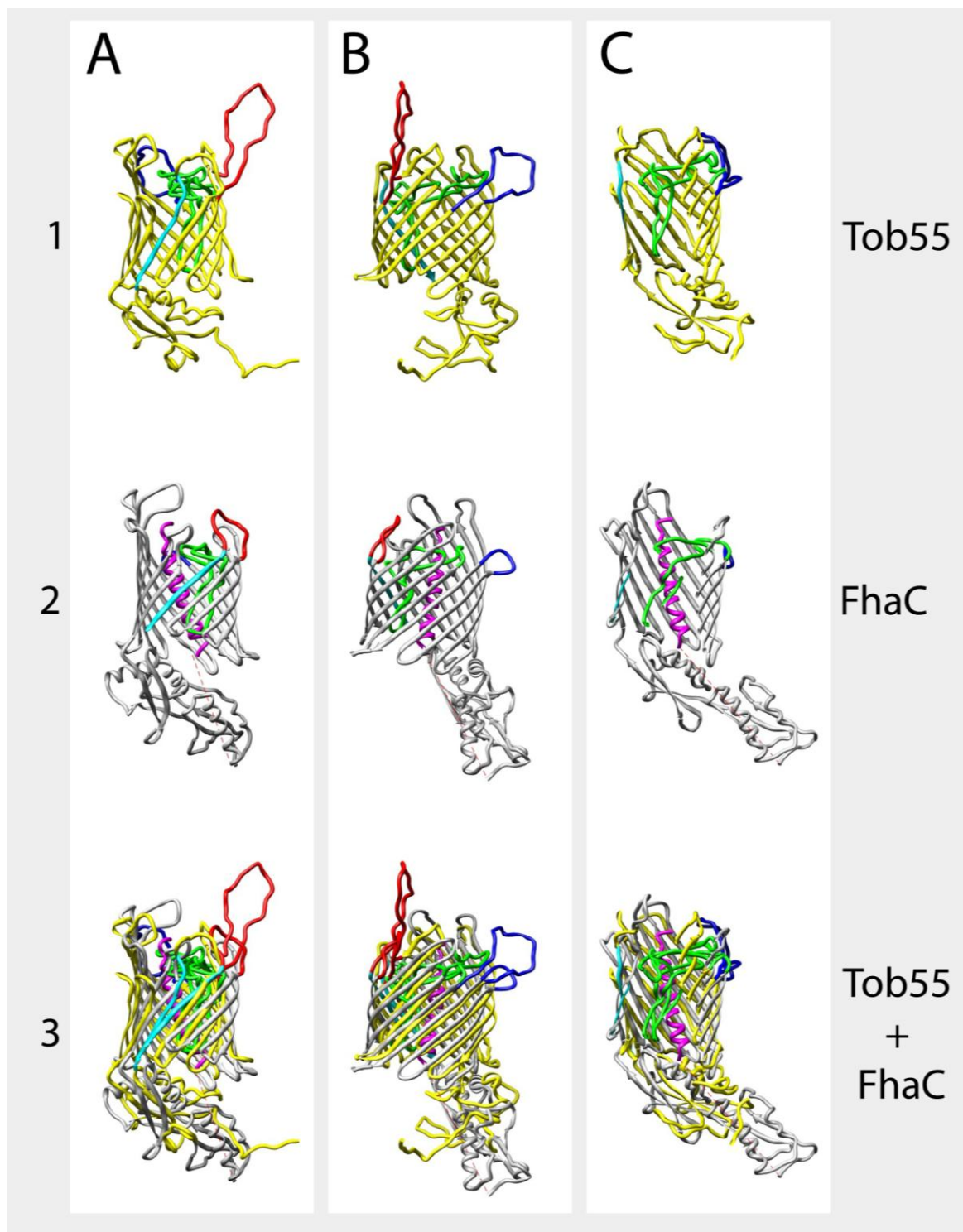


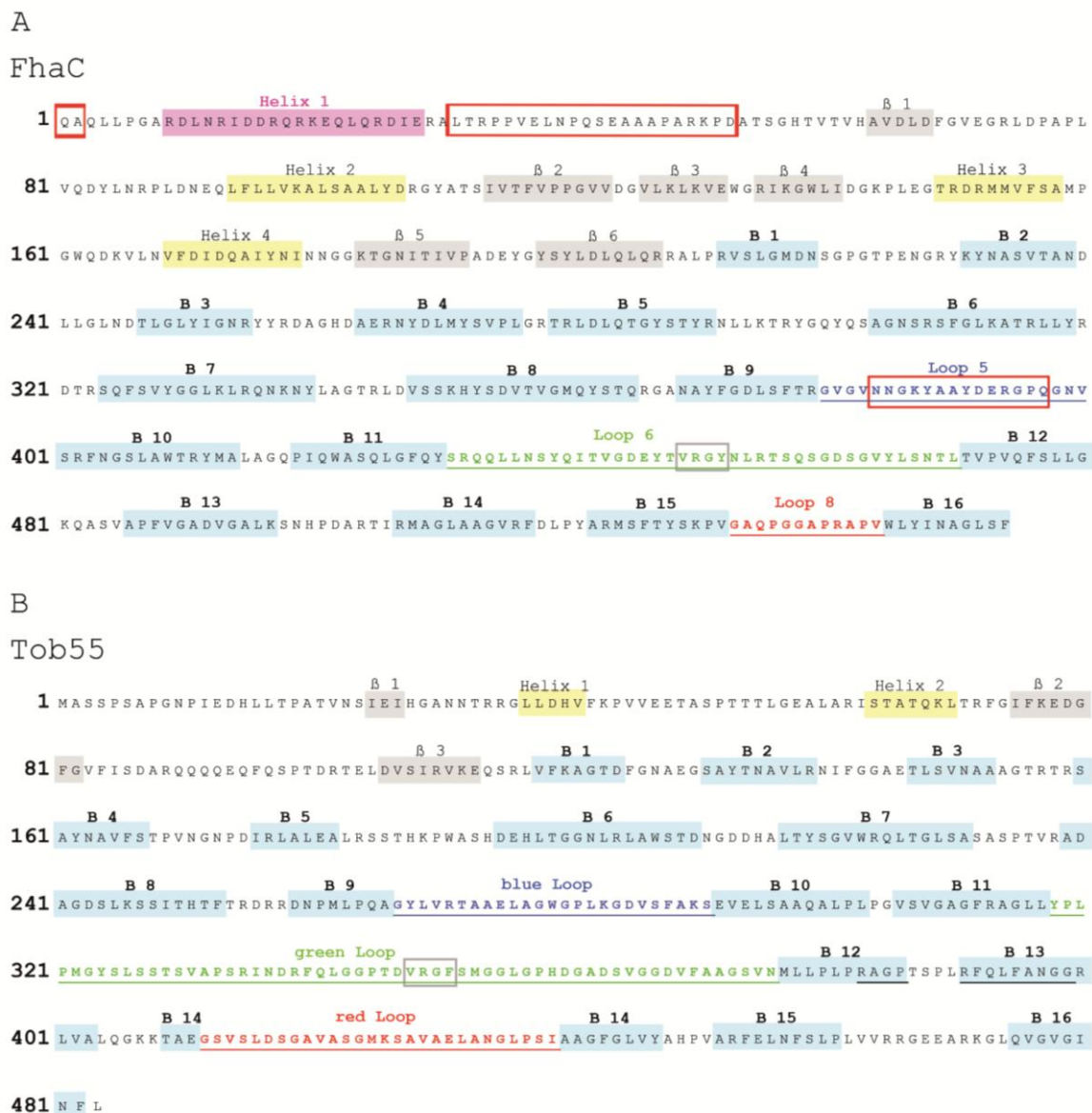
Figure 18

Superposition of Tob55 and FhaC illustrates corresponding elements in the architecture of both transporters

A and B: Ribbon representation of two corresponding views of the predicted structure of Tob55 (row 1, yellow) and the crystal structure of FhaC (row 2, grey) are illustrated. Row 3 depicts an overlay of both structures.

C: Insight into cutaway views of Tob55 and FhaC is given.

The red and blue loops are located on similar sites in both structures. The C-terminus of both proteins is colored in light blue. The loops spanning the interior of the β -barrels are depicted in green. The N-terminal helix in the interior of the FhaC β -barrel is shown in pink.

**Figure 19****Analysis of the secondary structural elements of FhaC and Tob55**

A: Secondary structural elements of the FhaC structure

Helices and β -strands of the POTRA domains are presented in yellow and grey, respectively. β -strands which are forming the β -barrel are coloured in light blue. The FhaC model does not include the first two N-terminal residues, the loop after helix 1 as well as the residues 384 – 398 of loop 5 (red framing). The VRGY/F tetrad in the green loop is framed in grey.

B: The predicted structure of the short isoform of Tob55 is illustrated in the same way as in “A”. Amino acid residues which were not part of β -strands in the 2D structure prediction of Tob55 but turned out to contribute to the β -strands in the 3D modelling are underlined.

Results

TOB complexes bearing a His-tag either at the Tob37 or Tob38 subunit were placed on grids with a “lacey” carbon film. Lacey meaning the surface is mostly irregular holes in the film. The samples form a thin layer of liquid in the holes during blotting. These complexes are more homogenous than those isolated using His-tagged Tob55, as described earlier (chapter: 2.3, Figure 8, Figure 10).

Images of TOB complexes in vitreous ice were obtained (Figure 20). Particles visible in the images were boxed from the images in an automated manner.

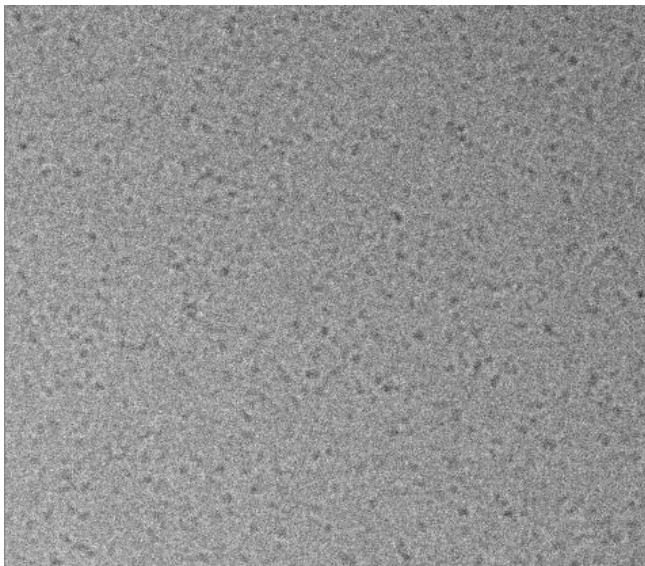


Figure 20

A typical micrograph of TOB complex particles obtained by cryo-electron microscopy
A micrograph of vitrified TOB complex, imaged at 20-25 e⁻ per Å, -2.2 μm ΔF is depicted.

Since there were no models available to begin alignment and reconstruction with, the first step of the image analysis was to perform a reference free alignment on the particles. Reference free alignment potentially can produce classified images representing closely related views of the particle whose orientations can be determined. At best, these views might be used to generate a starting model. At a minimum, it gives some insight into the basic architecture of the particle and non-particle images, such as carbon edges, can be identified (Figure 21C). Reference free alignment averages were determined from three different subsets of particle images collected in one session from one grid with TOB complex prepared from the His9-Tob37 *N. crassa* strain (Figure 21A). These averages are essentially the same although they appear shifted and rotated relative to one another. This shift and rotation is a result of each set of images starting from a different randomly determined starting point. These averages have one prominent globular protein mass.

After classification of reference free aligned particle images, the individual class averages show one or two additional masses occurring in different positions relative to the main mass (Figure 21, B and C). These appear much like different projections of a three dimensional complex containing three subunits. None of these class averages appear symmetric nor do they have a visible channel.

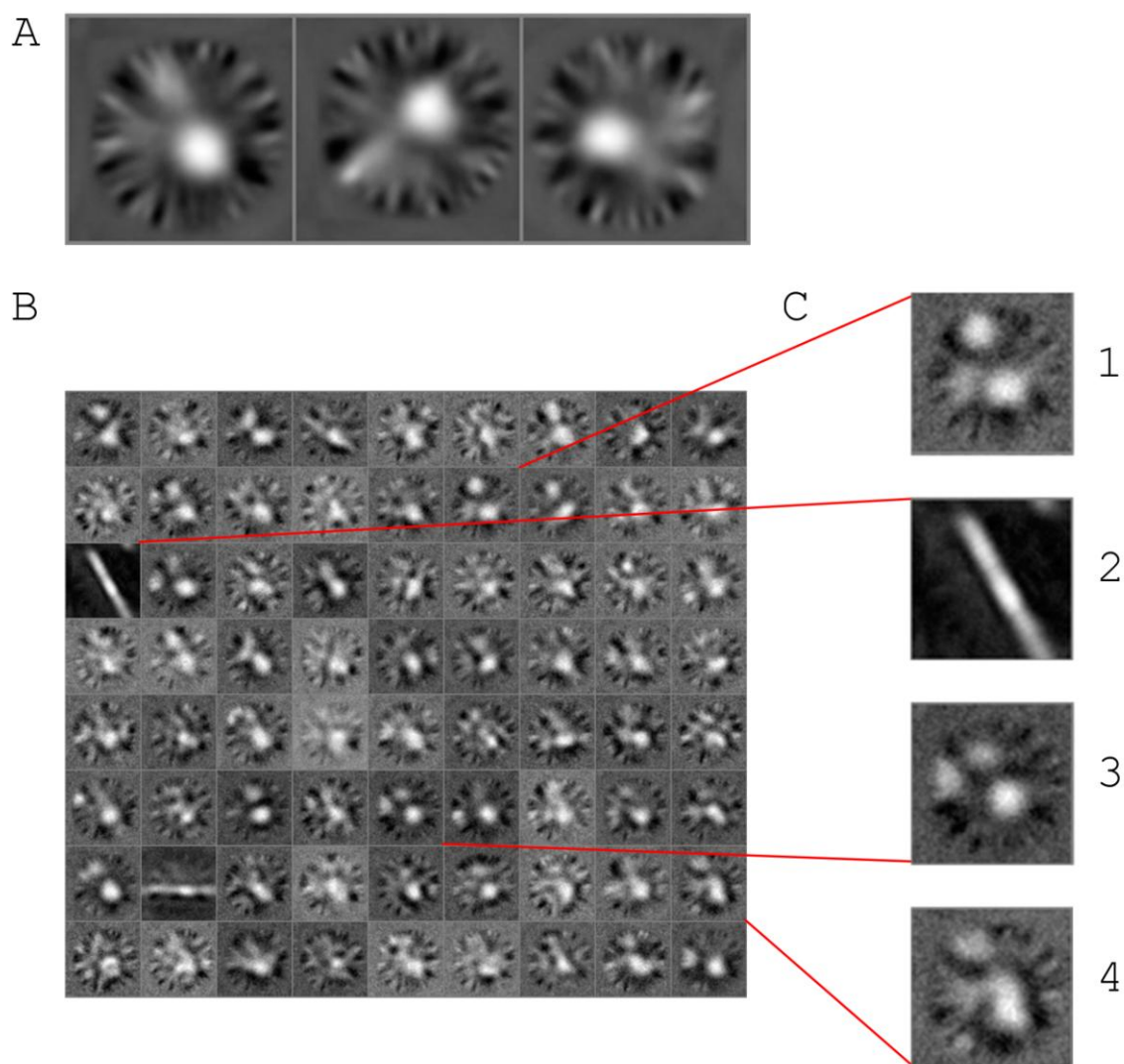


Figure 21

Reference free alignment of single particle images suggests that the TOB complex comprises three subunits

A: Particle images of the TOB complex collected in one session from one grid were divided into three subsets and subjected to reference free alignment.

B: Classification of reference free aligned particle images

C: Class averages out of “B” are enlarged. Images 1, 3 and 4 depict class averages of TOB complex particles; image 2 illustrates a class average of non-particle images, such as carbon edges.

Results

A 3D model could not be obtained from the class averages of the reference free alignment. Therefore, a starting model needed to be generated to be able to begin alignment and reconstruction of the complexes. Since the reference free alignment classes strongly suggested that there were three discrete domains or subunits, a reference with three subunits was an obvious starting point. The reference was centered on a density map calculated from the Tob55 model. Two subunits were expected to be found on the cytoplasmic surface of Tob55. Thus it seemed reasonable to place two spheres in the model that are associated with Tob55. However, there was no information to guide the placement of such spheres. Therefore, to avoid any bias in the reconstruction by a defined prepositioning of spheres for the subunits Tob38 and Tob37, an amorphous ring was placed above the cytoplasmic face of the Tob55 β -barrel.

With successive rounds of reconstruction, the ring shape converted into two defined spherical structures that are facing each other, presumably presenting the subunits Tob38 and Tob37 (Figure 22). The bulky central part of the structure retained the original overall appearance of the model of the β -barrel protein Tob55. However, after the formation of the two peripheral subunits and a progressing improvement of the reconstruction, conformational flexibility in the structure started to increasingly influence the alignment, thereby blurring the structure again (Figure 22, compare 5 and 6). A maximum-likelihood-analysis might be a good approach in the future for the separation of complexes with slight internal conformational differences.

In addition, the reconstruction is limited by the small molecular mass of the TOB complex. The analysis of the TOB complex in this study revealed that the complex has an apparent molecular mass of 140 kDa, which is much smaller than expected from previous results. The small size of the protein complex presents severe difficulties in the cryo-EM analysis due to a low signal-to-noise ratio in the image. The low signal-to-noise ratio is reflected in the minimal difference between cross-correlation intensities resulting from images of the TOB complex and those calculated from images of buffer background aligned against the same reference data projections (Figure 23). The cross correlations of data containing images are consistently above the background but by a much smaller margin than might be expected for larger complexes. This low signal-to-noise ratio results in errors in alignment and therefore errors in assignment of correct angles to images.

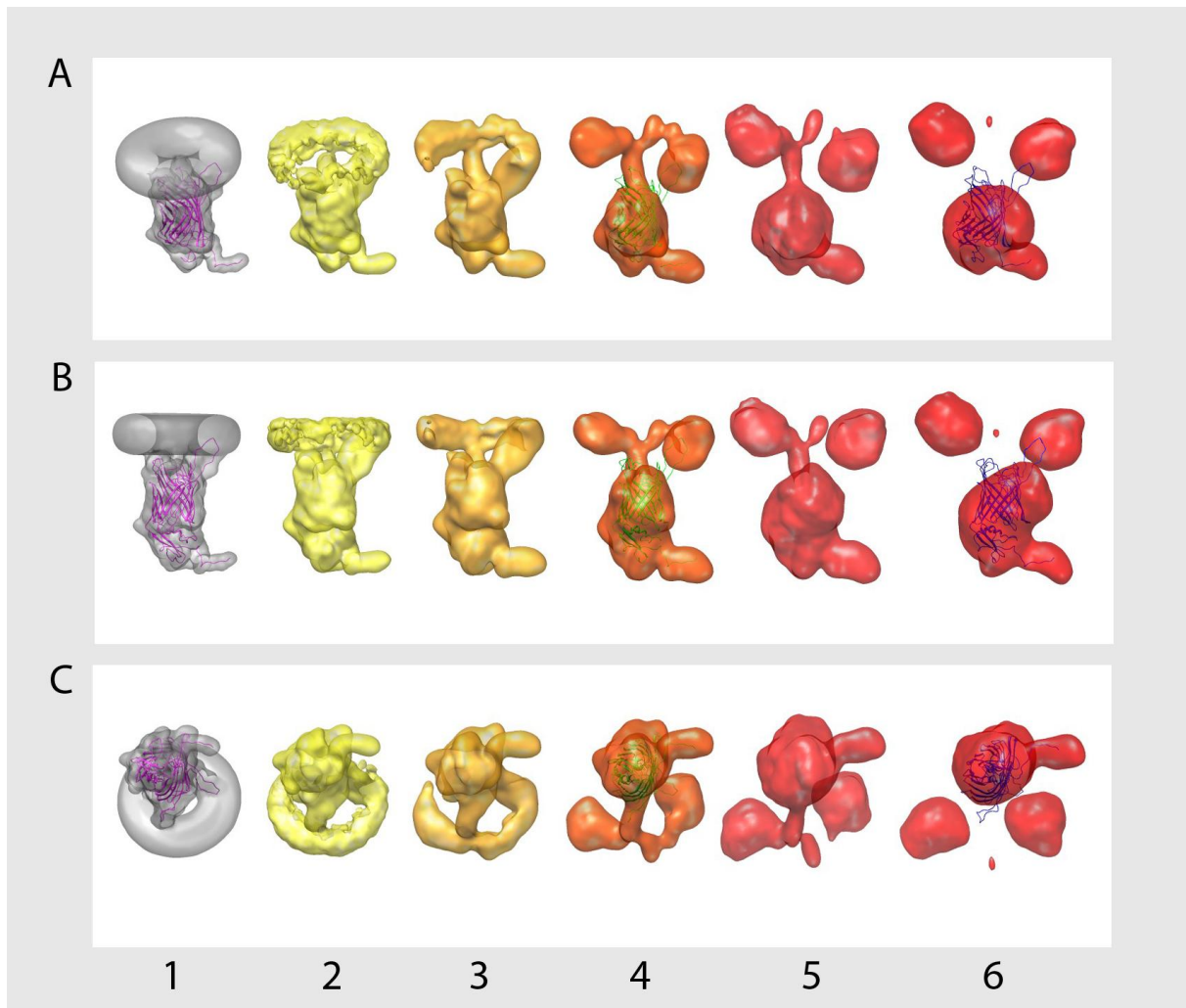


Figure 22

Reconstruction of the isolated TOB complex

TOB complex was isolated from the His9-Tob37 N.c. strain and subjected to cryo-electron microscopy single particle analysis. Progress with increasing rounds of alignment and reconstruction is illustrated from the left to the right. A superposition of the predicted structure of Tob55 and the reconstruction is shown (1, 4 and 6).

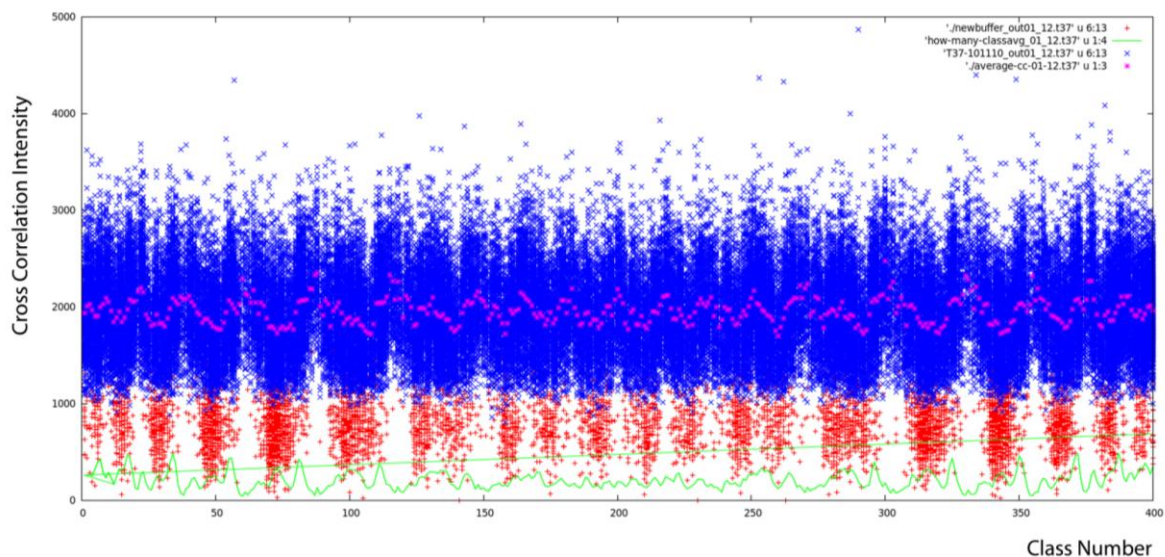


Figure 23

The small molecular mass of the TOB complex results in low signal-to-noise ratios

The cross-correlation intensities of classified particle images are depicted. The green line reveals the number of particle images assigned to a certain class number. The x-axis depicts the class number, the y-axis the intensity of cross correlation. Cross-correlation intensities originating from vitrified buffer are coloured in red, signals emerging from TOB complex particles in blue. The average cross-correlation intensities of the TOB complex particles are illustrated in pink.

Interestingly, fitting of the predicted structure of Tob55 into the reconstruction suggests that the extended loops at the cytoplasmic face of Tob55 are sticking out into the spheres of the subunits Tob37 and Tob38. They presumably form the connection sites between the latter proteins and Tob55 (Figure 24, A and B).

Samples of isolated TOB complex were incubated with Ni-NTA-Nanogold. This was done in order to identify and localize the His-tagged subunits and thereby determine the organization of the complex. Reconstructions of the TOB complex containing labelled or unlabelled 9His-Tob37 were obtained. After density difference calculations, extra mass could mainly be detected in one of the two spheres, identifying it as Tob37 (Figure 24, A and B). Furthermore, a mass strand between Tob37 and Tob55 or the membrane was observed. Such a structure was not recognized with Tob38 (Figure 24). In conclusion, the results obtained in this study, including analysis of stoichiometries, molecular masses, cryo-electron microscopy and molecular modeling allow a preliminary organization of structure of the TOB complex to be proposed (Figure 24C).

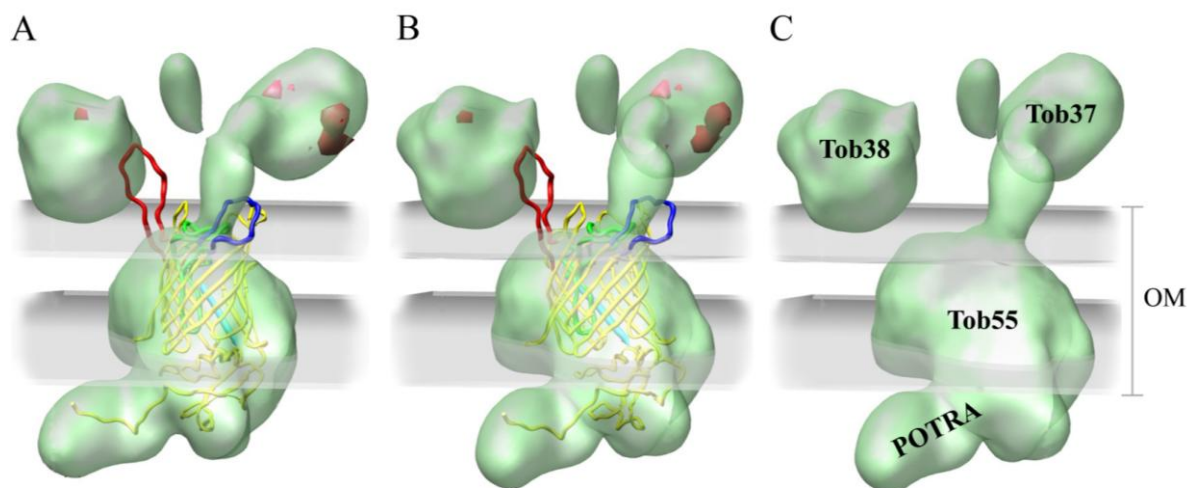


Figure 24

Two extracellular loops of the Tob55 β -barrel are likely to present sites of interaction with the peripheral subunits Tob38 and Tob37.

A and B: Superposition of the predicted structure (ribbon representation) and the next to last reconstruction of Tob55 (light green)

A density difference calculation of reconstructions of TOB complexes with 9His-Tob37, labelled or unlabelled with Ni-NTA-Nanogold, was performed (red areas).

C: Localization of Tob38, Tob37, Tob55 as well as the POTRA domain of Tob55

OM: outer mitochondrial membrane

2.6 The subunits of the TOB complex are tightly associated with the outer mitochondrial membrane

Cryo-electron microscopy analysis revealed a mass strand for Tob37 which might function as a membrane anchor. To get some further insight into the interaction of Tob37 and the other TOB subunits with the membrane, alkaline extraction was performed. By this, it should be determined whether the subunits of the TOB complex are only loosely attached or tightly anchored to the outer mitochondrial membrane. Tob37 turned out to be very resistant to alkaline extraction. It could not be removed from the membrane at pH values up to 12.5. The extra mass strand observed for Tob37 in the reconstruction of the TOB complex might represent a membrane anchor. Thus, Tob37 can be classified as a membrane anchored protein. Tob38 is slightly more sensitive to alkaline treatment than the signal-anchored protein Tom70 and roughly half of Tob38 is extracted at pH 12.5. Thus, Tob38 rather has the characteristics of a peripheral membrane protein.

Tob55 is predicted to be a β -barrel protein and thus is expected to have a tight interaction with the membrane. In agreement with this, even under very basic conditions no extraction of Tob55 could be observed (Figure 25). Mdm10 has also been assigned to the family of β -barrel membrane proteins and its membrane integration has been demonstrated (108). Taken together, all subunits of the TOB complex reveal a tight interaction with the membrane.

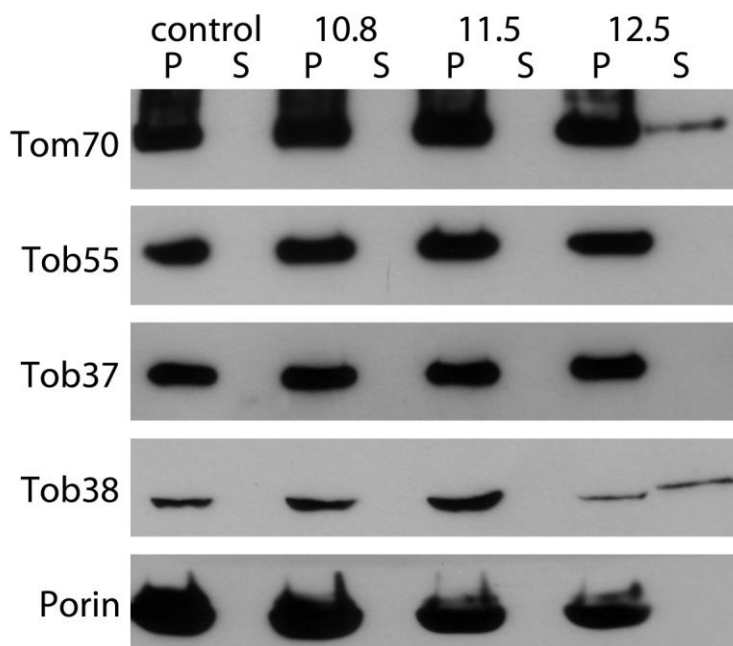


Figure 25

Tob55, Tob38 and Tob37 are tightly associated with the outer mitochondrial membrane

OMVs were subjected to alkali extraction with 0.1 M sodium carbonate adjusted to different pH values of 10.8, 11.5 and 12.5. As a control, proteins were treated with HEPES buffer at pH 7.4 (control). Membrane bound proteins were sedimented by centrifugation (P). Soluble proteins in the supernatant were precipitated with trichloroacetic acid (S).

2.7 The isolated TOB complex shows specific substrate binding behavior

In order to study the functionality of the isolated TOB complex, its ability to bind substrates was analyzed. To this end, the TOB complex was immobilized on a Ni-NTA matrix, thoroughly washed and incubated with radioactive mitochondrial precursor proteins. Tom40 precursor showed a weak binding, slightly above background level. In contrast, a distinct binding to the TOB complex was observed for Tom22. No significant binding of porin was found (Figure 26).

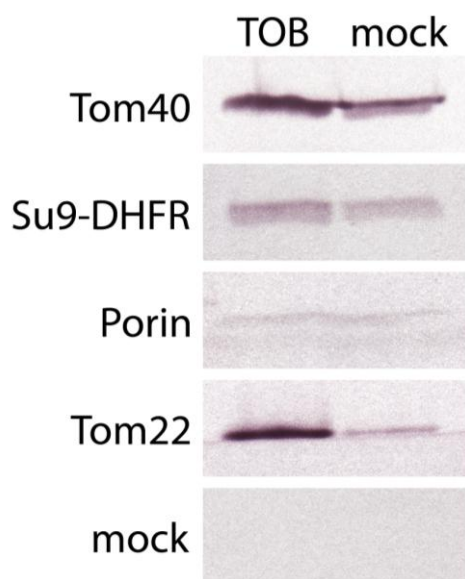


Figure 26

The immobilized TOB complex shows specific binding of certain substrates

TOB was affinity-purified from OMVs bearing a 9His-Tob37 on a Ni-NTA matrix by using TX-100. The isolated complex was incubated with different radioactive precursor proteins (TOB) before being eluted from the column. As a control, a mock isolation without OMVs was performed and the matrix was treated the same way with radioactive precursor proteins (mock). After washing, the bound precursor proteins were eluted and visualized by autoradiography.

Radioactive precursor proteins: Tom40, Porin, Su9-DHFR, Tom22; mock, no plasmid was added to the transcription/translation-reaction

The immobilization of the TOB complex on the matrix might have hindered the interaction with its substrates. Therefore, a pepspot binding assay was performed, which allows the isolated TOB to interact with peptide libraries of its substrates Tom40 and porin in a soluble state. The peptide libraries used in the assay consisted of amino acid residues covering the complete sequence of the respective substrates. The assay allows This enables the localization

of specific binding sites on the substrates. With both peptide libraries, TOB presented a distinct and reproducible binding pattern (Figure 27, Figure 28). Interestingly, binding to the “ β -signal” of the β -barrel substrate proteins could not be detected.

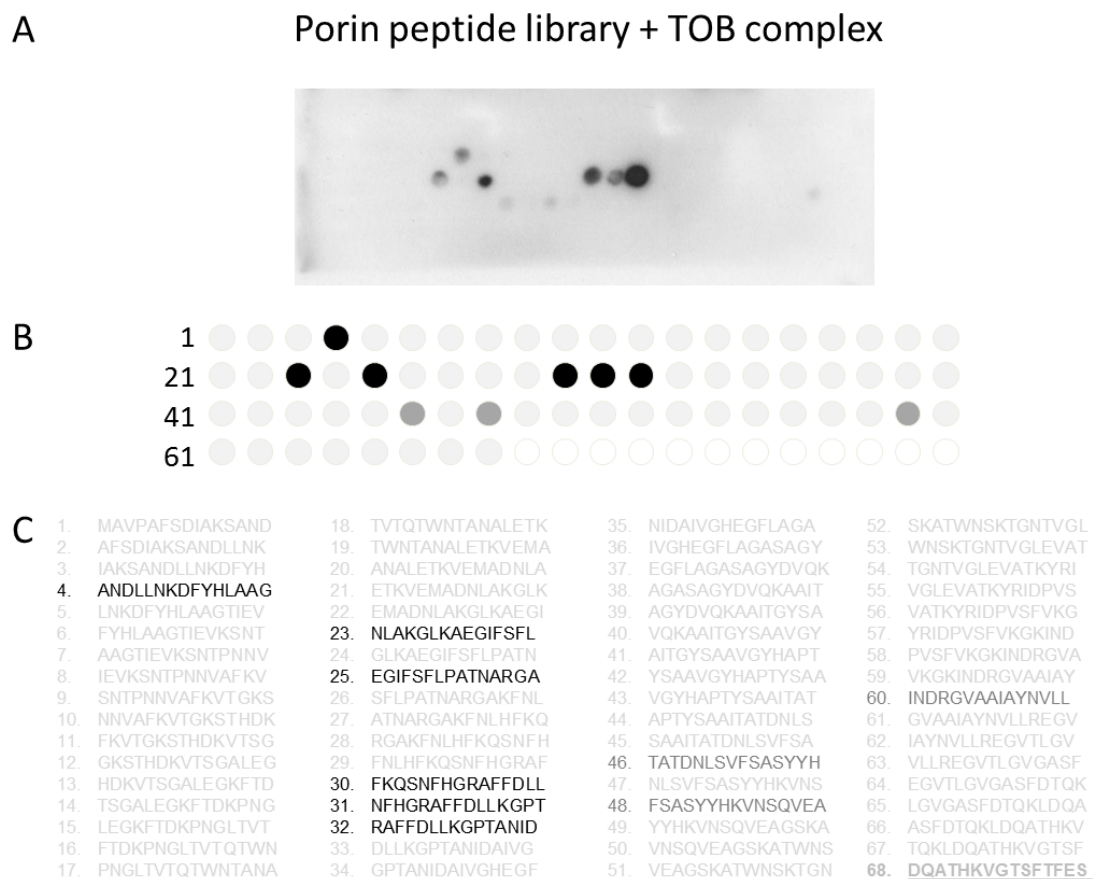


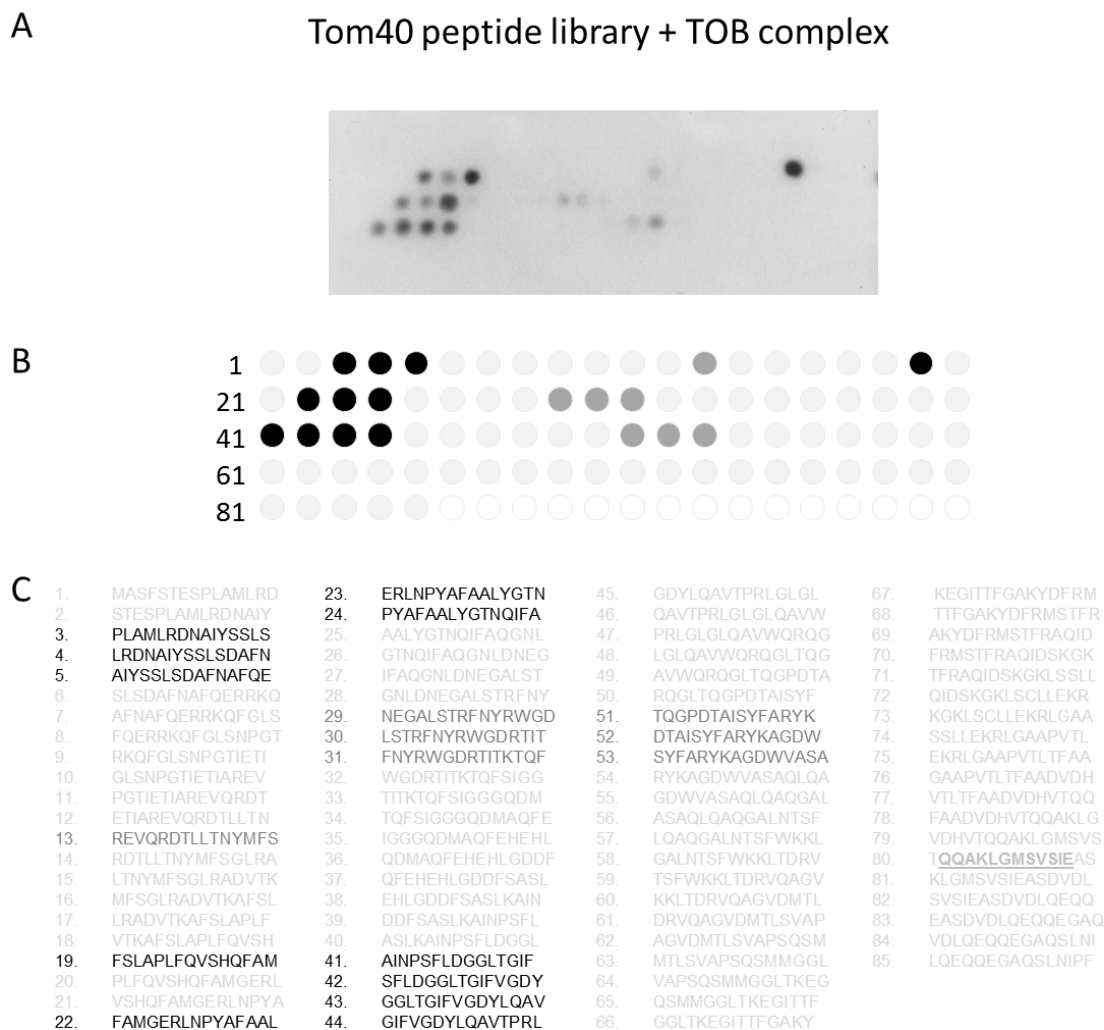
Figure 27

The isolated TOB complex interacts with distinct peptides of a porin peptide library

A: The TOB complex was isolated by Ni-NTA affinity purification from *N. crassa* by the use of TX-100. The porin peptide library was incubated with the isolated TOB complex. Bound TOB complex was blotted from the pepspot-membrane to a PVDF-membrane and immunodecorated with penta-His antibodies.

B and C: Schematic view of the binding sites on the peptide library

Strong binding of the TOB complex is indicated by black pepspot dots (B) and black peptide fragments in the peptide library overview (C). Weak interactions are in dark grey. The “ β -signal” is underlined (# 68).

**Figure 28**

The isolated TOB complex interacts with distinct peptides of a Tom40 peptide library

A: As in Figure 27, except for the use of the Tom40 peptide library

B and C: Schematic view of the binding sites on the peptide library

Interactions are indicated as in Figure 27. The β -signal is underlined (# 80).

As a control, the peptide libraries were incubated with isolated TOM core complex and the BCS1 complex isolated from mitochondria from *N. crassa* and yeast, respectively. The TOM complex exhibited a different binding pattern than the TOB complex, although several peptides in both libraries were recognized by both complexes, as highlighted in the figures (Figure 29, Figure 30). This indicates that some regions of the β -barrel precursor proteins might interact first with the TOM complex during their translocation and afterwards function as binding sites of the TOB complex. The peptide libraries of porin and Tom40 were incubated with His-tagged BCS1 complex which is not involved in the biogenesis of β -barrel precursor proteins. This was done to exclude that the binding of the protein complexes to the

peptide libraries resulted from unspecific hydrophobic protein interactions or was caused by the presence of the His-tag attached to the membrane protein complexes. There was a considerable overlap of the binding pattern of the BCS1 complex with that observed for the TOB complex (Figure 31, Figure 32). Therefore, the specificity of the binding of the TOB complex to the substrate peptides has to be further verified.

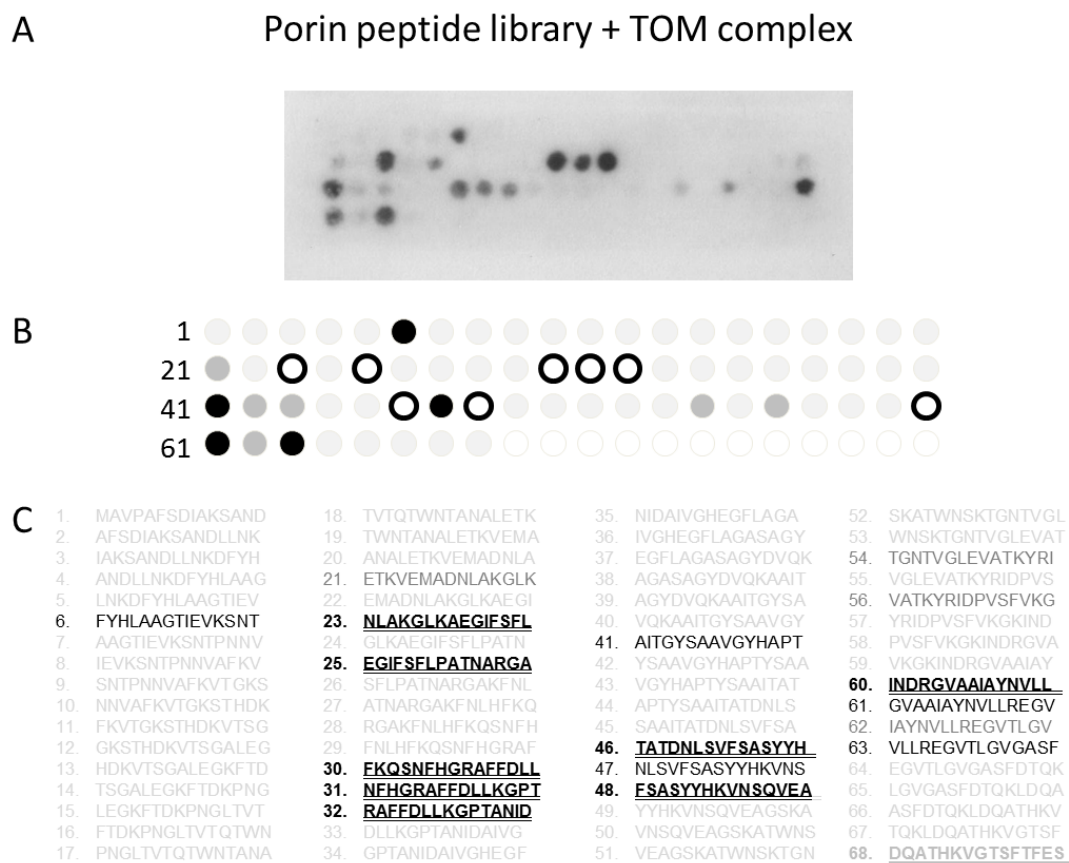


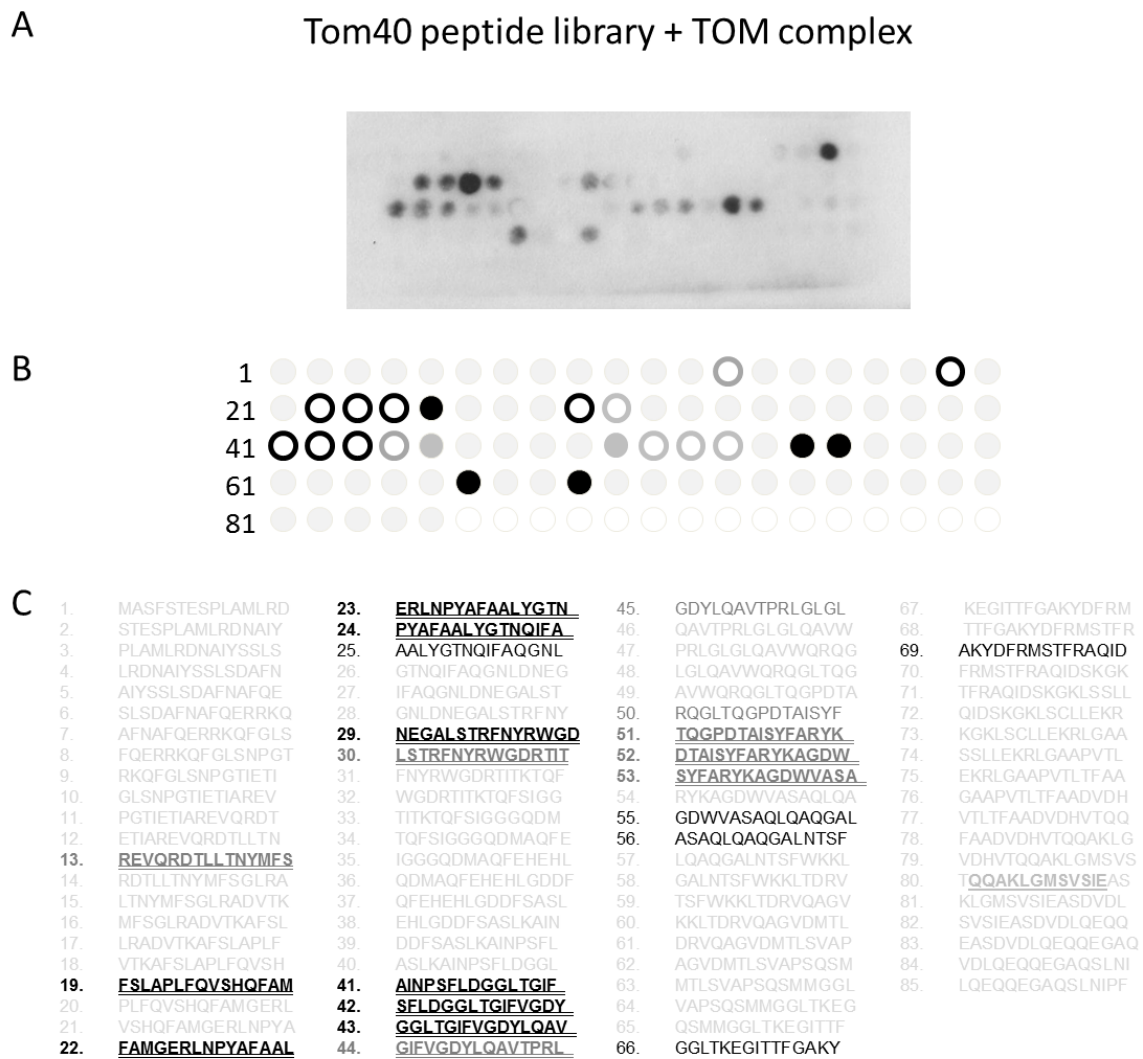
Figure 29

The isolated TOM core complex interacts with distinct peptides of a porin peptide library

A: The TOM core complex was isolated by Ni-NTA affinity purification from *N. crassa* by the use of DDM. The porin peptide library was incubated with the isolated TOB complex. Bound TOM core complex was blotted from the pepspot-membrane to a PVDF-membrane and immunodecorated with penta-His antibodies.

B and C: Schematic view of the binding sites on the peptide library

Strong binding of the TOM complex is depicted by black pepspot dots (B) and black peptide fragments in the peptide library overview (C). Weak interactions are colored in dark grey. Binding sites which are also recognized by the TOB complex are illustrated by open circles (B) and underlined peptide fragments (C). The “ β -signal” is underlined (# 68).

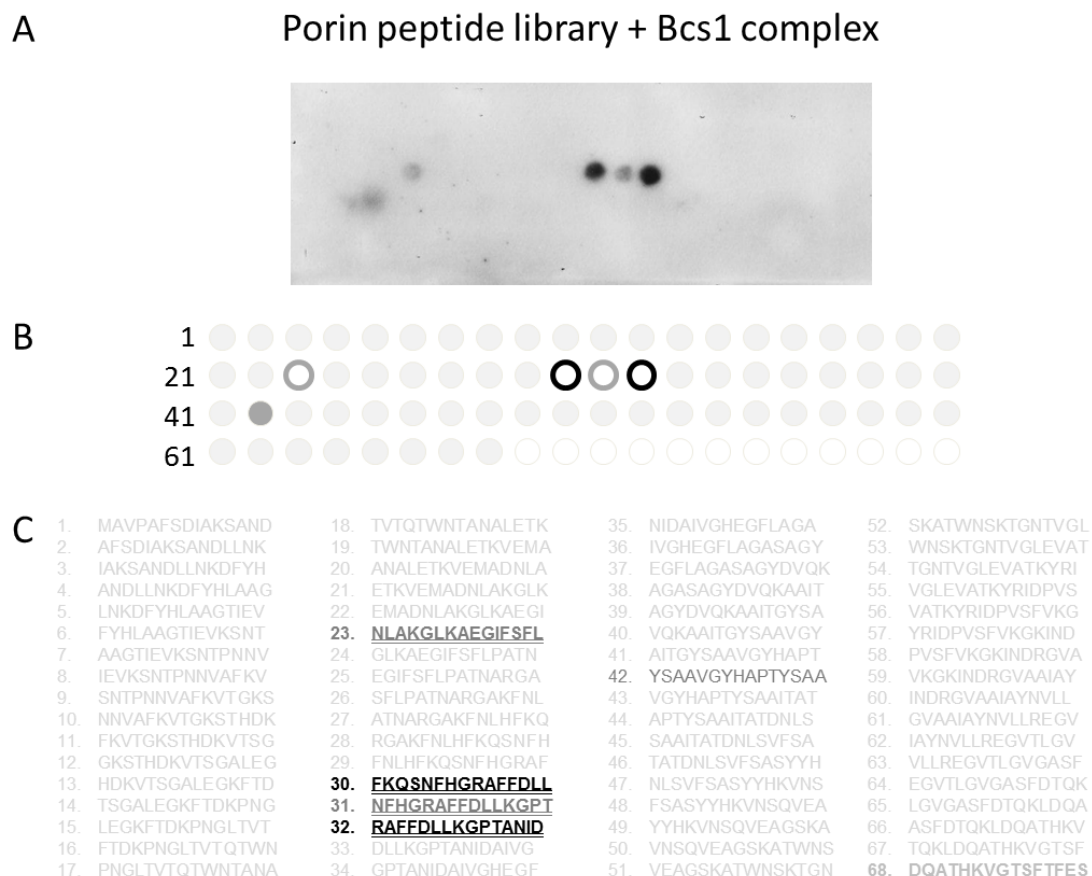
**Figure 30**

The isolated TOM core complex interacts with distinct peptides of a Tom40 peptide library

A: As in Figure 29, except for the use of the Tom40 peptide library

B and C: Schematic view of the binding sites on the peptide library

Interactions are indicated as in Figure 29. The β -signal is underlined (# 80).

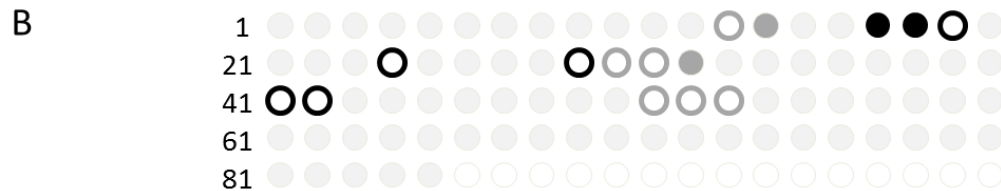
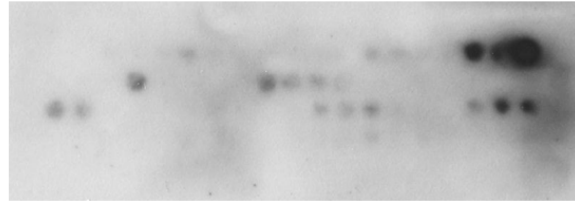
**Figure 31*****The isolated BCS1 complex interacts with distinct peptides of a porin peptide library***

A: The BCS1 complex was isolated by Ni-NTA affinity purification from yeast by the use of digitonin. The porin peptide library was incubated with the isolated TOB complex. Bound BCS1 complex was blotted from the pepsot-membrane to a PVDF-membrane and immunodecorated with penta-His antiserum.

B and C: Schematic view of the binding sites on the peptide library

Strong binding of the BCS1 complex is depicted by black pepsot dots (B) and black peptide fragments in the peptide library overview (C). Weak interactions are colored in dark grey. Binding sites which are also recognized by the TOB complex, are illustrated by open cycles (B) and underlined, bold peptide fragments (C). The β -signal is underlined (# 68).

A Tom40 peptide library + Bcs1 complex



C

1. MASFSTESPLAMLRD	23. ERLNPYAFAAALYGTN	45. GDYLQAVTPRLGLGL	67. KEGITTFGAKYDFRM
2. STESPLAMLRDNIAY	24. <u>PYAFAAALYGTNQIEA</u>	46. QAVTPRLGLGLQAVW	68. TTFGAKYDFRMS TFR
3. PLAMLRDNIAYSSLS	25. AALYGTNQIFAQGNL	47. PRLGLGLQAVWQRQG	69. AKYDFRMS TFR AQID
4. LRDNIAYSSLSDAFN	26. GTNQIFAQGNLDNEG	48. LGLQAVWQRQGLTQG	70. FRMSTFR AQIDSKGK
5. AIYSSLSDAFNAFQE	27. IFAQGNLDNEGALST	49. AVWQRQGLTQGPDTA	71. TFR AQIDSKGKLS SLL
6. SLSDAFNAFQERRKQ	28. GNLDNEGALSTRFNY	50. RQGLTQGPDTAISYF	72. QIDSKGKLSCLLEKR
7. AFNAFQERRKQFGLS	29. <u>NEGALSTRFNRYWGD</u>	51. <u>TQGPDTAISYFARYK</u>	73. KGKLSCLLEKRLGAA
8. FQERRKQFGLSNPGT	30. <u>LSTRFNRYWGDRTIT</u>	52. <u>DTAISYFARYKAGDW</u>	74. SSLEKRLGAAPVTL
9. RKQFGLSNPGTIETI	31. <u>FNRYWGDRTITKTQF</u>	53. <u>SYFARYKAGDWVASA</u>	75. EKRLGAAPVTLTFAA
10. GLSNPGTIETIAREV	32. WGDRTITKTQFSIGG	54. RYKAGDWVASAQLQA	76. GAAPVTLTFAADVHD
11. PGTIETIAREVQRDT	33. TITKTQFSIGGGQDM	55. GDWVASAQLQAQGGAL	77. VTLTFAADVHDVHTQQ
12. ETIAREVQRDTLLTN	34. TQFSIGGGQDMAQFE	56. ASAQLQAQGALNTSF	78. FAADVHDVHTQQAKLG
13. <u>REVQRDTLLTNMFES</u>	35. IGGGGQDMAQFEHEHL	57. LQAQGALNTSFWKKL	79. VDHVTQQAKLGMSVS
14. RDTLLTNMFSGLRA	36. QDMAQFEHEHLGDDF	58. GALNTSFWKKLTDRV	80. <u>TQQA KLGMSVSIEAS</u>
15. LTNMFSGLRADVTK	37. QFEHEHLGDDFSASL	59. TSFWKLTDRVQAGV	81. KLGMSVSIEASDVLD
16. MFSGLRADVTKAFSL	38. EHLGDDFSASLKAIN	60. KKLTDVQAGVDMTL	82. SVSIEASDVLDLQEQQ
17. LRADVTKAFSLAPLF	39. DDFSASLKAINPSFL	61. DRVQAGVDMTL SVAP	83. EASDVLDLQEQQEGAQ
18. VTKAFSLAPLFQVSH	40. ASLKAINPSFLDGGI	62. AGVDMTL SVAPSQSM	84. VDLQEQQEGAQSLNI
19. <u>FSLAPLFQVSHQFAM</u>	41. <u>AINPSFLDGGITGIF</u>	63. MTL SVAPSQSMGGI	85. LQEQQEGAQSLNIPF
20. PLFQVSHQFAMGERL	42. <u>SFLDGGITGIFVGDY</u>	64. VAPSQSMGGITKEG	
21. VSHQFAMGERLNPYA	43. GGLTGIFVGDYLAQV	65. QSMGGITKEGITTF	
22. FAMGERLNPYAF AAL	44. GIFVGDYLAQVTPRL	66. GGLTKEGITTFGAKY	

Figure 32

The isolated BCS1 complex interacts with distinct peptides of a Tom40 peptide library

A: As in Figure 31, except for the use of the Tom40 peptide library

B and C: Schematic view of the binding sites on the peptide library

Interactions are indicated as in Figure 31. The β -signal is underlined (# 80).

3 Discussion

3.1 Composition of the TOB complex

The aim of the present study was to enhance our knowledge about the composition and biochemical as well as functional characteristics of the TOB complex in the outer mitochondrial membrane. Such an analysis necessitated the isolation of the complex in a pure form. Up to now, the TOB complex has not been purified. So far, only small scale preparations resulting from affinity columns were reported that could be analyzed by decoration with antibodies. In a first step *Neurospora* strains were generated that had a His-tag on one of its subunits. His-tagged Tob55 was used because it was predicted to form the main component of the TOB complex as a membrane inserted β -barrel protein (97, 105, 113, 114).

The TOB complex was isolated by Ni-NTA affinity purification from OMVs which were solubilized either with the mild detergent digitonin or with TX-100. With both detergents Tob55, Tob38 and Tob37 were the only proteins which were considerably enriched in the eluate and only traces of Mdm10 were present. Therefore the loss of subunits due to the use of the comparatively harsher detergent TX-100 could be excluded.

Since the His9-Tob55ST strain was only expressing the short but not the long and intermediate Tob55 isoforms, the loss of further subunits due to the absence of these isoforms had to be considered. Therefore, strains with His-tagged Tob38 or Tob37 were created which are expressing all three Tob55 isoforms. Preparations of the TOB complex from these strains yielded the same results as obtained by the use of His-tagged Tob55. Thus, Tob55, Tob38 and Tob37 could be identified as the components of the TOB complex in *N. crassa*. This finding is consistent with observations made in yeast (98, 105, 107). Since only minor amounts of Mdm10 were detected in the eluate, it was suggested that Mdm10 is not a subunit of the TOB complex, but rather functions as an interaction partner of the TOB complex. By being a β -barrel protein itself, Mdm10 might also copurify with the complex as a substrate. However, no other substrates such as the β -barrel proteins porin or Tom40 could be coisolated.

In a next step, the TOB complex isolated from all three different strains with His-tagged Tob55, Tob38 or Tob37 was subjected to BNGE analysis. Several protein complexes could be identified in the eluate. Independent of the detergent used, two complexes were found with all three strains, the TOB complex and very minor amounts of a TOB-Mdm10 complex. By immunodecoration Tob55, Tob38 and Tob37 were identified as constituents of the TOB

Discussion

complex and Mdm10 was additionally found in the TOB-Mdm10 complex. Using membrane protein complexes from the respiratory chain of bovine heart mitochondria as a protein standard indicated an apparent molecular size between 130 and 160 kDa for the TOB complex. Association of Mdm10 with the TOB complex resulted in a complex with an apparent molecular mass of 200 kDa. This is in contrast to former publications suggesting a molecular mass of 200 - 250 kDa for the TOB complex (97, 135, 136). However, in those published studies, hydrophilic, soluble proteins were used as protein standards for the mass estimation of the TOB complex in BNGE analysis. Considerable discrepancies between the migration behavior of membrane integrated and soluble proteins demonstrate that soluble markers are not appropriate for the mass estimation of membrane proteins (140). In contrast to soluble proteins, membrane proteins contain substantial amounts of bound lipids, detergent and Coomassie-Blue when subjected to BNGE. The latter dye binds preferentially to hydrophobic surfaces of proteins and to basic amino acid residues. Therefore, soluble proteins bind this anionic dye which enables anodic migration to different degrees and provide these proteins with a different number of negative charges (142). Different amounts of protein-bound lipids additionally bias the running behavior of membrane proteins and thereby severely compromise mass estimations of membrane proteins by soluble markers. Thus, respiratory chain complexes of bovine heart mitochondria represent a more reliable marker for the mass determination of the TOB complex.

The apparent molecular masses determined by BNGE analysis in combination with membrane protein markers are also highly consistent with the stoichiometry of the TOB complex. The stoichiometry was measured by isotope diluted mass spectrometry which is a novel and highly precise method to analyze the relative amounts of proteins within a mixture (143, 144). A 1:1:1 ratio between the TOB complex components Tob55, Tob38 and Tob37 was measured, resulting in a calculated molecular protein mass for the TOB complex of 140 kDa. BNGE analysis and volume estimations of the cryo-EM structure of the TOB complex exclude a composition of two or more of each TOB complex subunit (e.g. a 2:2:2 stoichiometry).

Although the same stoichiometry for the TOB complex isolated either with TX-100 or digitonin was measured, a slight difference in their running behavior could be observed in the BNGE. This might be attributed to the different properties of the detergents, the relative harsh TX-100 as compared to the mild digitonin. Although it was shown that protein-bound detergent is replaced by Coomassie-dye during the BNGE (145), the detergent used causes differences in the migration behavior of the protein. On the one hand, the proteins are solubilized with different efficiencies, leaving different amounts of lipids on the protein (140),

on the other hand, differences in the ratios of hydrophilic and hydrophobic, membrane embedded parts of membrane complexes might also cause slight variations in the amount of protein-bound lipids remaining on membrane proteins of comparable mass, although they were solubilized with the same detergent. Thus, moderate differences in the migration behavior between sample and standard proteins in various detergents are a common observation, especially when proteins are analyzed that were solubilized with a mild detergent such as digitonin.

Association of one Mdm10 molecule with the 140 kDa TOB complex, results in a complex of calculated 190 kDa, which is in agreement with the migration behavior of this TOB-Mdm10 complex in BNGE. BN-shift analysis demonstrated that Mdm10, but no Tom40 or Porin, can be shifted with the TOB complex. This suggests that Mdm10 is not a substrate, but rather an interaction partner of the TOB complex.

In accordance with this, a regulatory function of Mdm10 in the biogenesis of β -barrel membrane proteins has been described. Mdm10 was suggested to be responsible for the release of Tom40 from the TOB complex and thereby to coordinate its assembly process (135-137). Moreover, the TOB-Mdm10 complex in yeast was found to promote the membrane integration of Tom22 (92). Differences in the regulatory processes between the organisms may exist, since Mdm10 was described to play a crucial role not only for the assembly of Tom40, but also for porin in *N. crassa* (108), which conflicts with findings in yeast (135-137).

Mim1 (91) and Tom40 (92) were also reported to associate with the TOB complex as interaction partners in yeast, adjusting them for the specific interplay with different substrates. However, even with the use of the mild detergent digitonin, the eluates of our TOB isolation from *N. crassa* were entirely devoid of Tom40 and Mim1 and therefore do not support those findings. Analysis from Waizenegger et al. in yeast also provides further evidence that Mim1 is not a constituent of the TOB complex (105), although the presence of precursor proteins might be necessary for the association of Mim1 with the complex (92). Taken together these data conclusively show that Tob55, Tob38 and Tob37 are the only stoichiometric subunits of the TOB complex in *N. crassa*. The flexible interplay of this complex with other proteins, as for example Mdm10, might provide a regulatory mechanism to facilitate the insertion and assembly of different substrates in the outer mitochondrial membrane.

In preparations of the TOB complex performed with TX-100 a complex was present in addition to the TOB and TOB-Mdm10 complex, which is composed by Tob55 and Tob38 only, the Tob55-Tob38 complex. Since isolation with digitonin did not yield a Tob55-Tob38

Discussion

complex form, it seems likely that by using the detergent TX-100 a small fraction of the TOB complex is destabilized and Tob37 dissociates from the complex. In agreement with this, Tob55 and Tob38 were described to form a tight complex in yeast, whereas the interaction of these proteins with Tob37 was suggested to be more labile (105). Consistent with this, complexes between Tob55 and Tob37 or Tob37 with Tob38 could not be detected in the absence of Tob38 and Tob55, respectively. This indicates that Tob37 is the only dynamic constituent of the TOB complex whose detachment does not lead to a complete disintegration of the whole complex. Nevertheless, Tob37 is crucial for the functionality of the TOB complex as it is involved in the release of substrate proteins from the complex in yeast (132) and essential in *N. crassa* (F. Nargang, University of Edmonton, Alberta, CA; personal communication). Moreover, Tob37 was found to be required and needed for embryonic development in mice (146).

Furthermore, in preparations using the 9His-Tob55ST strain Tob55 dimers and small amounts of monomeric Tob55 were present. This was not only observed upon immunodecoration of the complexes but also by IDMS measurement. A striking excess of Tob55 over Tob38 and Tob37 was measured in the 100 kDa species of preparations from the strain containing His-tagged Tob55. Thus, Tob55 dimers exist beside small amounts of the Tob55-Tob38 in these 100 kDa species. BN-shift experiments revealed that Tob55 dimers are not generated in the course of the isolation but are already present in the solubilized OMVs. They can be observed not only in the strains with a His-tagged TOB subunit but also in the wild type strain. Therefore, it is unlikely that they result from a destabilization and disintegration of the TOB complex, caused by the modification of the TOB complex by the attachment of a His-tag. Furthermore, as described earlier, disintegration of the TOB complex would lead to the presence of monomeric Tob38 and Tob37. In preparations from strains carrying 9His-Tob38 or 9His-Tob37, such species should be observed but are not detectable. Therefore it was concluded that mitochondria contain Tob55 which is not assembled in a TOB complex. The function of those Tob55 monomers and dimers will be subject of experimental investigations in the future.

Taken together, this study describes for the first time an isolation of a highly purified TOB complex. Tob55, Tob38 and Tob37 were identified as the components of the complex. The stoichiometry and molecular mass of a highly purified TOB complex were determined. Isotope diluted mass spectrometry (IDMS) analysis revealed a ratio between these constituents of 1:1:1. The TOB complex comprises one of each subunit. This resulted in a calculated molecular mass of 140 kDa which is in very good agreement with results from

BNGE analysis and which is much smaller than expected before. Mdm10 is suggested to function as an interaction partner of the complex. Moreover, a second population of Tob55 which is not associated with the TOB complex but is present predominantly in form of dimers exists in the mitochondrial outer membrane. Its function is not clear so far.

3.2 Structure of the TOB complex

Secondary structure prediction analysis demonstrates a striking similarity between the TpsB-transporter FhaC from *Bordetella pertussis* and Tob55 from *N. crassa*. A crystal structure of FhaC shows the presence of a 16-stranded β -barrel (121). The same structure is suggested by our prediction for Tob55. Moreover, additional traits, such as the presence of a conserved VRGY/F tetrad at the tip of the loops of FhaC and Tob55 as well as the high similarity in the arrangement of the loops at the cytosolic face in both proteins, support the predicted Tob55 model with a 16-stranded β -barrel. In line with this, sequence alignments of Omp85 from *Neisseria meningitides* and BamA from *Escherichia coli* also indicate a 16-stranded β -barrel for these proteins (115). This is in contrast to earlier studies, by which 12 antiparallel β -strands were predicted (113). However, recent structure prediction analyses of human Tob55 on the basis of the resolved FhaC structure also show a sufficiently clear similarity between both proteins to assign Tob55 to the group of 16-stranded β -barrel proteins (116).

Another common characteristic feature of FhaC and Tob55 is the POTRA domain. The POTRA domain is a module of approximately 75 amino acid residues found in various numbers at the N-terminus of all members of the Omp85-TpsB superfamily. The POTRA domain is characterized by a fold including three β -strands, the first and second strands being separated by two α -helices (β - α - α - β - β motive) (103, 117, 147). Slight variations exist, as seen for example in the POTRA domains of FhaC, where the first helix of POTRA1 is replaced by a loop (121). According to these results, the structure of Tob55 was suggested to be highly similar to that described for TpsB transporters, in particular FhaC.

The cryo-electron microscopy analysis presented in this study together with the quantitative mass spectrometry analysis is in agreement with the biochemically determined composition of the TOB complex of one Tob55, Tob38 and Tob37 each. The POTRA domain at the N-terminus of Tob55 is localized at the inner face of the outer membrane whereas Tob38 together with Tob37 are localized at the outer face of the β -barrel pointing to the cytosol. As indicated by the superposition of the secondary structure of Tob55 and the reconstruction obtained from cryo-EM analysis, long loops between the β -strands of Tob55 are most likely representing the connections between the β -barrel and Tob38 and Tob37.

The composition of the TOB complex of only three subunits with a resulting mass of 140 kDa is perfectly in line with the stoichiometry and BNGE analysis. Nevertheless, these features are not in accordance with the preliminary structure of the TOB complex from yeast presented by Paschen et al. (97). In that study, cryo-negative staining analysis suggested a contribution of

several Tob55 subunits to the TOB complex. Initial image processing steps of our study included a reference free alignment of the particle images which can provide some insight into the basic architecture of the particle analyzed. Our study suggests a complex of three subunits and is therefore not supporting a pentameric structure. Furthermore, in contrast to these previous studies of the TOB complex structure, evidence for the presence of the subunits Tob55, Tob38 and Tob37 in stoichiometric amounts and high purity could be demonstrated for the complex isolated from *N. crassa*. On the other hand, formation of higher order complexes of TOB cannot be excluded. Of note, larger species of the TOB complex were consistently observed upon BNAGE of preparations gained by the use of TX-100.

In our final model of the TOB complex the structure was inserted in a 4-nm thick bilayer in a way that the Tob55 β -barrel protein is embedded in the membrane, its N-terminus is reaching into the IMS and the subunits Tob38 and Tob37 are located at the cytosolic face of the membrane. This orientation is based on several findings presented in the literature. Proteinase K (PK) treatment in combination with osmotic shock or solubilization of the mitochondrial envelope demonstrated that the POTRA domain at the N-terminus of Tob55 is exposed to the IMS (114). The same results were obtained in studies with mitochondria from *N. crassa* (own data, not shown). Furthermore, when Tob55 is embedded in such an orientation in the membrane, the VRGF tetrad is at the tip of the loop which is spanning the interior of the β -barrel and reaching into the IMS. This is in line with findings for FhaC, where the VRGY tetrad is also at the tip of this loop reaching into the periplasm.

Treatment of mitochondria at alkaline pH characterized Tob37 as well as Tob38 as peripheral membrane proteins ((105-107, 148) and this study), while PK treatment additionally revealed that they are exposed to the cytosolic side of the outer membrane (105-107) (F. Nargang, University of Edmonton, Alberta, CA; personal communication).

The presence of the Tob55-Tob38 complex in our preparations of TOB demonstrates that Tob55 and Tob38 still form a complex when Tob37 is detached, an observation which was also made in yeast (105) and which most likely can be attributed to a direct connection between these two proteins. Thus, this connection is probably made by a loop of the Tob55 β -barrel sticking out into the cytosol.

Tob37, on the other hand, is not forming a complex with Tob55 when Tob38 is missing (105) and a direct interaction between Tob55 and Tob37 has not been demonstrated so far. In contrast to Tob37, Tob38 does not include a predicted transmembrane segment (133). Moreover, Tob37 is more resistant to alkali extraction than Tob38 suggesting that there is a tighter connection to the membrane than in the case of Tob38. Therefore, Tob38 might need a

Discussion

strong bond to Tob55 to stay attached to the membrane, whereas Tob37 might be anchored into the outer mitochondrial membrane by an additional transmembrane segment and therefore does not depend on its association with Tob55 to stay in a membrane bound state. Hence, it seems reasonable to suggest that a transmembrane segment anchors Tob37 in the outer mitochondrial membrane and that a further interaction between Tob55 and Tob37 is made by an exposed loop of the β -barrel. An extra mass which might represent the membrane anchor of Tob37 but is missing in Tob38 can be seen in our cryo-electron microscopy reconstruction of the TOB complex (Figure 24).

Taken together, our detailed analysis of the TOB complex by cryo-electron microscopy yielded a structure of the TOB complex with one Tob55, Tob38 and Tob37 each. It is reflecting all the characteristics obtained from further analysis, as there are composition and stoichiometry of the subunits, molecular size as well as the relative orientation of the subunits towards each other. A superposition of the predicted Tob55 structure demonstrated a nice fit into the cryo-electron microscopy reconstruction of the complex and indicated a specific role of the loops sticking out from the cytoplasmic β -barrel side in connecting the peripheral subunits Tob38 and Tob37 to the β -barrel of Tob55. An exemplary embedding of our final cryo-electron microscopy structure of the TOB complex is consistent with all topological characteristics of its subunits known so far and the dimension of a biological membrane with a thickness of 3 – 5 nm.

3.3 The functional mechanism of the TOB complex

According to our structural analysis, Tob55 bears a striking resemblance to the X-ray structure of FhaC. Both proteins belong to the same Omp85-TpsB superfamily and epitomize all the features which seem to be characteristic for this transporter family, as there are one or several N-terminal POTRA domains, a C-terminal β -barrel, and a loop between two β -strands of the barrel harboring a highly conserved and functional important VRGY/F tetrad at its tip (109, 115, 121, 122, 124, 141). The similarity of the architecture of both protein transporters suggests a comparable functionality of their components.

The first component which the substrates are encountering in the periplasmic or intermembrane space is most likely the POTRA domain. In the TpsB-family, the POTRA domain functions as a specific interface between the transporter and its dedicated TpsA substrate (115, 149). The function of FhaC absolutely depends on the presence of both POTRA domains. Binding of incoming substrates to the POTRA domain was demonstrated (121, 149). In agreement with this, the POTRA domains of BamA were described to play a key role in the recruitment of lipoproteins and deletion mutants depict severe phenotypes (103). A construct encoding BamA without the fifth POTRA domain (Δ POTRA5) could not be introduced into a BamA-deletion strain, even in the presence of the expression of wild type BamA. Therefore, Kim et al. suggested that the Δ POTRA5 construct of BamA “mishandles nascent β -barrel substrates, producing harmful misfolded or aggregated OMPs” (103). A similar important role of the most carboxy-terminal POTRA domain was demonstrated for Omp85. POTRA5 of Omp85, preceding the β -barrel, turned out to be essential, whereas deletion of POTRA1-4 only had minor effects on the assembly of OMPs (118). Here, the membrane integration of large OMPs by Omp85 was more sensitive to the deletions of the POTRA domains 1-4 than that of smaller OMPs.

Conflicting results were reported for the role of the POTRA domain of Tob55. While Habib et al. provided evidence for the involvement of the POTRA domain in binding of the precursor proteins and their subsequent membrane insertion (114), Kutik et al. later described that the POTRA domain can be removed with only a minor effect on the membrane insertion of β -barrel precursor proteins (133). However, the POTRA domain in yeast was predicted to comprise the amino acids 29-120 (117, 133). Since deletion of the first N-terminal 102 amino acids causes severe import defects of precursor proteins (114), but not the deletion of the N-terminal 120 amino acids (133), it is most likely, that the remaining 18 amino acids (102 – 120) impair the insertion mechanism of the TOB complex. One explanation might be that the

interaction between the POTRA domain of Tob55 and incoming precursor proteins facilitates their membrane insertion rather than being essential for it and primes a conformational change by which the POTRA domains are rearranged in favor of the following membrane integration of the precursor protein. In case of only a partial deletion of the POTRA domain, such a conformational rearrangement of the remaining POTRA stretch might not be possible. Nevertheless, the strong and specific interaction of the POTRA domain with precursor proteins (114) indicates a role of the POTRA domain as an anchor and interaction platform for incoming substrate proteins in the IMS and thereby resembles the role of the POTRA domains in the periplasmic space of the prokaryotic homologues.

A second component of the transporters which is conceivable to play an important role in the subsequent processing of substrate proteins is a large loop connecting the β -strands 11 and 12 of the β -barrel. This loop is predicted to pass the interior of the β -barrel and, together with the first half of β 12, forms a conserved motif, motif3, in this transporter superfamily (115, 141). Alignment analysis in representative members of the TpsB- as well as Omp85 family revealed that this loop harbors the highly conserved VRGY/F tetrad. In FhaC and Tob55, this tetrad is located at the tip of the loop reaching into the periplasmic or intermembrane space, respectively. The arginine residue is invariant in all tetrads. Point mutation analysis in FhaC revealed that substitution of this arginine suffices to inhibit secretion of FHA by FhaC and thus indicates the importance of this loop and the tetrad for transport activity (141). In view of the observation that loop6 of motif3 in FhaC is mobile and changes its conformation in the course of the secretion process (121, 150) it has been suggested that the loop might be expelled from the barrel after its interaction with the substrate at the periplasmic side (121). The removal of the loop from the interior of the barrel is expected to result in considerable structural changes, as deletion of the loop has substantial influence on the stability and channel activity of the β -barrel (115, 141). This is in line with the finding of a further conserved motif, motif4, which corresponds to the β -strands 14 and 15 and forms part of the inner surface of the barrel covered by the loop of motif3 (121). Interaction between motif3 and motif4 might have a stabilizing effect on the barrel and removal of the loop of motif3 therefore might end up in a severe destabilization. Thus the binding of incoming substrates to the POTRA domain and most likely subsequently to the tip of the β -barrel spanning loop seems to trigger rearrangement of the β -barrel and induce transport activity. Considering the high resemblance in the structural features, this mechanism might not only be true for FhaC, but for all members of this transporter superfamily, including the TOB complex.

The further processing of the substrates is thought to be different between those two transporter families, since their substrates do not only differ in their final structure but are also directed to different destinations. Members of the TpsB-family transport their substrates to the membrane surface where they are secreted in form of β -helical soluble proteins (123). In contrast, Omp85 transporters mediate the membrane insertion of β -barrel precursor proteins (122). Furthermore, TpsB transporters consist only of a single β -barrel protein (123), whereas members of the Omp85 transporter family possess further subunits beside the β -barrel protein as the core component of the complex (122). The presence of additional subunits, as for example Tob38 and Tob37 for the TOB complex or BamB-E for the BAM complex (147) might be attributed to the fact that Omp85 transporters are responsible for membrane insertion of a variety of substrates. In contrast to this, each TpsB transporter exclusively secretes its dedicated TpsA substrate.

The model of the TOB complex presented here suggests possible mechanisms of how the membrane insertion of β -barrel proteins might function. On the one hand, the embedding of the substrate into the membrane could be facilitated by the concerted action of several TOB complexes. An oligomer of TOB complexes might form a cavity whose interior is lined by the hydrophobic outer sheaths of the contributing β -barrels and thereby could have a scaffolding function in the formation of a new β -barrel in the interior of the cavity. This functional mechanism is reminiscent to the principle of an “Anfinsen cage”, which was described to provide a protective environment for precursor folding (151, 152). A similar model was also proposed for the insertion of α -helical transmembrane protein by the TOM complex (88). The presence of a small amount of complexes with an estimated molecular mass of around 400 and 1000 kDa in our TOB preparations could support this possibility. However, complex oligomers could only be seen upon preparations performed with TX-100 but not with digitonin and could also result from partial aggregation.

With this latter model it is difficult to imagine how the hydrophilic inner face of the new barrel can be integrated into the hydrophobic surrounding of the lipid bilayer. Nonetheless, an instance which argues for such an insertion mechanism is that a lateral opening of the β -barrel is not required. Although channel activity and thereby the presence of a pore in Omp85 transporter has been described (97, 133, 153), the folding of a new β -barrel within the pore would require lateral opening for the release of the substrate into the membrane. Such a scenario was suggested to be highly unlikely in respect to thermodynamics since the opening of a β -barrel requires significant displacement of the β -strands which are tightly interconnected by hydrogen bonds (102, 110, 154).

Discussion

On the other hand, diverse transporters of the Omp85 superfamily such as BamA, FhaC or Tob55 exhibit pore activity that is responsive to substrate binding (110, 121, 133). This is suggesting an active role of the pore in the transport process. The analysis of the conserved motif4 and the loop of motif3 indicate a substantial rearrangement of the β -barrel induced by the binding of a substrate protein. Thus, it cannot be excluded that such a rearrangement of the complex leads to a transient opening of the barrel, which may either take place in the conserved motif4 or between β -strands 1 and 16, as they are not connected by a turn within the barrel. A new barrel might be generated by a sequence of antiparallel β -strands from one end of the β -barrel. After the arrangement of all 16 antiparallel β -strands, both β -barrels, the Tob55 and the client barrel, might close and separate. In this manner, the outer, hydrophobic sheath of the old and new barrel would stay in a hydrophobic surrounding. The same would be true for the hydrophilic inner sheath facing the hydrophilic interior of the barrel. Such a mechanism would allow the TOB complex to act as a monomeric complex.

During the rearrangement of the β -barrel after substrate binding, the loop flapping out of the interior of the β -barrel might still be connected to the incoming substrate, thereby pulling it through the pore and bringing it in proximity of Tob38 at the outer face of the membrane. This would be in line with an interaction of the β -signal of incoming β -barrel precursor proteins and Tob38 which has been proposed in the recent literature (133). A similar interaction might take place at the C-terminal signature sequence of bacterial β -barrel proteins, which presumably corresponds to the eukaryotic β -signal (133, 155). In agreement with this, a high conservation of this interaction mechanism is likely, since the C-terminal signature sequence in precursor proteins was reported to be processed by the TOB complex in yeast (156).

To date, our knowledge about what drives the membrane insertion of β -barrel proteins is still elusive. No obvious energy source required for the assembly of β -barrel proteins could be determined so far (26). The protein folding and insertion of β -barrels into the hydrophobic environment of a membrane are likely to be energetically favorable reactions, bringing the protein into a free energy minimum. The free energy minimum of proteins is determined by their surroundings, comprising interactions of the peptide chains with each other, with water, the lipid bilayer hydrocarbon core and the bilayer interface (157). Thus, the free energy of folding the soluble precursor form into the stable membrane-inserted form was suggested to provide the energy needed for the whole process. Increasing affinities of the folding intermediates with their binding partners might provide unidirectionality to the transport pathway (26).

Structural and functional analysis of Tob55 and FhaC shed light on the architecture of these transporters and provide further indications of how they interact with and process their substrates. However, the elements of the various constituents which are crucial for the functionality of the transport process are just about to be determined and further analysis will be needed to improve our knowledge about this enigmatic mechanism.

3.4 Alternative splicing of *tob55*

In the course of our studies of the TOB complex *N. crassa* Tob55 was observed to be expressed in three different isoforms due to alternative splicing. This was an observation made for the first time for a component of the mitochondrial import machinery (120). Expression of isoforms of one protein might serve the purpose of specialization, varying for example in different tissues (158) or under certain growth condition, such as upon exposure to chemical oxidants or environmental stress (159). Thus it was analyzed whether the different Tob55 isoforms might have specialized functions in *N. crassa* (120). The strain exclusively expressing the long Tob55 isoform had growth defects at elevated temperatures (37°C) and in the presence of high salt concentrations. Furthermore, assembly of mitochondrial β -barrel proteins of this strain was severely impaired. However, strains expressing only the short or intermediate Tob55 isoform showed no differences in growth or import efficiencies compared to the wild type strain (120). The substrates of the TOB complex are either essential (120, 160, 161) or their deletion results in reduced growth rates or import defects of β -barrel proteins (108, 162). Therefore, substrate specific interaction of the different Tob55 isoforms with incoming precursor proteins seems unlikely. Since the differences in the Tob55 isoforms are at the N-terminus just in front of the POTRA domain, it was proposed that the interaction of the TOB complex with incoming precursor proteins might be compromised under stress conditions when only the long Tob55 isoform is present (120). An explanation for this might lie in divergent affinities of the Tob55 isoforms to incoming substrates, with the long Tob55 isoform possessing the lowest affinity. The efficiency of membrane insertion of precursor proteins by the TOB complex might be regulated in this way, a suggestion which has to be verified. Altogether, our knowledge about possible differences in the functionality of the different Tob55 isoforms is still elusive and awaits further analysis.

3.5 α -Helical substrates of the TOB complex

Functionality of the isolated TOB complex was tested by diverse binding assays. Although only a slightly increased binding above background level was observed for β -barrel precursor proteins, an especially strong binding of Tom22 could be detected. This supports the surprising finding made by Stojanovski et al. in *Saccharomyces cerevisiae* that the TOB complex is essential for the efficient membrane insertion and assembly of the α -helical outer mitochondrial membrane protein Tom22 into the TOM complex (95). The involvement of the TOB complex in the biogenesis of Tom22 is also reflected in the observations that a downregulation of the essential protein Tob55 in *N. crassa* not only resulted in decreased levels of β -barrel proteins, but also severely reduced the steady state levels of Tom22 (120). To our knowledge this is the first time a direct interaction between the TOB complex and Tom22 is reported.

Additionally to Tom22, the α -helical proteins Tom5, Tom6 and Tom7 were found to depend on the TOB complex (92, 95). However, in contrast to Tom22, the TOB complex is only needed for the assembly of the small Tom proteins into the TOM complex, but not for their membrane insertion (95). Thus, the substrate spectrum of the TOB complex is not only restricted to β -barrel precursor proteins but also includes α -helical proteins of the outer mitochondrial membrane.

Akin to β -barrel precursor proteins, Tom22 first interacts with the TOM complex (163) and is subsequently integrated into the membrane with the help of the TOB complex. However, the membrane interaction of Tom22 with the TOM complex is suggested to be “a loose association with the mitochondrial surface followed by the SAM (TOB)-stimulated insertion into the outer membrane” (95). Therefore, a passage of the TOM complex might not be necessary for the assembly of Tom22. This is in contrast to β -barrel precursor proteins which have to be translocated to the IMS by the TOM complex before they interact with the TOB complex (114). This indicates some differences in the interaction of α -helical and β -barrel substrates with the TOB complex during the import process.

4 Summary

β -Barrel membrane proteins are exclusively present in the outer membrane of Gram-negative bacteria and in the outer envelope of organelles of endosymbiotic origin, mitochondria and chloroplasts. The assembly of β -barrel precursor proteins into the outer mitochondrial membrane is mediated by the TOB (topogenesis of mitochondrial outer membrane β -barrel proteins) complex. Tob55 together with Tob38 and Tob37 constitutes the TOB complex. Tob55 is a putative β -barrel protein and represents the core component of the complex. The work presented here describes a functional and structural analysis of the TOB complex of *Neurospora crassa*. Tob55 was found to be expressed in three different isoforms. It is the first component of the mitochondrial import machinery described to be expressed in different isoforms due to alternative splicing.

The stoichiometry analysis of the TOB complex was performed by isotope dilution mass spectrometry (IDMS) and revealed a 1:1:1 ratio between these subunits. This, together with the results obtained by electrophoretic analysis of the TOB complex led to the conclusion that one Tob55 associates with one Tob38 and one Tob37 to a complex of 140 kDa molecular mass. Association of Mdm10 with this complex results in the formation of the TOB-Mdm10 complex, which only makes up a minority of the isolated complexes. A second population of Tob55 was detected which is not contributing to the TOB complex but was present predominantly in form of dimers. The physiological role of this Tob55 population still has to be determined.

Molecular modeling based on the X-ray structure of the FhaC transporter and cryo-electron microscopy studies of the TOB complex revealed a high similarity between both proteins. FhaC and Tob55 expose their N-terminal POTRA domain into the periplasmic or intermembrane space, respectively. They are embedded into the membrane by their β -barrel domain. The interior of the β -barrels of both proteins harbors a large loop with a conserved VRGY/F tetrad at its tip, which plays a crucial role in the function of FhaC. Tob38 and Tob37 are associated with Tob55 at the cytosolic face of the outer membrane. Tob37 interacts firmly with the membrane and with Tob55. Based on these results the mechanism of how the TOB complex mediates the insertion of β -barrel proteins into the outer membrane of mitochondria is discussed.

The TOB complex was described not only to participate in the assembly of β -barrel precursor proteins, but also of α -helical proteins such as Tom22 of the TOM complex. Here, a direct interaction of the isolated TOM complex with the Tom22 precursor protein is demonstrated.

5 Zusammenfassung

β -Barrel-Proteine kommen ausschließlich in der Außenmembran von Gram-negativen Bakterien, Mitochondrien und Chloroplasten vor. Für die Insertion von β -Barrel Proteinen in die mitochondriale Außenmembran ist der TOB- (topogenesis of mitochondrial outer membrane β -barrel proteins) Komplex verantwortlich. Der TOB-Komplex umfaßt die drei Untereinheiten Tob55, Tob38 und Tob37. Tob55 bildet die Hauptuntereinheit des TOB-Komplexes. Die hier vorliegende Arbeit beschäftigt sich mit der funktionellen sowie strukturellen Analyse des TOB-Komplexes von *Neurospora crassa*. Es konnte herausgefunden werden, daß die Tob55-mRNA alternativ gespleißt wird und Tob55 dadurch in drei verschiedenen Isoformen exprimiert wird. Tob55 ist damit die erste Komponente der mitochondrialen Translokasen, für die eine Expression in verschiedenen Isoformen aufgrund alternativen Spleißings bekannt ist.

Durch Isotopen verdünnte Massenspektrometry (IDMS) konnte ein stoichiometrisches Verhältnis von Tob55, Tob38 und Tob37 von 1:1:1 ermittelt werden. Unter Berücksichtigung der elektrophoretischen Mobilität des nativen Komplexes ergibt sich, daß jede Untereinheit einmal im TOB Komplex vorliegt und dieser demnach ein errechnetes Molekulargewicht von 140 kDa hat. Ein geringfügiger Anteil des TOB-Komplexes assoziiert mit Mdm10 zum TOB-Mdm10-Komplex. Zudem wurde gefunden, daß Tob55 nicht nur an der Bildung des TOB-Komplexes beteiligt ist, sondern zudem auch in Dimeren vorkommt. Die funktionelle Bedeutung dieser Dimere ist derzeit noch offen.

Mittels Strukturvorhersage und cryo-Elektronenmikroskopie konnte eine starke Ähnlichkeit zwischen dem FhaC-Transporter und dem TOB-Komplex ermittelt werden. Beide Proteine verfügen über eine N-terminale POTRA-Domäne und sind über ein C-terminales β -Barrel in der Membran verankert. Der Innenraum des β -Barrels von FhaC als auch von Tob55 wird von einer großen Schleife durchspannt, welche an ihrer Spitze das konserviert VRGY/F-Motif besitzt. Dies ist essentiell für die Funktion von FhaC. Tob38 und Tob37 sind auf der cytosolischen Membranseite mit Tob55 assoziiert, wobei Tob37 eine stärkere Verbindung mit der Membran aufweist als Tob38. Anhand der bekannten strukturellen Eigenschaften des TOB-Komplexes werden mögliche Funktionsmechanismen zur Insertion der β -Barrel-Proteine in die Membran diskutiert.

Neben der Insertion von β -Barrel-Proteinen wurde auch eine Beteiligung des TOB Komplexes bei der Assemblierung von α -helicalen Proteinen, wie z.B. Tom22, beschrieben. Eine direkte Interaktion von Tom22 mit dem TOB Komplex wird in der vorliegenden Arbeit gezeigt.

6 Material and Methods

6.1 Materials

6.1.1 Equipment

Equipment	Prescription
Autoclave Bioclav	Schütt, Göttingen, GER
Autoclave Varioclav 400E	H + P Labortechnik, Oberschleißheim, GER
Autoclave Systec DX-150, D1167	Systec GmbH, Wettengel, GER
Cannulae	Braun, Melsungen, GER
Centrifuge Allegra X-22 R	Beckman Instruments, München, GER
Centrifuge Avanti J-20 XP	Beckman Instruments, München, GER
Centrifuge Avanti J-25	Beckman Instruments, München, GER
Centrifuge Optima Max-E Ultracentrifuge	Beckman Instruments, München, GER
Centrifuge Optima LE-80 K Ultracentrifuge	Beckman Instruments, München, GER
Centrifuge Optima L-90 K Ultracentrifuge	Beckman Instruments, München, GER
Centrifuge L8-M Ultracentrifuge	Beckman Instruments, München, GER
Centrifuge 5417 R	Eppendorf, Hamburg, GER
Centrifuge 5810 R	Eppendorf, Hamburg, GER
Centrifuge 5415 D	Eppendorf, Hamburg, GER
Centrifuge 3 K 30	Sigma, München, GER
Centrifuge RC-3B Refrigerated Centrifuge	Sorvall Instruments, Newtown, USA
Colloid mill	Workshop, Institute for Physiological Chemistry, LMU Munich
Developer machine AGFA Gevamat 60	Agfa-Gevaert, Munich, GER
Erlenmeyer flask for <i>N.c.</i> -cultivation, 300 ml, wide-necked	Fisherbrand, Schwerte, GER
Excicator	Duran, Wertheim/Main, GER
Foam Caps for <i>N.c.</i> -cultivation	Schaumstoffe-Mayer, München, GER
Freezer -20°C	Liebherr, Ochsenhausen, GER
Freezer -80°C	GFL, Burgwedel, GER
Fridge 4°C	Liebherr, Ochsenhausen, GER
Gas burner Fireboy eco 50/60 Hz, 5 W	Integra Biosciences AG, Wallisellen, CH
Geoelectrophoresis chamber	Workshop, Institute for Physiological Chemistry, LMU Munich
Glass-teflon homogenizer	Workshop, Institute for Physiological Chemistry, LMU Munich
Glass ware	Schott, Mainz, GER
Glas ware	Duran, Wertheim/Main, GER

Heating Cabinet	Memmert, Hannover, GER
HPLC Ultimate 3000 system	Dionex, Benelux B.V.
Incubator B 5042 E	Heraeus Christ, Osterode, GER
Incubator BA3	Heraeus Christ, Osterode, GER
Magnetic stirrer MR 3001 K	Heidolph, Schwabach, GER
Orbitrap mass spectrometer	Thermo Electron, Rockford, USA
Overhead shaker	Workshop, Institute for Physiological Chemistry, LMU Munich
Peristaltic pump P-1	Amersham Biosciences, Freiburg, GER
pH-Meter Lab 850	Schott, Mainz, GER
Photometer BioPhotometer	Eppendorf, Hamburg, GER
Photometer Biochrom Libra S11	Biochrom Ltd., Cambridge, GB
Pipettes	Gilson, Inc., Middleton, WI, USA
Pipet tips	Sarstedt, Bad Homburg, GER
Poly-Prep Chromatography Columns	Bio-Rad Laboratories, Hercules, CA
Power supply EPS 600	Amersham Biosciences, Freiburg, GER
Power supply EPS 601	Amersham Biosciences, Freiburg, GER
PP-Test tubes, 15 and 50 ml (falcons)	Greiner bio-one, Frickenhausen, GER
Pure water plant PURELAB plus UV/UF	USF, Ransbach-Baumbach, GER
Pure water plant PURELAB classic UVF	ELGA, Bucks, GB
Quarz precision cuvettes 105.201-QS	Hellma GmbH & Co. KG, Müllheim, GER
Reaction tubes	Sarstedt, Bad Homburg, GER
Rotor HLR6	Sorvall Instruments, Newtown, USA
Rotor JA 10	Beckman Instruments, München, GER
Rotor SW28	Beckman Instruments, München, GER
Rotor Ti70	Beckman Instruments, München, GER
Semi-dry blotting chamber	Workshop, Institute for Physiological Chemistry, LMU Munich
Shaker Multitron II	Infors AG, Bottmingen, CH
SpeedVac vacuum centrifuge	ScanSpeed MaxiVac, Scanvac, Lynge (DK)
Steampot Varioklav	H + P Labortechnik, Oberschleißheim, GER
Sterile Bench	BDK, Genkingen, GER
Sterile filters	Schleicher & Schüll, Kassel, GER
Table shaker	Workshop, Institute for Physiological Chemistry, LMU Munich
Table shaker LS10	Gerhardt, Bonn, GER
Thermomixer comfort	Eppendorf, Hamburg, GER
Thermostat Julabo ED	Julabo Labortechnik GmbH, Seelbach, GER
Universal mixer GT, 4l, polycarbonate bucket, 500 – 17000 / min, 800W	Carl Roth GmbH, Karlsruhe, GER
Venting filter Midisart 2000, Sterile-EO, non-pyrogenic, PTFE- membrane, PP-housing, 0.2 µm	Sartorius Stedim Biotech GmbH, Göttingen, GER

Material and Methods

Vortex Mixer Vortex Genie 2	Bender & Hobein, Zurich, CH
Vortex Mixer VF2	Janke & Kunkel, IKA Labortechnik, Staufen, GER
Voyager-DE STR Time Of Flight mass spectrometer	Applied Biosystems, Carlsbad, CA, USA
Washbottle without head, 10 l for <i>N.c.</i> -cultivation	Duran, Wertheim/Main, GER
Washbottle-head 60/46 without filter disc for 10 l Wash bottle without head for <i>N.c.</i> -cultivation	Stricker, Tutzing, GER
Weighing machine CP2202 S	Sartorius, Mainz, GER
Weighing machine QS 4000	Sartorius, Mainz, GER
Weighing machine L610-D	Sartorius, Mainz, GER
Weighing machine A120S	Sartorius, Mainz, GER
Weighing machine 1475A MP8-2	Sartorius, Mainz, GER
Weighing machine XS205 Dual Range	Mettler Toledo, Giessen, GER
X-Cell SureLock Mini-Cell, gelelectrophoresis chamber	Invitrogen, Carlsbad, CA

6.1.2 Chemicals

All chemicals not listed below were obtained from Merck, Darmstadt, GER.

Chemical	Manufacturer
ACN	Rotisolv Ultra LC-MS, Roth, Karlsruhe (GER)
Acrylamid-Bis (37.5 : 1), 30% (w/v)	Serva, Heidelberg, GER
Agar-agar	Serva, Heidelberg, GER
Amicon Ultra 30 k device	Millipore, Cork, IRL
Amino Acids	Sigma, München, GER
Amino acid minus methionine, 1 mM	Promega, Madison, USA
Aminohexanoic acid	Sigma, St. Louis, MO, USA
Ammonium nitrate	Grüssing, Filsum, GER
Ampicillin	AppliChem, Darmstadt, GER
Anti-Guinea Pig IgG (whole molecule) Peroxidase, Developed in Goat, Affinity isolated antigen specific antibody	Sigma, St. Louis, USA
APS	AppliChem, Darmstadt, GER
Bacto-pepton	DIFCO, Detroit, USA
Bacto-Trypton	DIFCO, Detroit, USA
β-DDM	Glycon Biochemicals, Luckenwalde, GER
β-mercaptoethanol	Sigma, München, GER
Bio-Rad Protein Assay (Bradford reagent)	Bio-Rad Laboratories, München, GER
Bio-Rad Protein Assay Standard I	Bio-Rad Laboratories, Hercules, CA
Bromphenolblue	Serva, Heidelberg, GER
BSA Grade VIII (fatty acid free)	Sigma, München, GER
C18 micro column (75 μm i.d. x 15 cm, packed with C18 PepMap, 3 μm, 100 Å)	Dionex, Benelux B.V.
Coomassie Brilliant Blue R-250	Serva, Heidelberg, GER
DH5α E.coli	Takara Bio Europe/Clontech, Saint-Germain-en-Laye, FR
DMSO	Sigma, St. Louis, MO, USA
Developer for medical X-ray film processing G153 A + B	Agfa Healthcare NV, Mortsels, BEL
Digitonin, high purity	Calbiochem, Darmstadt, GER
DTT	Gerbu Biotechnik GmbH, Gaiberg, GER
EDTA-free complete protease inhibitor	Roche Mannheim GmbH, Mannheim, GER
Ethanol	Serva, Heidelberg, GER
Fuji medical X-ray film Super RX, 100 NIF	FujiFilm Deutschland, Düsseldorf, GER
Freund's Adjuvant incomplete	Sigma, St. Louis, MO, USA

Material and Methods

Gel Drying Film	Promega Corporation, Madison, WI, USA
Glycerol	SIGMA, München, GER
Goat-Anti-Mouse IgG (H + L)-HRP Conjugate	Bio-Rad Laboratories, Hercules, CA
Goat-Anti-Rabbit IgG (H + L)-HRP Conjugate	Bio-Rad Laboratories, Hercules, CA
HEPES	Serva, Heidelberg, GER
Hydrogen peroxide	AppliChem, Darmstadt, GER
Imidazol	AppliChem, Darmstadt, GER
Kodak Bio Max MR film, X-ray film	Carestream Health, Rochester, USA
Lacey carbon film on molybdenum EM grid	Plano GmbH, Wetzlar, GER
Luminol (5-Amino-2,3-dihydro-1,4-phthalazinedione free acid)	Sigma, St. Louis, MO, USA
m ⁷ G(5')ppp(5')G RNA Cap Structure Analog	Amersham Biosciences, Freiburg, GER
Methanol	Serva, Heidelberg, GER
Methionine, non-radioactive	Sigma, St. Louis, MO, USA
Monoclonal Anti-FLAG, antibody produced in mouse, Clone M2, purified immunoglobulin	Sigma, St. Louis, MO, USA
NativePAGE Sample Buffer	Invitrogen, Carlsbad, CA, USA
NativePAGE 5% G-250 Sample Additive	Invitrogen, Carlsbad, CA, USA
NativeMark Unstained Protein Standard	Invitrogen, Carlsbad, CA, USA
NativePAGE 4-16% Bis-Tris Gel, 1.0 mm x 10 well	Invitrogen, Carlsbad, CA, USA
NativePAGE Running Buffer (20x)	Invitrogen, Carlsbad, CA, USA
NativePAGE Cathode Buffer Additive (20x)	Invitrogen, Carlsbad, CA, USA
NHS-activated Sepharose 4 Fast Flow	GE Healthcare, Piscataway, NJ, USA
Ni-NTA agarose	QIAGEN, Hilden, GER
Ni-NTA-Nanogold	Nanoprobe, Yaphank, NY, USA
NuPAGE Transfer Buffer (20x)	Invitrogen, Carlsbad, CA
PageRuler Plus Prestained Protein Ladder	Fermentas, St. Leon-Roth, GER
Parafilm	American National Can, Neenah, WI, USA
PCA	Sigma, St. Louis, MO, USA
Penta-His Antibody, BSA-free, mouse monoclonal IgG ₁	QIAGEN, Hilden, GER
Peptide libraries	JPT Peptide Technologies GmbH, Berlin, GER
PMSF	Serva, Heidelberg, GER
Ponceau S	Serva, Heidelberg, GER
Protease arrest	Calbiochem, Darmstadt, GER
Protran nitrocellulose membrane B A83	Schleicher & Schüll, Kassel, GER

PVDF membrane	Carl Roth GmbH, Karlsruhe, GER
Rabbit Reticulocyte Lysate, nuclease treated	Promega, Madison, USA
Rapit Fixer for medical x-ray film processing G354	Agfa Healthcare NV, Mortsels, BEL
rNTPs, Ribonucleosidtriphosphate set, (100 mM lithium salt solution, 4 x 20 µmol (200 µl))	Boehringer Mannheim GmbH, Mannheim, GER
RNasin Rnase inhibitor, (ribonuclease inhibitor), 40 u/µl	Promega, Madison, USA
SDS	Serva, Heidelberg, GER
³⁵ S-methionine, 10 mCi/ml	ICN Pharmaceuticals, Eschwege, GER
Skimmed milk powder	AppliChem, Darmstadt, GER
SP6-RNA-polymerase, 25 u/µl	Epicentre, Madison, WI, USA
Spermidine, (N-[3-aminopropyl]-1,4-butanediamine)	Sigma, St. Louis, MO, USA
Sucrose, (Saccharose)	Carl Roth GmbH, Karlsruhe, GER
Sulfo Link Coupling Gel	Thermo Scientific, Rockford, USA
TEMED	Serva, Heidelberg, GER
TFA, for peptide synthesis	Roth, Karlsruhe (GER)
TiterMax Gold Adjuvant	Sigma, St. Louis, MO, USA
TNT Reaction buffer	Promega, Madison, USA
TNT Rabbit Reticulocyte Lysate	Promega, Madison, USA
TNT SP6 Polymerase	Promega, Madison, USA
Tris	AppliChem GmbH, Darmstadt, GER
Triton X-100	Sigma, München, GER
Trypsin (sequencing grade modified trypsin)	Promega, Madison, USA
Tween20 (Polyoxyethylene-sorbitan Monolaurate)	Sigma, St. Louis, MO, USA
Unstained Protein Molecular Weight Marker	Fermentas, St. Leon-Roth, GER
Yeast extract	Serva, Heidelberg, GER
Whatman filter paper	Schleicher & Schüll, Kassel, GER
Whatman´s #1 filter paper	Whatman, Maidstone, GBR

6.1.3 Preparation Kits

Preparation Kit	Use	Manufacturer
Flag-Immunoprecipitation Kit	Affinity purification of Flag-tagged proteins	Sigma-Aldrich, Steinheim, GER
Promega Pure Yield Plasmid Midiprep System	Plasmid isolation out of bacteria	Promega, Heidelberg, GER
TNT SP6 Coupled Reticulocyte Lysate System	<i>In vitro</i> synthesis of radioactive precursor protein	Promega, Madison, USA

6.1.4 Medias and buffers

In general, all solutions and medium were prepared with bidestillized water (ddH₂O, Millipore) and were autoclaved or sterile filtered if required. Unless stated otherwise, the pH-value was adjusted with hydrochloric acid and sodium hydroxide solution.

NAME	PRESCRIPTION
<i>Neurospora crassa</i> cultivation	
Biotin solution	dissolve 20 g biotin in 100 ml H ₂ O + 100 ml 95% ethanol
Trace elements solution	(dissolved in H ₂ O) 50 mg/ml Citric acid, 50 mg/ml ZnSO ₄ , 10 mg/ml Fe[(NH ₄) ₂ SO ₄], 2.5 mg/ml CuSO ₄ , 0.5 mg/ml MnSO ₄ ·H ₂ O, 0.5 mg/ml water-free H ₃ BO ₃ , 0.5 mg/ml Na ₂ MoO ₄
Vogel's 50x stock solution	(amounts for 1 l 50x stock solution) 150 g Na ₃ -citrate·2H ₂ O, 100 g KH ₂ PO ₄ , 10 g MgSO ₄ , 5 g CaCl ₂ , 2.5 ml biotin solution and 5 ml stock solution of trace elements
Histidine 100x stock solution	2 mg/ml
Vogel's minimal liquid medium	1x Vogel's, 2% Sucrose, 1x histidine if needed
Vitamin solution	0.01 mg/ml vitamin B1, 0.005 mg/ml vitamin B2, 0.005 mg/ml vitamin B6, 0.005 mg/ml, aminobenzoic acid 0.005 mg/ml nicotinamide, 0.1 mg/ml cholin-hydrochloride, 0.001 mg/ml folic acid, 0.1 mg/ml inositol, 0.05 mg/ml calcium pantothenate
Vogel's minimal solid medium	(for 50 ml medium / Erlenmeyer flask) 1 ml Vogel's 50x stock solution, 1 ml 50% sucrose solution, 0.5 ml 100x histidine stock solution if needed, 1 g agar powder, autoclave and allow the medium to solify
Vogel's full solid medium	(for 50 ml medium / Erlenmeyer flask) 1 ml Vogel's 50x stock solution, 1 ml 50% sucrose solution, 0.5 ml 100% glycerine, 0.25 ml vitamin solution, 0.125 g yeast extract, 0.05 g casein hydrolysate, 0.5 ml 100x histidine stock solution 1 g agar powder, autoclave and

	allow the medium to solify
10 % (w/v) Skimmed milk for silica stocks	10 g skimmed milk powder in 100 ml water, autoclave and store at 4°C
Silica gel	O ₂ Si, ~ 0.2 – 1 mm Ø granules, aliquots of 1 g were heat sterilized at 180°C for 3 hours in glas vials
Isolation of mitochondria and OMVs from <i>Neurospora crassa</i>	
0.25 M SET-buffer	250 mM Sucrose, 1 mM EDTA, 1 mM PMSF, 20 mM Tris, pH 8.5
0.25 M ST-buffer	250 mM Sucrose, 1 mM PMSF, 20 mM Tris, pH 8.5
0.7 M SET-buffer	0.7 M Sucrose, 1 mM EDTA, 20 mM Tris, pH 8.5
0.9 M SET-buffer	0.9 M Sucrose, 1 mM EDTA, 20 mM Tris, pH 8.5
2 M SET-buffer	2 M Sucrose, 1 mM EDTA, 20 mM Tris, pH 8.5
Tris/EDTA-buffer	1 mM EDTA, 20 mM Tris, pH 8.5
OMV-buffer	1mM PMSF, 20 mM Tris, pH 8.5
Cultivation of <i>Saccharomyces cerevisiae</i>	
Lactate medium, liquid	0.3% (w/v) yeast extract, 0.1% (w/v) KH ₂ PO ₄ , 0.1% (w/v) NH ₄ Cl, 0.05% (w/v) CaCl ₂ · 2 H ₂ O, 0.05% (w/v) NaCl, 0.11% (w/v) MgSO ₄ · 6 H ₂ O, 0.0003% (w/v) FeCl ₃ , 2 % (v/v) lactic acid, pH 5.5 adjusted with KOH
Lactate medium, solid	0.3% (w/v) yeast extract, 0.1% (w/v) KH ₂ PO ₄ , 0.1% (w/v) NH ₄ Cl, 0.05% (w/v) CaCl ₂ · 2 H ₂ O, 0.05% (w/v) NaCl, 0.11% (w/v) MgSO ₄ · 6 H ₂ O, 0.0003% (w/v) FeCl ₃ , 2 % (v/v) lactic acid, 2% (w/v) agar, pH 5.5 adjusted with KOH
Isolation of mitochondria from <i>Saccharomyces cerevisiae</i>	
Resuspension buffer	10 mM DTT, 100 mM Tris, pH 9.4
Sorbitol buffer	1.2 M sorbitol, 20 mM KH ₂ PO ₄ , pH 7.4 adjusted with KOH
Homogenization buffer	0.6 M sorbitol, 1 mM EDTA, 0.2% (w/v) BSA, 1 mM PMSF, 10 mM Tris, pH 7.4
SEH-buffer	0.6 M sorbitol, 1 mM EDTA, 20 mM HEPES, pH 7.4 adjusted with KOH
Chemical competent <i>E. coli</i> cells	
CaCl ₂ -solution	0.1 M CaCl ₂
LB-medium	1% (w/v) (bacto-)trypton, 0.5% (w/v) yeast extract, 1% (w/v) NaCl (for culture plates ad 1.5% (w/v) agar
Plasmid transformation into <i>E. coli</i> cells	
LB-medium with selective antibiotics	in general: ampicillin, 100 µg/ml
<i>In vitro</i> synthesis of radioactive precursor proteins	
DTT-solution	0.1 M
MgAc	15 mM
m ⁷ G(5')ppp(5') G RNA Cap Structure Analog	2.5 mM
methionine solution (non-radioactive)	58 mM
ribonucleoside triphosphates (rNTPs)	2.5 mM ATP, GTP, UTP, CTP diluted in H ₂ O
Sucrose solution	1.5 M

Transcription buffer (5x)	50 mM MgCl ₂ , 10 mM spermidine, 200 mM Tris, pH 7.5
Isolation of the TOB complex by Ni-NTA affinity purification	
Ni-NTA solubilization buffer	10% (v/v) glycerol, 1 mM PMSF, 15 mM imidazole, 50 mM HEPES, pH 8.5
Ni-NTA wash buffer	1 mM PMSF, 50 mM HEPES, pH 8.5
Isolation of the TOB complex by Flag-tag affinity purification	
Flag solubilization buffer	10% (v/v) glycerole, 1 mM PMSF, 50 mM HEPES, pH 8.5
Flag washing buffer	1 mM PMSF, 0.084% (v/v) Triton X-100, 50 mM HEPES, pH 8.5
Isolation of the TOM core complex	
Solubilization buffer	300 mM NaCl, 20% (v/v) glycerol, 20 mM imidazole, 1% (w/v) β -DDM, 1 mM PMSF (freshly added), 20 mM Tris-Cl pH 8.5
Equilibration buffer	20% (v/v) glycerol, 0.2% (w/v) β -DDM, 1mM PMSF, 50 mM Tris-Cl pH 8.5
TOM washing buffer 1	300 mM NaCl, 10% (v/v) glycerol, 20 mM imidazole, 0.1% (w/v) β -DDM, 1 mM PMSF, 20 mM Tris-Cl pH 8.5
TOM washing buffer 2	10% (v/v) glycerol, 40 mM imidazole, 0.1% (w/v) β -DDM, 1 mM PMSF, 50 mM KAc/MOPS pH 7.2
TOM elution buffer	10% (v/v) glycerol, 300 mM imidazole, 0.1% (w/v) β -DDM, 1 mM PMSF, 50 mM KAc/MOPS pH 7.2
ResQ low salt buffer	10% (v/v) glycerol, 0.03% (w/v) β -DDM, 50 mM KAc/MOPS pH 7.2
ResQ high salt buffer	10% (v/v) glycerol, 7.457% (w/v) KCl, 0.03% (w/v) β -DDM, 50 mM KAc/MOPS pH 7.2
Gel filtration buffer	0.03% (w/v) β -DDM, 10 mM KAc/MOPS pH 7.2
Isolation of the BCS1-complex	
NaPi-buffer	1 M Na ₂ PO ₄ was titrated with 1M NaH ₂ PO ₄ to pH 8.0
Protease arrest, 100x	dissolved in DMSO according to instructions
Solubilisation buffer	3% (w/v) digitonin, 100 mM NaCl, 20 mM imidazole, 5% (v/v) glycerol, 1x protease arrest, 50 mM NaPi-buffer, pH 8.0
Washing buffer	0.1% (w/v) digitonin, 100 mM NaCl, 20 mM imidazole, 5% (v/v) glycerol, 50 mM NaPi-buffer, pH 8.0
Elution buffer	0.1% (w/v) digitonin, 100 mM NaCl, 400 mM imidazole, 5% (v/v) glycerol, 50 mM NaPi-buffer, pH 8.0
SDS PAGE and TCA precipitation	
72% TCA	72% (w/v) TCA in H ₂ O
4x Laemmli	8% (w/v) SDS, 20% (v/v) β -mercaptoethanol, 240 mM Tris, pH 6.8, 40% (v/v) glycerol, 0.02% (w/v) bromphenolblue
2x Laemmli	4% (w/v) SDS, 10% (v/v) β -mercaptoethanol, 120 mM Tris, pH 6.8, 20% (v/v) glycerol, 0.01% (w/v) bromphenolblue
5 % SDS-gel	5 % acrylamide-bis (37.5 : 1), 30% (w/v), 60 mM Tris, pH 6.8, 0.1% (w/v) SDS, 0.05% (w/v) APS, 0.1% (v/v) TEMED
12.5% SDS-gel	12.5 % acrylamide-bis (37.5 : 1), 30% (w/v), 380 mM Tris, pH 8.8 0.1% (w/v) SDS, 0.06% (w/v) APS, 0.06% (v/v) TEMED
SDS-running buffer	24.8 mM Tris, 1.9 M glycine, 0.1% (w/v) SDS

Western blotting	
SDS-transfer buffer	0.1% (w/v) SDS, 192 mM glycine, 25 mM Tris, pH not adjusted
Staining of proteins	
Coomassie destaining solution	30% (v/v) methanol, 10% (v/v) acetic acid, pH not adjusted
Coomassie staining solution	45% (v/v) methanol, 40% (v/v) acetic acid, 0.2% (w/v) Coomassie Brilliant Blue R-250, pH not adjusted
Ponceau S solution	0.2% (w/v) Ponceau S, 3% (w/v) TCA, pH not adjusted
Peppspot protein interaction assay	
Blocking buffer	3% BSA (w/v), 2.7 mM KCl, 137 mM NaCl, 50 mM Tris, pH 8.0
Anode buffer I	20% (v/v) methanol, 30 mM Tris, pH not adjusted
Anode buffer II	20% (v/v) methanol, 300 mM Tris, pH not adjusted
Cathode buffer	20% (v/v) methanol, 40 mM aminohexanoic acid, 25 mM Tris, pH 9.2
PBS-buffer (10x)	150 mM NaCl, 9.2 mM Na ₂ HPO ₄ , 1.6 mM NaH ₂ PO ₄ , pH 7.2
Regeneration buffer IA	2% (w/v) SDS, 100 mM β-mercaptoethanol, 62.5 mM Tris, pH 6.7
TBS-buffer	2.7 mM KCl, 137 mM NaCl, 50 mM Tris, pH 8.0
T-TBS-buffer	0.05% (v/v) Tween20, 2.7 mM KCl, 137 mM NaCl, 50 mM Tris, pH 8.0
Binding studies of mitochondrial precursor proteins to the isolated TOB complex	
Beads binding buffer	0.084% (v/v) TX-100, 15 mM imidazole, 50 mM HEPES, pH 7.8
Beads washing buffer	0.084% (v/v) TX-100, 5 mM imidazole, 5 mM MgCl ₂ , 50 mM HEPES, pH 7.8
Tryptic digestion of protein samples for mass spectrometry analysis	
ACN/TFA-solution	50% (v/v) ACN, 0.25% TFA, pH not adjusted
DTT-solution	10 mM DTT, 25 mM NH ₄ HCO ₃ , pH not adjusted
IAA-solution	55 mM IAA, 25 mM NH ₄ HCO ₃ , pH not adjusted
NH ₄ HCO ₃ -buffer	25 mM NH ₄ HCO ₃ , pH 7.6
Trypsin-solution	200 ng/μl trypsin in 50 mM acetic acid, pH not adjusted
Mass spectrometry analysis of protein samples by electrospray ionisation	
Buffer A	0.1% (v/v) FA in HPLC grade water, pH not adjusted
Buffer B	80% (v/v) ACN, 0.1% (v/v) FA in HPLC grade water, pH not adjusted
Immunodecoration	
TBS-buffer	154 mM NaCl, 10 mM Tris, pH 7.5
ECL-reagent	1.24 mM luminol, 0.2 mM PCA, 100 mM Tris, pH 8.5; add H ₂ O ₂ to a final concentration of 0.012% (v/v) directly before use
Flag-TBS-buffer	138 mM NaCl, 2.7 mM KCl, 50 mM Tris, pH 8.0
Luminol	248 mM luminol (= 5-Amino-2,3-dihydro-1,4-phthalazinedione free acid) in DMSO
PCA	91.35 mM in DMSO
Affinity purification of antibodies	
Antiserum solution	6.5 ml rabbit antiserum, 1.2 ml 25 x EDTA free complete protease inhibitor solution, 22.3 ml 10 mM Tris, pH 7.5

Material and Methods

Cystein-buffer	50 mM (L)-cysteine, 5 mM EDTA, 50 mM Tris, pH 8.5
Glycine-solution	100 mM glycine, pH 2.5
NaCl-solution	1 M NaCl
Na ₂ HPO ₄ -solution	100 mM Na ₂ HPO ₄ , pH 11.5
NaN ₃ -buffer	0.05% NaN ₃ , 5 mM EDTA, 50 mM Tris, pH 8.5
Sodium citrate solution	100 mM trisodium citrate (C ₆ H ₅ Na ₃ O ₇ ·2H ₂ O), pH 4.0
Sulfo Link-buffer	5 mM EDTA, 50 mM Tris, pH 8.5
10 mM Tris-buffer, pH 7.5	10 mM Tris, pH 7.5
10 mM Tris-buffer, pH 8.8	10 mM Tris, pH 8.8
1 M Tris-buffer, pH 8.8	1 M Tris, pH 8.8
Tris/NaCl-buffer	0.5 M NaCl, 10 mM Tris/HCl, pH 7.5
NHS-Sepharose Coupling buffer	200 mM NaHCO ₃ , 500 mM NaCl, pH 8.3
NHS-Sepharose Tris buffer	100 mM Tris, pH 8.5
PBS-buffer	137 mM NaCl, 2.7 mM KCl, 10 mM Na ₂ HPO ₄ , 1,76 mM KH ₂ PO ₄
Cryo-electron microscopy	
Nanogold washing buffer	1 mM PMSF, 0.084% (v/v) Triton X-100, 50 mM HEPES, pH 8.5

6.1.5 *Neurospora crassa* strains

Strain	Genotype	Origin or source and reference (if applicable)
NCN251 (also called 74A)	A	FGSC 2489
76-26	<i>his-3 mtrR a</i> (<i>mtrR</i> imparts fpa resistance)	R.L. Metzenberg
71-18	<i>pan-2 BmlR a</i> (<i>BmlR</i> imparts benomyl resistance)	R.L. Metzenberg
HP1	Heterokaryon of 76-26 plus 71-18	F. Nargang
Δ Tob55 (Tob55KO-1)	Sheltered heterokaryon. As HP1, but with replacement of the <i>tob55</i> gene in 76-26 nucleus with a hygromycin resistance (<i>hygR</i>) cassette.	F. Nargang (120)
Δ Tob55 (Tob55KO-3)	As Tob55KO-1	As Tob55KO-1
T55His6-1	<i>his-3 mtrR a Δtob55 ::hygR</i> contains an ectopic copy of genomic <i>tob55</i> with N-terminal hexahistidinyl tag. Also bleomycin resistant.	F. Nargang (120)
T55His6-3	As T55His6-1, but different clone	As T55His6-1
ST55-2	<i>his3 mtrR a Δtob55 ::hygR</i> contains an ectopic copy of <i>tob55</i> cDNA specific for the short form.	F. Nargang (120)
IT55-8	<i>his3 mtrR a Δtob55 ::hygR</i> contains an ectopic copy of <i>tob55</i> cDNA specific for the intermediate form.	F. Nargang (120)
LT55-2	<i>his3 mtrR a Δtob55 ::hygR</i> contains an ectopic copy of <i>tob55</i> cDNA specific for the long form.	F. Nargang (120)
His9-Tob55 (H6C4-5)	<i>his-3 mtrR a Δtob55 hygR</i> Contains an ectopic copy of genomic <i>tob55</i> with an N-terminal nine His tag. Also bleomycin resistant.	F. Nargang (108)
His9-Tob55ST	<i>his-3 mtrR a Δtob55 ::hygR</i> contains an ectopic copy of <i>tob55</i> cDNA specific for the short form with an N-terminal nine His-tag. Also bleomycin resistant.	F. Nargang

55FH123	<i>his-3 mtrR a Δtob55 hygR</i> Contains an ectopic copy of <i>tob55</i> cDNA specific for the short form with with an N-terminal nine His-tag, and an ectopic copy of <i>tob55</i> cDNA specific for the intermediate form with an N-terminal Flag-tag. Also bleomycin and benomyl resistant.	F. Nargang
ΔTob37 (Tob37KO-5)	Sheltered heterokaryon. As HP1, but with replacement of <i>tob37</i> gene in 76-26 nucleus with a hygromycin resistance (<i>hygR</i>) cassette.	F. Nargang
His9-Tob37 (9His-Tob37-2)	<i>his-3 mtrR a Δtob37 hygR</i> Contains an ectopic copy of genomic <i>tob37</i> with a C-terminal nine His tag. Also bleomycin resistant.	F. Nargang, (108)
ΔTob38 (Tob38KO-6)	Sheltered heterokaryon. As HP1, but with replacement of <i>tob38</i> gene in 76-26 nucleus with a hygromycin resistance (<i>hygR</i>) cassette.	F. Nargang
His9-Tob38 (9His-Tob38-3)	<i>his-3 mtrR a Δtob38 hygR</i> Contains an ectopic copy of genomic <i>tob38</i> with a C-terminal nine His tag. Also bleomycin resistant.	F. Nargang (108)
Δmdm10	Δmdm10 <i>his-3 mtrR hygR a</i> Replacement of <i>mdm10</i> gene in 76-26 with hygromycin resistance (<i>hygR</i>) cassette	F. Nargang (108)
GR 107	expression of a Tom22 with a hexahistidiny tag at its C-terminus	W. Neupert (31, 164)

6.1.6 *Saccharomyces cerevisiae* strain

Strain	Genotype	Origin or source and reference (if applicable)
N-His6-Bcs1 in Δ bcs1	W303a	Kai Hell, N. Wagener, W. Neupert

6.1.7 Peptides

Name of peptide	Sequence	Use	Origin
Tob38Nc-8	RDPEYTDLLDRFYI TPASS	Injection into rabbits for synthesis of polyclonal antibodies against Tob38 from <i>N. crassa</i> ; the peptide was coupled to KLH before injection.	Peptide corresponds to the residues 146 – 182 of the Tob38 protein from <i>N. crassa</i> .
Tob38Nc-4	C - RDPEYTDLLDRFYI TPASS	Used for affinity purification of antibodies against Tob38 from <i>N. crassa</i> out of antiserum	Peptide corresponds to the residues 146 – 182 of the Tob38 protein from <i>N. crassa</i> with an extra cystein at the N-terminus.
Tob38Nc-9	KYMSDAEGEVEGN MGFILASRK	Injection into rabbits for synthesis of polyclonal antibodies against Tob38 from <i>N. crassa</i> ; the peptide was coupled to KLH before injection.	Peptide corresponds to the residues 269 – 290 of the Tob38 protein from <i>N. crassa</i> .
Tob38Nc-5	C- KYMSDAEGEVEGN MGFILASRK	Used for affinity purification of antibodies against Tob38 from <i>N. crassa</i> out of antiserum	Peptide corresponds to the residues 269 – 290 of the Tob38 protein from <i>N. crassa</i> with an extra cystein at the N-terminus.
Tob37Nc-10	DTDAEMERLEREE REREAAG	Injection into rabbits for synthesis of polyclonal antibodies against Tob37 from <i>N. crassa</i> ; the peptide was coupled to KLH before injection. Used for affinity purification of antibodies against Tob37 out of antiserum.	Peptide corresponds to the residues 165 – 184 of the Tob37 protein from <i>N. crassa</i> .

Tob37Nc-11	KRRIKLEGLAAEVF DVLGEVDF	Injection into rabbits for synthesis of polyclonal antibodies against Tob37 from <i>N. crassa</i> ; the peptide was coupled to KLH before injection. Used for affinity purification of antibodies against Tob37 out of antiserum.	Peptide corresponds to the residues 212 – 233 of the Tob37 protein from <i>N. crassa</i> .
Tob37Nc-12	VGLGSFGAAGAMF AGLA	Injection into rabbits for synthesis of polyclonal antibodies against Tob37 from <i>N. crassa</i> ; the peptide was coupled to KLH before injection. Used for affinity purification of antibodies against Tob37 out of antiserum.	Peptide corresponds to the residues 426 – 442 of the Tob37 protein from <i>N. crassa</i> .
Mdm10Nc-22	EDNKYNELNATSR HELELID	Injection into rabbits for synthesis of polyclonal antibodies against Mdm10 from <i>N. crassa</i> ; the peptide was coupled to KLH before injection.	Peptide corresponds to the residues 20 – 32 of the Mdm10 protein from <i>N. crassa</i> , primary sequence modified in the Nargang lab (108).
Mdm10Nc-C22	C- EDNKYNELNATSR HELELID	Used for affinity purification of antibodies against Mdm10 from <i>N. crassa</i> out of antiserum	Peptide corresponds to the residues 20 – 32 of the Mdm10 protein from <i>N. crassa</i> , primary sequence modified in the Nargang lab (108) with an extra cystein at the N-terminus.
Mdm10Nc-23	ATKNDEYKGVLKA RLD	Injection into rabbits for synthesis of polyclonal antibodies against Mdm10 from <i>N. crassa</i> ; the peptide was coupled to KLH before injection.	Peptide corresponds to the residues 332 - 333 and 423 – 425 of the Mdm10 protein from <i>N. crassa</i> , primary sequence modified in the Nargang lab (108).

Mdm10Nc-C23	C- ATKNDEYKGVLKA RLD	Used for affinity purification of antibodies against Mdm10 from <i>N. crassa</i> out of antiserum	Peptide corresponds to the residues 332 - 333 and 423 – 425 of the Mdm10 protein from <i>N. crassa</i> , primary sequence modified in the Nargang lab (108) with an extra cysteine at the N-terminus.
Mdm10Nc-25	HKLGEPFRSLGEVQ YSS	Injection into rabbits for synthesis of polyclonal antibodies against Mdm10 from <i>N. crassa</i> ; the peptide was coupled to KLH before injection.	Peptide corresponds to the residues 463 – 480 of the Mdm10 protein from <i>N. crassa</i> , primary sequence modified in the Nargang lab (108).
AQUA55	EDGFGVFISDAR	Isotopic labelled peptide (heavy peptide) used for the quantification of the Tob55 subunit in the isolated TOB complex; arginine substituted by isotopic arginine (bold) (¹³ C ₆ , ¹⁵ N ₄), mass shift +10 Da	Thermo Fisher Scientific GmbH, Ulm, GER
AQUA38	DPEYTDLLDR	Isotopic labelled peptide (heavy peptide) used for the quantification of the Tob38 subunit in the isolated TOB complex; arginine substituted by isotopic arginine (bold) (¹³ C ₆ , ¹⁵ N ₄), mass shift +10 Da	Thermo Fisher Scientific GmbH, Ulm, GER
AQUA37	VYADSQAYK	Isotopic labelled peptide (heavy peptide) used for the quantification of the Tob37 subunit in the isolated TOB complex; lysine substituted by isotopic lysine (bold) (¹³ C ₆ , ¹⁵ N ₂), mass shift +8 Da	Thermo Fisher Scientific GmbH, Ulm, GER

6.1.8 Whitehead codes and molecular masses of selected proteins from *Neurospora crassa*

Protein	Whitehead code	Molecular mass (kDa)
Tob55	NCU05593	54.7 (long), 54.1 (intermediate), 50.7 (short)
Tob37	NCU00923	48.6
Tob38	NCU01401	37.3
Tom40	NCU01179	38.1
Mdm10	NCU07824	52.7
porin	NCU00431	30

For further information seek the complete *N. crassa* genome database:

<http://www.broadinstitute.org/annotation/genome/neurospora/FeatureSearch.html>

6.1.9 Antibodies

Primary antibody	Blocking buffer	Dilution primary antibody	Secondary antibody	Dilution secondary antibody
anti-His Penta-His Antibody, BSA-free, mouse monoclonal IgG ₁	3% (w/v) BSA in TBS-buffer	1 : 1000 in 3% (w/v) BSA in TBS-buffer	Goat-Anti-Mouse IgG (H + L)-HRP Conjugate	1:3000 in 10% (w/v) skimmed milk powder in TBS-buffer
anti-Flag Monoclonal Anti-FLAG, antibody produced in mouse, Clone M2, purified immunoglobulin	3% (w/v) skimmed milk powder in Flag-TBS-buffer	1:1900 in 3% (w/v) skimmed milk powder in Flag-TBS-buffer	Goat-Anti-Mouse IgG (H + L)-HRP Conjugate	1:3000 in 3% (w/v) skimmed milk powder in Flag-TBS-buffer
rabbit antisera or affinity purified antibodies Polyclonal Antibodies risen in rabbits by antigen injection; affinity purification was performed if required	5% (w/v) skimmed milk powder in TBS-buffer	1:30 – 1:24000 in 5% (w/v) skimmed milk powder in TBS-buffer	Goat-Anti-Rabbit IgG (H + L)-HRP Conjugate	1:10000 in 5% (w/v) skimmed milk powder in TBS-buffer

6.1.10 Plasmids

Plasmid	Description	Reference
pGEM4	empty	Promega, Madison, USA
pGEM4PorinNc	Porin from <i>N. crassa</i> expressed under control of Sp6-promotor, ampicillin resistance	W. Neupert (165)
pGEM4Su9DHFR	fusion protein of mitochondrial targeting sequence of subunit 9 of F _o -ATPase from <i>N. crassa</i> and dihydrofolate reductase (DHFR) from mouse expressed under control of Sp6-promotor, ampicillin resistance	W. Neupert (166)
pGEM4Tom22Nc	Tom22 from <i>N. crassa</i> expressed under control of Sp6-promotor, ampicillin resistance	N. Pfanner (163)
pGEM4Tom40Nc	Tom40 from <i>N. crassa</i> expressed under control of Sp6-promotor, ampicillin resistance	N. Pfanner (167)

6.2 Methods

Unless stated otherwise, methods were performed at room temperature.

6.2.1 Cell biology

6.2.1.1 Cultivation of *Neurospora crassa*

Growth and handling of *N. crassa* were performed as described previously (168). For the cultivation of *N. crassa*, solid Vogel's growth medium was inoculated with a few granules of the silica stock of the strain of interest in Erlenmeyer flasks. These A-flasks were incubated for 48 hours in the dark at 30°C and subsequently for around 190 hours at light at room temperature. With mycelium from the A-flasks, a second lot of flasks was inoculated and cultivated as described for the A-flasks. The fungus was harvested from the solid medium with 50 ml sterile water per flask and vigorous swirling and used for inoculating liquid medium.

For a 2 l-culture, 1.9 l of Vogel's minimal liquid medium were mixed with 100 ml of harvested *N. crassa*. For a 50 l-culture, a 10 l-preculture was started with 1 liter of harvested mycelium and 9 l Vogel's minimal liquid medium containing 40 µg/ml chloramphenicol. After 6 hours, 40 liters of Vogel's minimal medium were mixed with this preculture and cultivated for another 14 – 16 hours. Cultivation in liquid medium was performed at 30°C with constant aeration. The mycelium was harvested by filtration of the liquid medium.

6.2.1.2 Preparation of silica stocks from *Neurospora crassa*

Mycelium of one to two A-flasks was harvested with a total volume of 50 ml 10 % (w/v) skimmed milk and vigorous swirling. The solution was filtered through an autoclaved funnel filled with cotton batting. 300 µl of the filtrate were mixed with 1 g silica gel in a glass vial, dried in an exicator at room temperature for 3 weeks and stored at -20°C.

6.2.1.3 Isolation of mitochondria from *Neurospora crassa*

Mycelia were ground in the presence of sand and 0.25 M SET-buffer. The sand was separated from the cell extract by two sequential centrifugation steps at 2594 x g for 5 minutes. The cell organelles in the supernatant were sedimented at 10976 x g for 50 minutes at 4°C. The mitochondria were scraped off from the very top of the resulting pellet and resuspended in 0.25 M ST-buffer. After homogenization of the mitochondria they were again sedimented at 10976 x g for 50 minutes at 4°C, resuspended in a smaller amount of 0.25 M ST-buffer and

homogenized. The concentration of mitochondrial proteins was determined by Bradford assay.

6.2.1.4 Isolation of outer mitochondrial membrane vesicles from *Neurospora crassa*

Mycelia were ground in the presence of sand and 0.25 M SET-buffer. The sand was separated from the cell extract by two sequential centrifugation steps at 2594 x g for 5 minutes. The cell organelles in the supernatant were sedimented at 10976 x g for 50 minutes at 4°C. The mitochondria were scraped off from the very top of the resulting pellet and resuspended in 0.25 M SET-buffer. After homogenization of the mitochondria the amount of mitochondrial protein was determined by Bradford assay. The homogenized mitochondria were spun down at 10976 x g for 50 minutes at 4°C, resuspended in 0.25 M SET-buffer and incubated at 37°C for 5 minutes. Afterwards, mitochondria were transferred into swelling buffer under stirring at 4°C to a final concentration of 1 g mitochondrial proteins per litre of swelling buffer. Following 30 minutes of stirring, the resulting mitoplasts were sedimented at 10976 x g for 30 minutes and resuspended in a smaller volume of 0.25 M SET-buffer. With an automated glass-teflon-homogenizer, the outer mitochondrial membrane was sheared off the mitoplasts for 40 minutes at 4 °C. 20 ml of the homogenate was applied on a step gradient of 20 ml 0.9 M - SET buffer at the bottom and 9 ml of 0.25 M SET-buffer and centrifuged for 1 hour at 141370 x g, 4°C. The vesicles of the outer mitochondrial membrane could be taken from a thin layer between the 0.9 M SET-buffer and the 0.25 M SET-buffer and were mixed with half of the volume of 2 M SET-buffer. 15 ml of these outer mitochondrial membrane vesicles (OMVs) were overlaid with 20 ml 0.7 M SET-buffer and 3 ml Tris/EDTA-buffer and centrifuged at 141370 x g overnight at 4°C. OMVs could be collected from the interface between the Tris/EDTA-buffer and the 0.7 M SET-buffer. The double volume of OMV-buffer was added and the OMVs were centrifuged for 1 hour at 183960 x g. Finally, the sedimented OMVs were dissolved in OMV-buffer. The protein concentration was determined by Bradford assay and aliquots of the OMVs were shock frozen in liquid nitrogen and stored at -80°C.

6.2.1.5 Cultivation of *Saccharomyces cerevisiae*

Cultivation of the *Saccharomyces cerevisiae* yeast strain “N-His6-Bcs1 in $\Delta bcs1$ ” was performed according to standard procedures (169). Yeast from a glycerine-stock were struck out on solid lactate complete medium and cultivated at 30°C. After 2 days of cultivation, yeast from the solid medium were used for the inoculation of liquid lactate medium and incubated under moderate shaking at 30°C.

6.2.1.6 Preparation of glycerol stocks from *Saccharomyces cerevisiae*

For the preparation of stocks of *S. cerevisiae*, yeast cells from solid medium plates were mixed with 15% (v/v) glycerol in water and stored at -80°C.

6.2.1.7 Isolation of mitochondria from *Saccharomyces cerevisiae*

Mitochondria from *S. cerevisiae* were isolated according to standard procedures as described before (170). Yeasts were cultivated in liquid medium to an OD₆₀₀ of 1 – 1.5 and harvested by centrifugation at 2800 x g for 5 min at room temperature (RT). The cells were washed with sterile water and resuspended to a final concentration of 0.5 g/ml yeast cells in resuspension buffer and incubated for 10 min at 30°C under moderate shaking. Following centrifugation 2000 x g for 5 min at 4°C, the cells were washed again with a final concentration of 0.16 g/ml yeast cells in sorbitol buffer. For the digestion of the cell wall, 2.5 mg zymolyase were added per g yeast cell and incubation was performed for 30 – 45 min at 30°C under moderate shaking. Resulting spheroplasts were harvested by centrifugation at 2000 x g for 5 min at 4°C and homogenized 10 times in a Dounce-homogenizer at 4°C with a final concentration of 0.16 g/ml spheroplasts in homogenization buffer. After centrifugation at 2000 x g for 5 min at 4°C, the supernatant was stored on ice and the remaining pellet was again resuspended and homogenized as described before. The supernatants of the first and second homogenization were pooled and centrifuged at 2000 x g for another 5 min at 4°C to sediment cell remnants. Mitochondria were spun down by centrifugation at 17000 x g for 12 min at 4°C and resuspended in SEH-buffer. Cell remnants were again separated by centrifugation at 2000 x g for 5 min at 4°C and the mitochondria in the supernatant were pelletized by centrifugation at 17000 x g for 12 min at 4°C. Mitochondria were resuspended in SEH-buffer with a final concentration of 10 mg/ml protein, aliquotted, frozen in liquid nitrogen, and stored at -80°C.

6.2.1.8 Preparation of cryostocks from *Escherichia coli* cells

For storage 1 ml of an *Escherichia coli* (*E. coli*) overnight culture was mixed with 1 ml 87% glycerol and kept at -80°C.

6.2.1.9 Chemical competent *Escherichia coli* cells

500 ml of LB-medium were inoculated with 5ml overnight-culture of *E. coli* and grown at 37°C to an OD₆₀₀ of 0.4. Following incubation on ice for 15 minutes the bacteria were spun down at 1756 x g for 15 minutes at 4°C. The pellet was resuspended in 40 ml CaCl₂-solution and after 30 minutes on ice, the bacteria were harvested by centrifugation at 1756 x g for 15 minutes at 4°C. After resuspending the pellet in 20 ml CaCl₂-solution, 4 ml glycerol, 100% were added and the bacteria were incubated on ice for 2 hours. 200 µl aliquots of the suspension were shock-frozen in liquid nitrogen and subsequently stored at -80°C.

6.2.2 Molecular biology

6.2.2.1 Plasmid transformation into Escherichia coli cells

For amplification, in general plasmids were transformed into DH5 α *E. coli* cells. For that, 100 μ l of chemical competent *E. coli* cells were thawed on ice and mixed with 1 μ l of purified plasmid and incubated on ice for 15 minutes. After a heat shock for 30 seconds at 42°C, the cells were placed on ice for 2 minutes. Subsequently, 800 μ l LB-medium without any selective antibiotics was added and the cells were shaken at 37°C for 45 minutes. A small amount of the bacteria were outplated on LB-medium with and without selective antibiotics and incubated overnight at 37°C to monitor the transformation efficiency. 55 ml of LB-medium with selective antibiotics were inoculated with the remaining bacteria suspension and incubated over night at 37°C for the following plasmid isolation.

6.2.2.2 Plasmid isolation out of Escherichia coli cells

Plasmids were isolated from 50 ml overnight bacteria culture with the Promega Pure Yield Plasmid Midiprep System - Kit according to the instructions. For the determination of the DNA-content, the eluate with the purified plasmid was diluted 1 : 50 with water and analyzed photometrically as described (6.2.2.3). The yield of ~ 400 μ l purified plasmids was stored at -20°C.

6.2.2.3 Photometrical quantification of nucleic acids

The DNA-concentration was determined photometrically by measuring the absorption of the solution at 260 nm in a quartz crystal cuvette. Absorption of 1 corresponds to 50 μ g/ml double strand DNA.

6.2.2.4 In vitro synthesis of radioactive precursor proteins

6.2.2.4.1 In vitro transcription

For the synthesis of radioactive precursor proteins, plasmid DNA encoding for the protein of interest under the control of the SP6-promotor was transcribed by the SP6-RNA-polymerase to RNA. For that, a transcription mix (50µl) with 3 - 10 µg of purified plasmids, 10 mM MgCl₂, 2 mM spermidine, 10 mM DTT, 1.6 u/µl RNasin RNase (ribonuclease) inhibitor, 0.5 mM ribonucleoside triphosphates (rNTPs), 0.13 mM m⁷G(5')ppp(5')G, 0.75 u/ml SP6-RNA-polymerase and 40 mM Tris (pH 7.5) was incubated for 1 hour at 37°C. The RNA was precipitated at -20°C for 30 minutes in the presence of 244 mM LiCl and 73% ethanol. Following a centrifugation at 36000 x g for 20 minutes at 2°C, the pellet was washed with 150 µl cold 70% (v/v) ethanol and DNA was spun down again at 36000 x g for 20 minutes at 2°C. After evaporation of the ethanol at RT, the pellet was resuspended in water supplemented with 1.54 u/µl RNasin RNase inhibitor solution. RNA was stored at -20°C.

6.2.2.4.2 In vitro translation

For the translation of the protein of interest from the isolated mRNA, a translation mix (45 µl) with 6.25 µl RNA, 25 µl rabbit reticulocyte lysate, 0.875 µl amino-acid mix without methionine, 0.25 µl RNasin RNase inhibitor and 3 µl ³⁵S-methionine (radioactive methionine) was incubated for one hour at 30°C. The synthesis of radioactive protein was stopped by adding 3.2 mM methionine (non-radioactive methionine) and 167 mM sucrose. 1 µl and 3 µl of the synthesized protein were analyzed by SDS-PAGE and Western blotting followed by autoradiography. The protein was shock-frozen in aliquots in liquid nitrogen and stored at -80°C.

6.2.2.4.3 TNT coupled reticulocyte lysate system

In the TNT coupled reticulocyte lysate system, transcription and translation were performed in the same reaction mix. The TNT-mix (50 µl), containing 25 µl TNT rabbit reticulocyte lysate, 2 µl TNT Reaction buffer, 1 µl TNT SP6 Polymerase, 1 µl amino-acid mix without methionine, 4 µl ³⁵S-methionine (radioactive methionine), 1 µl RNasin RNase inhibitor and 1-3 µg plasmid-DNA, was incubated for 1.5 hours at 30°C. When radioactive porin precursor was synthesized, the reaction was already stopped after 40 minutes. Following the addition of 3.7 mM methionine (non-radioactive) and 194 mM sucrose, the protein was shock-frozen in

Material and Methods

aliquots in liquid nitrogen and stored at -80°C . 1 μl and 3 μl of the synthesized protein were analyzed by SDS-PAGE and Western blotting followed by autoradiography.

6.2.3 Protein biochemistry

6.2.3.1 Autoradiography

Radioactive proteins were detected by exposing a X-ray film (Kodak) on the dried membrane with immobilized proteins for different time spans, ranging from a few hours to 15 days. Exposure times depended on the signal intensities observed after developing the films

6.2.3.2 Isolation of the TOB complex by Ni-NTA affinity chromatography

OMVs from *N. crassa* were solubilized in Ni-NTA solubilization buffer for 2 hours in the presence of 0.192% (v/v) Triton X-100 or 0.64% (w/v) digitonin, resulting in an detergent/protein ratio of 6/1 (TX-100) and 20/1 (digitonin), respectively. After a centrifugation step for clarification at 36000 x g for 20 minutes, the supernatant was loaded on a Ni-NTA agarose column (1.66 mg solubilized protein / 100 µl matrix, 100%) for affinity purification. The column was rinsed stepwise with 16 column volumes (CVs) of Ni-NTA washing buffer with 15 mM imidazole, 25 CVs with 20 mM imidazole and 10 CVs with 40 mM imidazole. Bound proteins were eluted with Ni-NTA washing buffer with 200 mM imidazole. Depending on the detergent used, the Ni-NTA washing buffer contained either 0.084 % Triton X-100 or 0.24% (w/v) digitonin. The isolation was performed at 4°C.

6.2.3.3 Isolation of the TOB complex by Flag-tag affinity purification

OMVs from *N. crassa* were solubilized in Flag solubilization buffer for 2 hours in the presence of 0.192 % Triton X-100. After a centrifugation step for clarification at 36000 x g for 20 minutes, the supernatant was loaded on ANTI-FLAG M2-Agarose Affinity Gel (1.66 mg solubilized protein / 10 µl matrix, 100%) and incubated for 2 hours with gentle agitation. Following a centrifugation at 4000 x g for 3 minutes, the supernatant with the unbound proteins was removed. The ANTI-FLAG M2-Agarose Affinity Gel with the bound proteins was transferred to a Mini-frit column in an 2 ml reaction tube and rinsed 5 times with 10 CVs of Flag washing buffer. After an incubation of 2 minutes, the washing buffer was removed by a centrifugation step at 4000 x g for one minute each. For elution, 2.5 CVs of Flag washing buffer with 5 µg/µl three fold Flag peptide was added to the matrix and incubated for 30 minutes with gentle agitation. Bound proteins were sedimented at 4000 x g for 1 minute. The isolation was performed at 4°C.

6.2.3.4 Isolation of the TOM core complex

The TOM core complex was isolated according to a protocol established by Patrick Schreiner in the group of W. Neupert (LMU, Munich, GER), as listed below. The protocol was adapted from “Structural investigation of two supramolecular complexes of the eukaryotic cell: the proteasome and the mitochondrial TOM complex”, (171).

TOM core complex was isolated from a *N. crassa* strain (GR-107) that carried a version of Tom22 with a hexahistidiny tag at its C-terminus. The TOM core complex was isolated according to Ahting et al., 1999 (172), with some modifications in the protocol. Isolated mitochondria were solubilized in solubilization buffer at a protein concentration of 10 mg/ml for 30 min at 4°C. Insoluble material was removed by centrifugation, and the clarified extract was loaded onto the equilibrated Ni-NTA agarose column using 4 ml resin per g of total mitochondrial protein. The column was washed with 5 CVs of TOM washing buffer 1 and with 10 CVs of TOM washing buffer 2. The bound protein was eluted with 4 CVs of TOM elution buffer. The eluted fraction of the Ni-NTA column was loaded onto an equilibrated Resource Q anion exchange column. The complex was eluted with a linear potassium chloride gradient. For further purification, the fractions containing TOM core complex were pooled, concentrated to 500 µl (spin filtration devices from Pall Corporation, 100 kDa cut-off) and loaded onto a Superose 6 size exclusion column. Proteins were eluted in gel filtration buffer. Stock solutions of purified TOM core complex were stored at a protein concentration of 10-20 mg/ml at 4°C. An average preparation of the protein started with ~1.5 kg of *Neurospora* cells (wet weight) which yielded about 5 g of mitochondrial proteins and 1-2 mg of purified TOM core complex.

6.2.3.5 Isolation of the BCS1 complex

Mitochondria isolated from the “N-His6-Bcs1 in $\Delta bcs1$ ” *Saccharomyces cerevisiae* strain were resuspended in solubilisation buffer by pipetting. After incubation for 10 min on ice in the presence of 3% (w/v) digitonin, unsolubilized mitochondria were sedimented by centrifugation at 10000 x g for 10 min at 4°C and the supernatant was loaded on a Ni-NTA agarose batch (5 mg solubilized protein / 100 µl matrix, 100%) for affinity purification. Following incubation of 1 hour at 4°C under gentle agitation, the beads were subjected to three washing steps in which the matrix beads were resuspended in washing buffer, spun down at 1000 x g for 1 min at 4°C and resuspended again in fresh buffer. For elution of the bound proteins, the matrix was incubated for 10 min in elution buffer at 4°C and eluted proteins were separated from the matrix beads by centrifugation at 1000 x g for 1 min at 4°C.

The isolation of the BCS1 complex was performed according to a protocol established by N. Wagener (Neupert group, LMU, Munich, GER).

6.2.3.6 Carbonate extraction

OMVs were resuspended in 100 mM Na₂CO₃ with different pH values of 10.8, 11.5 and 12.5 and incubated for 30 minutes on ice. As a control, proteins were treated with 10 mM HEPES-KOH, pH 7.4. By centrifugation for one hour at 125800 x g, transmembrane proteins were sedimented and could thereby be separated from the soluble and membrane associated proteins in the supernatant. The proteins in the supernatant were precipitated with trichloroacetic acid as described (6.2.3.8).

6.2.3.7 Protein concentration

If needed, the isolated proteins of the TOB complex were concentrated by using an Amicon Ultra 30k device. Centrifugation was performed at 4000 x g at 4°C.

6.2.3.8 Protein precipitation

Proteins in solution were mixed with 1/5th volume of 72% trichloroacetic acid (TCA) and frozen overnight at -20°C. The precipitated proteins were sedimented at 36000 x g for 15 minutes at 4°C and washed with 100% acetone. The pellet was dried at 35°C for 30 minutes and, unless stated otherwise, resolved by cooking in 2 x Laemmli at 95°C for 5 minutes.

6.2.3.9 Determination of the protein concentration by Bradford assay

The protein concentration was determined by adding 1ml of a 1:5 dilution of the “Bio-Rad Protein assay” solution to the samples of same volume. Following 5 minutes of incubation at RT, the absorbance at 595 nm was measured in a 10 mm path length microcuvette. The protein solution of interest was diluted and 2.5 µl, 5 µl and 7.5 µl were measured twice. The protein concentration was calculated according to a standard curve, measured in parallel with 48 µg, 24 µg, 12 µg, 6 µg, 3 µg, 1.5 µg and 0 µg of the “Bio-Rad Protein Assay Standard I”.

6.2.3.10 SDS-Polyacrylamide gel electrophoresis (SDS-PAGE)

By denaturing discontinuous sodiumdodecylsulfate polyacrylamide gelelectrophoresis (SDS-PAGE) proteins were separated according to their molecular mass as described previously

(173). Proteins were solved in 2 x Laemmli and cooked for 5 minutes at 95°C, applied on a 5% SDS-gel and separated on a 12.5% SDS-gel. The gels used had a size of 140 mm x 140 mm and a thickness of 1 mm. Standard running conditions were 30 mA for 2 – 3 hours at RT in SDS-running buffer. By comparison with marker proteins of known size running on the same gel, the molecular weight of the sample proteins could be estimated.

6.2.3.11 Blue Native-Polyacrylamide gel electrophoresis (BN-PAGE)

Proteins from mitochondria (60 – 120 µg) or OMVs (10 – 30 µg) were solubilized in 1 x NativePAGE sample buffer containing 0.9% - 1.8% (v/v) TX-100 or 0.75% - 6% (w/v) digitonin, resulting in a protein/detergent ratio of 6/1 (TX-100) and 10/1 – 40/1 (digitonin), respectively. Following 1 hour of incubation on ice, the samples were centrifuged for clarification at 20 000 x g for 30 minutes and the supernatant was mixed with NativePAGE 5 % G-250 sample additive to adjust the final G-250 concentration in the sample to at least 1/4th of the detergent concentration. BN-PAGE was performed as previously described (142, 174) with NativePAGE Novex 4-16 % Bis-Tris Gel according to the instructions. All buffers were used and gelelectrophoresis was performed at 4°C. The bovine heart mitochondria used as protein standard for the mass estimation in the BN-PAGE analysis were provided by Ilka Wittig (Schägger group, Goethe-University Frankfurt, Frankfurt am Main, GER).

6.2.3.12 In gel staining of proteins with Coomassie brilliant blue

After SDS- or BN-PAGE, the separated proteins in the gel were stained with the Coomassie Brilliant Blue dye. The gel was shaken in Coomassie staining solution for at least 30 minutes at RT. Subsequently, the stained gel was rinsed several times with water and incubated with Coomassie destaining solution until distinct bands became visible. After scanning for documentation, the gel was dried overnight between two gel-drying films.

6.2.3.13 Transfer of proteins to a nitrocellulose membrane (Western blotting)

Unless stated otherwise, proteins separated by SDS-PAGE were transferred by the semi-dry blotting procedure (175, 176) onto nitrocellulose membrane. SDS-gels, nitrocellulose membrane and Whatman filter paper were incubated in SDS-transfer buffer for ca. 1 minute at RT. One Whatman filter paper was placed on the anode electrode plate followed by the nitrocellulose membrane, the SDS-gel, another Whatman filter paper and the cathode

electrode plate. Transfer was performed at RT at 200 mA or 230 mA for 1 or 1.5 hours, respectively.

6.2.3.14 Transfer of proteins to a PVDF membrane (Western blotting)

For transferring proteins from BN-gels by the semi-dry blotting procedure, a PVDF (polyvinylidene fluoride) membrane was incubated in 100% methanol for 1 minute and afterwards rinsed in 1 x NuPAGE Transfer Buffer. The BN-gel was incubated in SDS-running buffer for 4 minutes and rinsed in 1 x NuPAGE Transfer Buffer. Whatman filter paper was also soaked with 1 x NuPAGE Transfer Buffer for 1 minute. One Whatman filter paper was placed on the anode electrode followed by the PVDF-membrane, the BN-gel, another Whatman filter paper and the cathode electrode plate. Transfer was performed at 130 mA for 1 hour. All buffers were used and protein transfer was performed at 4°C. After the blotting, the proteins were fixed on the membrane by shaking in 8% acetic acid for 15 minutes at RT and subsequently air-dried.

6.2.3.15 Reversible staining of blotted proteins by Coomassie Brilliant Blue solution

To visualize proteins transferred to a PVDF-membrane, the wet PVDF-membrane was incubated in Coomassie staining solution for 30 to 60 seconds at RT and rinsed in Coomassie destaining solution to remove the background staining. Visible marker proteins were marked with a pen on the membrane. The membrane was then further destained by shaking in 100% methanol for 1 to 2 minutes, rinsed in TBS-buffer and either air-dried or used for immunodecoration.

6.2.3.16 Reversible staining of blotted proteins by Ponceau S solution

To verify the transfer of proteins on a nitrocellulose membrane, the membrane was shaken in Ponceau S solution for two minutes at RT after blotting. The immobilized proteins were reversibly stained by the Ponceau dye and the membrane was rinsed in water to remove the background staining. Afterwards, the membrane was air-dried.

6.2.3.17 Pepspot protein interaction assay

To analyze specific binding of the isolated TOB complex to its substrates Tom40 and Porin and to identify their specific binding sites, a pepspot binding assay was performed.

Peptide libraries of peptides with 15 amino acids in length and an overlap of 11 amino acids were synthesized (JPT Peptide Technologies GmbH, Berlin, GER). Each peptide was covalently bound to a spot on a cellulose-PEG-membrane by the C-terminus (pepspot membrane). By acetylation the charged N-terminus was transformed into an uncharged peptide end and thereby provided the peptide with higher stability towards degradation and higher resemblance to the uncharged native peptide side. Cysteins were substituted with serins to prevent oxidation and cyclization of the peptide.

For the protein interaction assay, the pepspot membrane was rinsed in 100% methanol for one minute followed by three washing steps with TBS-buffer for 10 minutes at RT. After blocking unspecific sites of the pepspot membrane with blocking buffer for three hours, the membrane was washed in T-TBS-buffer for 10 minutes. Isolated TOB complex from the His9-Tob37 strain was added to the membrane at an estimated concentration of 5 µg/ml in blocking buffer supplemented with 0.042% (v/v) TX-100 and incubated overnight at 4°C with gentle agitation. The next day, the incubation was continued for three more hours at RT and subsequently rinsed three times for one minute with T-TBS-buffer. Bound TOB complex was transferred to a PVDF-membrane by the semi-dry blotting procedure as follows: two Whatman filter papers were incubated in anode buffer II and placed on the anode electrode followed by another two Whatman filter paper and a PVDF membrane soaked in anode buffer I. Subsequently, the pepspot membrane was put onto the stack upside down and covered with two Whatman filter paper pretreated with cathode buffer and the cathode electrode plate. The blotting was performed three times with 1.0 mA / cm² pepspot membrane; twice for 30 minutes and the last time for one hour at RT. After blotting, the PVDF-membranes were transferred to T-TBS-buffer.

The bound TOB complex was detected by immunodecoration against the histidin-tagged subunit of the TOB complex as described (6.2.4.1) with slight modifications: blocking was performed for three hours at RT, incubation with primary antibody was done overnight at 4°C and the secondary antibody was diluted 1:3000 in 5% (w/v) skimmed milk powder in TBS-buffer.

Pepspot membranes were washed in T-TBS-buffer three times for 10 minutes and stored at 4°C. To prepare the pepspot membranes for another protein-interaction assay, they were regenerated by shaking them three times for 10 minutes in water at RT, four times for 30

minutes in regeneration buffer I at 50°C, three times for 10 minutes in 10x-PBS-buffer at RT, three times for 20 minutes in T-TBS buffer at RT and finally three times for 10 minutes in TBS at RT. Regeneration efficiency was tested by blotting the pepspot membrane once for 2 hours and subsequent anti-histidin immunodecoration as described above.

To control the specificity of the binding sites of the TOB complex, pepspot protein interaction assays were performed with isolated TOM core complex out of *N. crassa* and BCS1 complex out of *S. cerevisiae*. The assay was performed in the very same way except for the fact that the complex was incubated with the peptide library in blocking buffer supplemented with 0.03% (w/v) DDM (TOM core complex) or 0.12% (w/v) Digitonin (BCS1 complex).

6.2.3.18 Binding studies of mitochondrial precursor proteins to the isolated TOB complex

As described in 6.2.3.2 “Isolation of the TOB complex by Ni-NTA affinity chromatography”, the TOB complex isolation was performed until the washing step of the bound proteins with buffer containing 40 mM imidazole. Subsequently, the column was rinsed with 5 CVs of Beads washing buffer. Aliquots of the beads with bound TOB complex were resuspended in 16 bead batch volumes (BVs) of Beads binding buffer supplemented with 2 mM ATP. Radioactive precursor proteins were added to the beads and incubated for 30 minutes on ice. Afterwards, the batch was washed twice with 16 BVs of Beads binding buffer. Beads were sedimented at 1000 x g for 2 minutes during the washing steps. All steps were performed at 4°C.

Subsequently, bound proteins were eluted with 2 x Laemmli and cooking for 5 min at 95°C. The eluted proteins were separated by SDS-PAGE and transferred on a nitrocellulose membrane. Co-purified radioactive proteins were detected by autoradiography.

6.2.3.19 Tryptic digestion of protein samples for mass spectrometry analysis

After SDS- or BN-PAGE followed by Coomassie blue staining, protein bands of interest were excised from the gel and frozen at -20°C in water until tryptic digestion. After thawing, the gel pieces were washed twice with water and twice with NH₄HCO₃-buffer for 10 minutes at RT. To dry the gel pieces, they were treated three times with acetonitrile (ACN) for 10 minutes at RT. Afterwards, remaining ACN was evaporated for 2 minutes. The gel pieces were reduced in dithiothreitol (DTT) solution for one hour at RT and subsequently treated with 2-Iodacetamide (IAA) solution for 30 minutes at RT avoiding light exposure. Next, they were washed once with NH₄HCO₃-buffer and three times with ACN for 10 minutes at RT.

Remaining ACN was again evaporated for 5 minutes. Trypsin (300 – 400 ng) was now added to each dried gel piece. After 2 - 3 minutes, the gel pieces were covered with NH₄HCO₃-buffer to a total volume of 50 µl and incubated for 12 – 16 hours at 37°C under moderate shaking (550 rpm).

6.2.3.20 Mass spectrometry analysis of protein samples by matrix-assisted laser desorption ionization-time of flight (MALDI-TOF)

For the identification of the different Tob55-protein isoforms, bands in the corresponding molecular weight range were excised and digested overnight with trypsin as described. Tryptic fragments in the range of 500 – 3500 Da were obtained by reflector matrix-assisted laser desorption ionization-time of flight (MALDI-TOF), whereas peptides in the range of 3500 – 6000 Da were analyzed by linear MALDI-TOF. Measurements were performed on a Voyager-DE STR Time Of Flight (TOF) mass spectrometer. With the PeptideMass program set for isotope averaging, predicted peptide masses could be obtained (177, 178). The automated database search of peptide spectra was performed with the MASCOT software (Matrix Science) on the complete *N. crassa* genome database (<http://www.broad.mit.edu/annotation/fungi/neurospora/>). MALDI-TOF analysis was performed in collaboration with Lars Israel (Imhof group, LMU Munich, GER).

6.2.3.21 Mass spectrometry analysis of protein samples by nano-electrospray ionisation-LC-tandem MS (ESI-LC-MS/MS)

For protein identification, the tryptic fragments were separated on a C18 reverse phase column by a linear acetonitrile gradient running from 5 – 60% (v/v) buffer B in buffer A within 40 minutes followed by 60 – 95% (v/v) within 10 minutes. The peptides eluting from the HPLC were directly analyzed by nano-electrospray ionization-LC-tandem MS (ESI-LC-MS/MS), recorded on an Orbitrap mass spectrometer. Spectra analysis was performed with the MASCOT software (Matrix Science) on the complete *N. crassa* genome database (<http://www.broad.mit.edu/annotation/fungi/neurospora/>). ESI-LC-MS/MS analysis was performed in collaboration with Lars Israel (Imhof group, LMU Munich, GER).

6.2.3.22 Peptide quantification by Isotope Dilution Mass Spectrometry (IDMS)

To determine the absolute and relative amounts the TOB complex subunits Tob55, Tob38 and Tob37 in the isolated TOB complex, the isolated complex was excised from a BN-gel and the

gel piece was dried as described (6.2.3.21, p. 110). A defined amount of AQUA- (AbsoluteQuantification-) peptides, quantified stable isotope ($^{13}\text{C}/^{15}\text{N}$) labelled internal peptide standards, were mixed with the shrunken gel pieces before tryptic digestion. Digested proteins were analyzed as described in 6.2.3.21 by ESI-LC-MS/MS. By comparison of the peak areas in the extracted ion chromatogram (EIC) of each AQUA peptide and the native counterpart, the amount of each native peptide was calculated. IDMS analysis was performed in collaboration with Lars Israel (Imhof group, LMU Munich, GER).

6.2.4 Immunology

6.2.4.1 Immunodecoration of immobilized proteins

By immunodecoration with specific antibodies, immobilized proteins of interest could be detected on a membrane. PVDF-membranes were prepared in 100% methanol for one minute and rinsed with TBS-buffer. Nitrocellulose- as well as PVDF-membranes with immobilized proteins were incubated for 10 minutes in TBS-buffer. Blocking of membrane sites not associated with immobilized proteins was performed by incubation with blocking buffer for 30 to 60 minutes. Afterwards, membranes were shaken in a solution of primary antibody for 1 to 2 hours at RT or overnight at 4°C, rinsed three times for 10 minutes with TBS-buffer, incubated for 45 minutes in a solution with horseradish peroxidase (HRP) coupled secondary antibody and washed again three times for 10 minutes with TBS-buffer. Following one minute of incubation with ECL-reagent, luminescence was recorded with X-ray films (FujiFilm). Blocking buffer, dilution of primary and secondary antibodies are listed in 6.1.9 “Antibodies” above. The dilution of the primary antibodies was dependant from the titer of the antiserum or antibody solution.

6.2.4.2 Synthesis of polyclonal antibodies in rabbits

For the synthesis of specific polyclonal antibodies, rabbits were injected with artificially synthesized antigen peptides from the protein of interest (see 6.1.7 “Peptides”). The antigen was injected subcutaneously into the upper shoulder area. The first injection was performed with 500 µg of peptide mixed with an equal volume of TiterMax Gold Adjuvant. After two weeks, the boost immunization was started, meaning that the rabbit was injected every four weeks with 250 – 500 µg of antigen peptide mixed with the equal volume of Freund’s Adjuvant Incomplete. 8 – 10 Days after injection 20 – 30 ml blood were taken from the ear artery of the rabbit. Following a centrifugation of the clotted blood at 3220 x g for 5 minutes at RT, the serum was transferred to a new tube and centrifuged again at 27200 x g for 15 minutes at RT. The clarified serum was incubated for 20 – 30 minutes at 56°C in a water bath to inactivate the complement system. The serum was stored at -20°C. For testing the sera, proteins from mitochondria and OMVs from *N.c. strains* expressing, as well as knock-out strains, lacking the protein of interest, were separated by SDS-PAGE, blotted and immunodecorated with the antisera.

6.2.4.3 Affinity purification of antibodies

To increase titer and specificity of the used antibody solution, specific antibodies were extracted out of antisera by affinity purification. For that, antigens were coupled to a matrix. In case of a Sulfo-Link matrix, antigens with an extra cysteine at one terminus were solved in Sulfo-Link buffer in a concentration of 1 mg/ml protein. The Sulfo-Link matrix was packed in a column and rinsed with 6 CVs Sulfo-Link buffer. Antigen peptides were given to the equilibrated matrix in the column and allowed to bind for 15 minutes at RT with gentle agitation. Afterward the column was fixed in a stand clamp and the matrix was left to sediment for 30 more minutes without agitation. Unbound antigens were removed by washing the column with 3 CVs of Sulfo-Link buffer. For blocking unspecific sites, the matrix was incubated with one CV of cysteine-buffer for 15 minutes at RT with gentle agitation and incubated for 30 more minutes without shaking. Then the matrix was washed with 16 CVs NaCl-solution. Before storage at 4°C, the column was washed with NaN₃-buffer.

In case of a NHS-activated sepharose matrix, peptides were bound by their amino group to an agarose matrix. For swelling, 1 g NHS-activated Sepharose 4 Fast Flow was incubated with 1 mM HCl at 4°C for 20 minutes. After mild centrifugation at 1000 x g for 15 seconds at 4°C, the supernatant was discarded and the beads were washed three times with NHS-Sepharose coupling buffer. 5-10 mg of peptides were solved in NHS-Sepharose coupling buffer in a concentration of 1-3 mg/ml and were immobilized on the Sepharose for 2 – 4 hours at RT with gentle agitation. Free binding sites on the Sepharose were blocked by incubation with NHS-Sepharose Tris-buffer for 1 hour at RT. The beads were intensively washed with PBS-buffer and stored in 20% ethanol at 4°C.

For antibody purification, the antigen-coupled matrix was equilibrated by rinsing with 10 CVs of 10 mM Tris-buffer, pH 7.5. Weakly bound antigen was removed by washing subsequently with 10 CVs of glycine-solution, 10 mM Tris-buffer (pH 8.8), Na₂HPO₄-solution, 10 mM Tris-buffer (pH 8.8) and 10 mM Tris-buffer (pH 7.5), each. The matrix was incubated with the antiserum solution for 1.5 hours and subsequently washed with 10 CVs 10 mM Tris-buffer (pH 7.5) and Tris/NaCl-buffer, each.

Elution of the antibodies was performed stepwise by washing with elution buffers of different pH-values. First, 10 CVs of sodium citrate solution were added. 1ml fractions were collected in tubes with 200 µl of 1M Tris-buffer (pH 8.8). Afterwards, 10 CVs of glycine-solution were loaded on the column and fractions were taken as described above. Subsequently, the column was rinsed with 10 CVs of 10 mM Tris-buffer (pH 8.8) and the last elution step consisted of rinsing the matrix with 10 CVs of Na₂HPO₄-solution. 1-ml fractions were collected in tubes

with 200 µl of glycine-solution. Finally, the column was washed with 10 CVs 10 mM Tris-buffer (pH 7.5) and 2 CVs of NaN₃-buffer and stored at 4°C.

The antibody content was initially assessed by application of 20 µl of each fraction on a nitrocellulose membrane and subsequent staining with Ponceau S solution. The best fractions were tested in an immunodecoration of membranes with immobilized test proteins.

6.2.4.4 Antibody supershifts of proteins in Blue Native-Polyacrylamide gel electrophoresis (BN-PAGE)

OMVs were treated with detergent as described above (6.2.3.11, BN-PAGE). Where indicated, 1 µg QUIAGEN Penta-His antibody was added to the solubilized proteins. Following one hour of incubation on ice, the samples were centrifuged for clarification at 36000 x g for 30 minutes and the supernatant was mixed with NativePAGE 5 % G-250 sample additive (Invitrogen, Carlsbad, CA) to adjust the final G-250 concentration in the sample to at least 1/4th of the detergent concentration and separated by BN-PAGE as stated before.

6.2.5 Cryo-electron microscopy

The TOB complex was isolated as described earlier (6.2.3.2) using TX-100. 4 μl were applied to a lacey carbon film on molybdenum EM grids blotted with Whatman's #1 filter paper and flash frozen in liquid ethane or an ethane-propane mixture cooled by liquid nitrogen. To identify a given subunit the His-tag used for isolation was labelled with Ni-NTA-Nanogold with gold particles of 1.8 nm. The Ni-NTA nanogold was mixed with the purified complex in ratios of 1:4, 1:6 and 1:9 (v/v). After incubation for 45 min on ice, the TOB/nanogold mixture was applied to EM grids as described above and serially washed three times on droplets of aqueous buffer to remove excess of gold label before they were blotted and flash frozen. The plunging of the grids was either performed at RT or at 4°C.

The samples are stored under liquid nitrogen and microscopy is performed at liquid nitrogen temperature ($\sim -175^\circ\text{C}$). Data acquisition was performed on a Tecnai F20 microscope operating at 120 kV, using a Gatan 656 cryo-holder. Images were recorded with the TOM_acquisition package (179) acquiring images on a 4K FEI EAGLE CCD (charge-coupled device) camera at 84270x magnification, corresponding to 1.78 Å/pixel. The images were collected with a defocus range (ΔF) from -0.7 and 3.5 μm with an electron dose of 15-25 $\text{e}^-/\text{Å}^2$. Initial selection of the images was done with WEB (180). The defocus contrast transfer function (CTF) for each image was determined and the image phases were corrected using *TOM_ctffindgui*. The power spectra could be examined and compared with the determined defocus. Images with incorrectly determined defocus or drift were excluded from analysis. Astigmatism was corrected. Particles were picked automatically from the phase corrected micrographs using a set of scripts written for SPIDER (System for Processing Image Data from Electron microscopy and Related fields) (180, 181). The picking algorithm calculates a band pass filter based on the expected size of the particle. The filter includes data from 1/2 to 4 times the particle diameter. A 2D average of unaligned particles is used as a reference for alignment. A number of cross correlation peaks in excess of the expected particle number per image is requested. This number is reduced by accepting only peaks corresponding to particles which are separated by more than 1.5 times the diameter, particles which overlap are excluded. The particles boxes are cut from the image and are then masked and realigned in x and y to the original reference. Particles which needed to be shifted more than 5 pixels were excluded from the data set. It was empirically determined that false positives tend to require significant shifts when masked and realigned.

Further data processing was performed with the SPIDER software package. Initially, the particle images underwent several iterations of reference free alignment and averaging. Reference free alignment starts with an arbitrary blob for a reference and then aligns all images to this. An average is calculated which then becomes the new reference. All images are sequentially aligned to the current average after the current image has been subtracted from the average. When the images no longer change alignment parameters the iterations stop. The aligned images were then subject to classification.

The particle images underwent several rounds of alignment by cross correlation to a set of reference projections. No high resolution structure of any component of the TOB complex has been determined to date. FhaC from *Bordetella pertussis*, a related transport machinery belonging to the same Omp85-TpsB superfamily as Tob55, has been solved (121) and is structurally homologous to Tob55. A 3D structural homology model of the Tob55 protein was made based on the FhaC structure and Tob55 secondary structure prediction (HHpred and MODELLER, LMU gene center). This 3D model was used as a starting point for building models of the complex. With these complex models starting references were generated. Models with spheres of uniform density were added on the cytoplasmic side of the Tob55 model approximating the volumes for Tob37 and Tob38. Two spheres, 6 spheres and a continuous ring of density were tried as starting models; the continuous ring seemed to bias the results the least.

Images are aligned to 2D projections through a 3D model along predetermined views. The views are calculated to be equally separated in distance on a hemi-sphere representing the approximate diameter of the object. The direction of the projection has a known Euler angle associated with it. When the images are aligned to the model projections the Euler angle of the best matching model projection is assigned to the image and used in generating the 3D reconstruction. Thereby, an improvement of the reconstruction of the TOB complex could be achieved with increasing rounds of alignment and reconstruction.

Superposition of structures was done with the UCSF Chimera program (Resource for Biocomputing, Visualization, and Informatics, University of California, San Francisco, CA, USA).

7 Abbreviations

AAC – ATP-ADP carrier

ACN – acetonitrile

APS – ammonium peroxy disulphate

AQUA – AbsoluteQuantification (peptides)

ADP – adenosine diphosphate

ATP – adenosine triphosphate

BAM – bacterial β -barrel assembly machinery

β -DDM - n-dodecyl- β -D-maltoside

BHM – bovine heart mitochondria

BN – blue native

BNGE – blue native gel electrophoresis

BN-PAGE – blue native polyacrylamide gel electrophoresis

BSA – bovine serum albumin

BV – batch volume

CCD – charged-coupled device

CCHL – cytochrome c heme lyase

CCPO – cytochrome c peroxidase

CTF – contrast transfer function

cDNA – complementary desoxyribonucleic acid

cryo-EM – cryo-electron microscopy

CTP – cytidine triphosphate

CV – column volume

Da – Dalton

ΔF – defocus range

$\Delta\psi$ – membrane potential

Abbreviations

DHFR – dihydrofolate reductase

DLD – D-lactate dehydrogenase

DMSO – dimethyl sulfoxide

DNA – deoxyribonucleic acid

DTT – dithiothreitol

E. coli – Escherichia coli

ECL – electrochemical luminescence

EDTA – ethylenedinitrilotetraacetic acid (also Titriplex III)

Erv – essential for respiration and viability

ESI-LC-MS/MS – nano-electrospray ionization-LC-tandem mass spectrometry

F₁β – β-subunit of ATP synthase

Fe/S cluster – iron-sulfur cluster

FGSC – Fungal Genetics Stock Center

Fha – filamentous haemagglutinin adhesin

FPA – p-fluorophenylalanine

GIP – general insertion pore

GTP – guanosine triphosphate

His – histidine

HEPES – 2-[4-(2-hydroxyethyl)piperazin-1-yl]ethanesulfonic acid

HPD – His-Pro-Asp

HRP – horseradish peroxidase

Hsp – heat shock protein

Hz – hertz

IAA – 2-Iodacetamide

IDMS – isotope diluted mass spectrometry

IMS – intermembrane space

kDa – kilodalton

KLH – keyhole limpet hemocyanin

LB – Luria-Bertani

LHON – Leber’s hereditary optic neuropathy

LMU – Ludwig-Maximilians-Universität München

MALDI-TOF – matrix-assisted laser desorption ionization time of flight

MELAS – mitochondrial encephalomyopathy with lactic acidosis and stroke-like episodes

MDM – mitochondrial distribution and morphology

MIA – mitochondrial intermembrane space import and assembly (machinery)

Mim – mitochondrial import (protein)

min – minute

MPP – matrix processing peptidase

mRNA – messenger ribonucleic acid

mtHsp – (mitochondrial) matrix heat shock protein

mtDNA – mitochondrial desoxyribonucleic acid

MS – mass spectrometry

mtHsp – matrix heat shock protein

MTS – matrix targeting signal

N.c. – *Neurospora crassa*

N. crassa – *Neurospora crassa*

NHS – N-hydroxysuccinimide

Ni-NTA – nickel-nitriloacetic acid

NBD – nucleotide binding domain

NTP – nucleoside triphosphate

Omp – outer membrane protein

OMV – outer mitochondrial membrane vesicle

OXA – oxidase assembly (complex)

PAGE – polyacrylamide gel electrophoresis

Abbreviations

PAM – presequence translocase-associated motor

pH – potentia Hydrogenii

Pi – inorganic phosphate

PBD – peptide binding domain

PBR – peripheral benzodiazepine receptor

PCA – p-coumaric acid

PMSF – phenylmethylsulfonylfluoride

POTRA – polypeptide transport associated (domain)

PVDF – polyvinylidene fluoride

RCSB PDB – **R**esearch **C**ollaboratory for **S**tructural **B**ioinformatics **P**rotein **D**ata **B**ank

RNA – ribonucleic acid

RNase – ribonuclease

rNTP – ribonucleoside triphosphate

RT – room temperature

SAM – sorting and assembly machinery

SDS – sodiumdodecylsulfate

SDS-PAGE – sodiumdodecylsulfate polyacrylamide gel electrophoresis

SPIDER – **S**ystem for **P**rocessing **I**mage **D**ata from **E**lectron microscopy and **R**elated fields

Su9 - subunit 9 of F_o-ATPase from *Neurospora crassa*

TBS – Tris buffered saline

TCA – trichloroacetic acid

TEMED - N, N, N', N'-Tetramethylethylenediamine

TFA – trifluoroacetic acid

TIM – translocase of the inner (mitochondrial) membrane

TOB – topogenesis of mitochondrial outer membrane β -barrel proteins (complex)

TOC – translocon at the outer envelope membrane of chloroplasts

TOF – Time of flight

TOM – translocase of the outer (mitochondrial) membrane

TPR – tetratricopeptide repeat

Tps – Two-partner secretion

tRNA – transfer ribonucleic acid

Tris – trishydroxyaminomethan

Tween20 – polyoxyethylene-sorbitan monolaurate

TX-100 – Triton X-100

UTP – uridine triphosphate

VDAC – voltage-dependent anion-selective channel

W – Watt

wt – wild type

8 References

1. Henze, K., and Martin, W. (2003) Evolutionary biology: essence of mitochondria, *Nature* 426, 127-128.
2. Alberts, B. (1994) *Molecular biology of the cell*, 3rd ed., Garland Pub., New York.
3. Voet, D., Voet, J. G., and Pratt, C. W. (2006) *Fundamentals of biochemistry : life at the molecular level*, 2nd ed., Wiley, Hoboken, N.J.
4. Emelyanov, V. V. (2003) Mitochondrial connection to the origin of the eukaryotic cell, *Eur J Biochem* 270, 1599-1618.
5. Gray, M. W., Burger, G., and Lang, B. F. (1999) Mitochondrial evolution, *Science* 283, 1476-1481.
6. Kurland, C. G., and Andersson, S. G. (2000) Origin and evolution of the mitochondrial proteome, *Microbiol Mol Biol Rev* 64, 786-820.
7. Martin, W., and Muller, M. (1998) The hydrogen hypothesis for the first eukaryote, *Nature* 392, 37-41.
8. Mokranjac, D., and Neupert, W. (2009) Thirty years of protein translocation into mitochondria: unexpectedly complex and still puzzling, *Biochim Biophys Acta* 1793, 33-41.
9. Wiesner, R. J., Ruegg, J. C., and Morano, I. (1992) Counting target molecules by exponential polymerase chain reaction: copy number of mitochondrial DNA in rat tissues, *Biochem Biophys Res Commun* 183, 553-559.
10. Chan, D. C. (2006) Mitochondria: dynamic organelles in disease, aging, and development, *Cell* 125, 1241-1252.
11. Futuyma, D. J. (2005) On Darwin's shoulders., *Natural History* 114, 64-68.
12. Reichert, A. S., and Neupert, W. (2004) Mitochondriomics or what makes us breathe, *Trends Genet* 20, 555-562.
13. Zeviani, M. (2004) Mitochondrial disorders, *Suppl Clin Neurophysiol* 57, 304-312.
14. Westermann, B. (2008) Molecular machinery of mitochondrial fusion and fission, *J Biol Chem* 283, 13501-13505.
15. Campbell, N. A., Williamson, B., and Heyden, R. J. (2006) *Biology: Exploring Life*, Pearson Prentice Hall, Boston, Massachusetts.
16. Hajnoczky, G., Csordas, G., Das, S., Garcia-Perez, C., Saotome, M., Sinha Roy, S., and Yi, M. (2006) Mitochondrial calcium signalling and cell death: approaches for assessing the role of mitochondrial Ca²⁺ uptake in apoptosis, *Cell Calcium* 40, 553-560.
17. Green, D. R. (1998) Apoptotic pathways: the roads to ruin, *Cell* 94, 695-698.
18. McBride, H. M., Neuspiel, M., and Wasiak, S. (2006) Mitochondria: more than just a powerhouse, *Curr Biol* 16, R551-560.
19. Taylor, R. W., and Turnbull, D. M. (2005) Mitochondrial DNA mutations in human disease, *Nat Rev Genet* 6, 389-402.

20. Chinnery, P. F., and Schon, E. A. (2003) Mitochondria, *J Neurol Neurosurg Psychiatry* 74, 1188-1199.
21. Schapira, A. H. (2006) Mitochondrial disease, *Lancet* 368, 70-82.
22. Pieczenik, S. R., and Neustadt, J. (2007) Mitochondrial dysfunction and molecular pathways of disease, *Exp Mol Pathol* 83, 84-92.
23. Blobel, G. (1980) Intracellular protein topogenesis, *Proceedings of the National Academy of Sciences of the United States of America* 77, 1496-1500.
24. Herrmann, J. M., and Neupert, W. (2000) Protein transport into mitochondria, *Curr Opin Microbiol* 3, 210-214.
25. Schmidt, O., Pfanner, N., and Meisinger, C. (2010) Mitochondrial protein import: from proteomics to functional mechanisms, *Nat Rev Mol Cell Biol* 11, 655-667.
26. Mokranjac, D., and Neupert, W. (2008) Energetics of protein translocation into mitochondria, *Biochim Biophys Acta* 1777, 758-762.
27. Neupert, W., and Herrmann, J. M. (2007) Translocation of proteins into mitochondria, *Annu Rev Biochem* 76, 723-749.
28. Hill, K., Model, K., Ryan, M. T., Dietmeier, K., Martin, F., Wagner, R., and Pfanner, N. (1998) Tom40 forms the hydrophilic channel of the mitochondrial import pore for preproteins [see comment], *Nature* 395, 516-521.
29. Becker, L., Bannwarth, M., Meisinger, C., Hill, K., Model, K., Krimmer, T., Casadio, R., Truscott, K. N., Schulz, G. E., Pfanner, N., and Wagner, R. (2005) Preprotein translocase of the outer mitochondrial membrane: reconstituted Tom40 forms a characteristic TOM pore, *J Mol Biol* 353, 1011-1020.
30. Kunkele, K. P., Juin, P., Pompa, C., Nargang, F. E., Henry, J. P., Neupert, W., Lill, R., and Thieffry, M. (1998) The isolated complex of the translocase of the outer membrane of mitochondria. Characterization of the cation-selective and voltage-gated preprotein-conducting pore, *J Biol Chem* 273, 31032-31039.
31. Ahting, U., Thieffry, M., Engelhardt, H., Hegerl, R., Neupert, W., and Nussberger, S. (2001) Tom40, the pore-forming component of the protein-conducting TOM channel in the outer membrane of mitochondria, *J Cell Biol* 153, 1151-1160.
32. van Wilpe, S., Ryan, M. T., Hill, K., Maarse, A. C., Meisinger, C., Brix, J., Dekker, P. J., Moczko, M., Wagner, R., Meijer, M., Guiard, B., Honlinger, A., and Pfanner, N. (1999) Tom22 is a multifunctional organizer of the mitochondrial preprotein translocase, *Nature* 401, 485-489.
33. Mayer, A., Nargang, F. E., Neupert, W., and Lill, R. (1995) MOM22 is a receptor for mitochondrial targeting sequences and cooperates with MOM19, *EMBO J* 14, 4204-4211.
34. Bolliger, L., Junne, T., Schatz, G., and Lithgow, T. (1995) Acidic receptor domains on both sides of the outer membrane mediate translocation of precursor proteins into yeast mitochondria, *The EMBO journal* 14, 6318-6326.

References

35. Esaki, M., Shimizu, H., Ono, T., Yamamoto, H., Kanamori, T., Nishikawa, S., and Endo, T. (2004) Mitochondrial protein import. Requirement of presequence elements and tom components for precursor binding to the TOM complex, *The Journal of biological chemistry* 279, 45701-45707.
36. Mayer, A., Neupert, W., and Lill, R. (1995) Mitochondrial protein import: reversible binding of the presequence at the trans side of the outer membrane drives partial translocation and unfolding, *Cell* 80, 127-137.
37. Komiya, T., Rospert, S., Koehler, C., Looser, R., Schatz, G., and Mihara, K. (1998) Interaction of mitochondrial targeting signals with acidic receptor domains along the protein import pathway: evidence for the 'acid chain' hypothesis, *EMBO J* 17, 3886-3898.
38. Mokranjac, D., Paschen, S. A., Kozany, C., Prokisch, H., Hoppins, S. C., Nargang, F. E., Neupert, W., and Hell, K. (2003) Tim50, a novel component of the TIM23 preprotein translocase of mitochondria, *The EMBO journal* 22, 816-825.
39. Yamamoto, H., Esaki, M., Kanamori, T., Tamura, Y., Nishikawa, S., and Endo, T. (2002) Tim50 is a subunit of the TIM23 complex that links protein translocation across the outer and inner mitochondrial membranes, *Cell* 111, 519-528.
40. Meinecke, M., Wagner, R., Kovermann, P., Guiard, B., Mick, D. U., Hutu, D. P., Voos, W., Truscott, K. N., Chacinska, A., Pfanner, N., and Rehling, P. (2006) Tim50 maintains the permeability barrier of the mitochondrial inner membrane, *Science* 312, 1523-1526.
41. Donzeau, M., Kaldi, K., Adam, A., Paschen, S., Wanner, G., Guiard, B., Bauer, M. F., Neupert, W., and Brunner, M. (2000) Tim23 links the inner and outer mitochondrial membranes, *Cell* 101, 401-412.
42. Chacinska, A., Lind, M., Frazier, A. E., Dudek, J., Meisinger, C., Geissler, A., Sickmann, A., Meyer, H. E., Truscott, K. N., Guiard, B., Pfanner, N., and Rehling, P. (2005) Mitochondrial presequence translocase: switching between TOM tethering and motor recruitment involves Tim21 and Tim17, *Cell* 120, 817-829.
43. Mokranjac, D., Popov-Celeketec, D., Hell, K., and Neupert, W. (2005) Role of Tim21 in mitochondrial translocation contact sites, *J Biol Chem* 280, 23437-23440.
44. Bauer, M. F., Sirrenberg, C., Neupert, W., and Brunner, M. (1996) Role of Tim23 as voltage sensor and presequence receptor in protein import into mitochondria, *Cell* 87, 33-41.
45. Meier, S., Neupert, W., and Herrmann, J. M. (2005) Conserved N-terminal negative charges in the Tim17 subunit of the TIM23 translocase play a critical role in the import of preproteins into mitochondria, *J Biol Chem* 280, 7777-7785.
46. Martinez-Caballero, S., Grigoriev, S. M., Herrmann, J. M., Campo, M. L., and Kinnally, K. W. (2007) Tim17p regulates the twin pore structure and voltage gating of the mitochondrial protein import complex TIM23, *J Biol Chem* 282, 3584-3593.

47. Marom, M., Azem, A., and Mokranjac, D. (2011) Understanding the molecular mechanism of protein translocation across the mitochondrial inner membrane: still a long way to go, *Biochimica et biophysica acta* 1808, 990-1001.
48. Bukau, B., Weissman, J., and Horwich, A. (2006) Molecular chaperones and protein quality control, *Cell* 125, 443-451.
49. Young, J. C., Agashe, V. R., Siegers, K., and Hartl, F. U. (2004) Pathways of chaperone-mediated protein folding in the cytosol, *Nat Rev Mol Cell Biol* 5, 781-791.
50. Schneider, H. C., Westermann, B., Neupert, W., and Brunner, M. (1996) The nucleotide exchange factor MGE exerts a key function in the ATP-dependent cycle of mt-Hsp70-Tim44 interaction driving mitochondrial protein import, *EMBO J* 15, 5796-5803.
51. Mokranjac, D., Sichting, M., Neupert, W., and Hell, K. (2003) Tim14, a novel key component of the import motor of the TIM23 protein translocase of mitochondria, *EMBO J* 22, 4945-4956.
52. Kozany, C., Mokranjac, D., Sichting, M., Neupert, W., and Hell, K. (2004) The J domain-related cochaperone Tim16 is a constituent of the mitochondrial TIM23 preprotein translocase, *Nat Struct Mol Biol* 11, 234-241.
53. Frazier, A. E., Dudek, J., Guiard, B., Voos, W., Li, Y., Lind, M., Meisinger, C., Geissler, A., Sickmann, A., Meyer, H. E., Bilanchone, V., Cumsky, M. G., Truscott, K. N., Pfanner, N., and Rehling, P. (2004) Pam16 has an essential role in the mitochondrial protein import motor, *Nat Struct Mol Biol* 11, 226-233.
54. Mokranjac, D., Bourenkov, G., Hell, K., Neupert, W., and Groll, M. (2006) Structure and function of Tim14 and Tim16, the J and J-like components of the mitochondrial protein import motor, *EMBO J* 25, 4675-4685.
55. Lee, C. M., Sedman, J., Neupert, W., and Stuart, R. A. (1999) The DNA helicase, Hmi1p, is transported into mitochondria by a C-terminal cleavable targeting signal, *J Biol Chem* 274, 20937-20942.
56. Hurt, E. C., Pesold-Hurt, B., and Schatz, G. (1984) The amino-terminal region of an imported mitochondrial precursor polypeptide can direct cytoplasmic dihydrofolate reductase into the mitochondrial matrix, *EMBO J* 3, 3149-3156.
57. Ostermann, J., Horwich, A. L., Neupert, W., and Hartl, F. U. (1989) Protein folding in mitochondria requires complex formation with hsp60 and ATP hydrolysis, *Nature* 341, 125-130.
58. Popov-Celeketic, D., Mapa, K., Neupert, W., and Mokranjac, D. (2008) Active remodelling of the TIM23 complex during translocation of preproteins into mitochondria, *EMBO J* 27, 1469-1480.
59. Popov-Celeketic, D., Waegemann, K., Mapa, K., Neupert, W., and Mokranjac, D. (2011) Role of the import motor in insertion of transmembrane segments by the mitochondrial TIM23 complex, *EMBO reports*.

References

60. Webb, C. T., Gorman, M. A., Lazarou, M., Ryan, M. T., and Gulbis, J. M. (2006) Crystal structure of the mitochondrial chaperone TIM9.10 reveals a six-bladed alpha-propeller, *Mol Cell* 21, 123-133.
61. Curran, S. P., Leuenberger, D., Oppliger, W., and Koehler, C. M. (2002) The Tim9p-Tim10p complex binds to the transmembrane domains of the ADP/ATP carrier, *EMBO J* 21, 942-953.
62. Sirrenberg, C., Endres, M., Folsch, H., Stuart, R. A., Neupert, W., and Brunner, M. (1998) Carrier protein import into mitochondria mediated by the intermembrane proteins Tim10/Mrs11 and Tim12/Mrs5, *Nature* 391, 912-915.
63. Kovermann, P., Truscott, K. N., Guiard, B., Rehling, P., Sepuri, N. B., Muller, H., Jensen, R. E., Wagner, R., and Pfanner, N. (2002) Tim22, the essential core of the mitochondrial protein insertion complex, forms a voltage-activated and signal-gated channel, *Mol Cell* 9, 363-373.
64. Koehler, C. M. (2004) New developments in mitochondrial assembly, *Annu Rev Cell Dev Biol* 20, 309-335.
65. Young, J. C., Hoogenraad, N. J., and Hartl, F. U. (2003) Molecular chaperones Hsp90 and Hsp70 deliver preproteins to the mitochondrial import receptor Tom70, *Cell* 112, 41-50.
66. Wiedemann, N., Pfanner, N., and Ryan, M. T. (2001) The three modules of ADP/ATP carrier cooperate in receptor recruitment and translocation into mitochondria, *EMBO J* 20, 951-960.
67. Herrmann, J. M., Neupert, W., and Stuart, R. A. (1997) Insertion into the mitochondrial inner membrane of a polytopic protein, the nuclear-encoded Oxa1p, *EMBO J* 16, 2217-2226.
68. Rojo, E. E., Stuart, R. A., and Neupert, W. (1995) Conservative sorting of F₀-ATPase subunit 9: export from matrix requires delta pH across inner membrane and matrix ATP, *EMBO J* 14, 3445-3451.
69. Herrmann, J. M., Koll, H., Cook, R. A., Neupert, W., and Stuart, R. A. (1995) Topogenesis of cytochrome oxidase subunit II. Mechanisms of protein export from the mitochondrial matrix, *J Biol Chem* 270, 27079-27086.
70. Hell, K., Herrmann, J. M., Pratje, E., Neupert, W., and Stuart, R. A. (1998) Oxa1p, an essential component of the N-tail protein export machinery in mitochondria, *Proc Natl Acad Sci U S A* 95, 2250-2255.
71. Hell, K., Neupert, W., and Stuart, R. A. (2001) Oxa1p acts as a general membrane insertion machinery for proteins encoded by mitochondrial DNA, *EMBO J* 20, 1281-1288.
72. Dolezal, P., Likic, V., Tachezy, J., and Lithgow, T. (2006) Evolution of the molecular machines for protein import into mitochondria, *Science* 313, 314-318.
73. Banci, L., Bertini, I., Cefaro, C., Ciofi-Baffoni, S., Gallo, A., Martinelli, M., Sideris, D. P., Katrakili, N., and Tokatlidis, K. (2009) MIA40 is an oxidoreductase that catalyzes oxidative protein folding in mitochondria, *Nat Struct Mol Biol* 16, 198-206.

74. Herrmann, J. M., and Kohl, R. (2007) Catch me if you can! Oxidative protein trapping in the intermembrane space of mitochondria, *J Cell Biol* 176, 559-563.
75. Hell, K. (2008) The Erv1-Mia40 disulfide relay system in the intermembrane space of mitochondria, *Biochim Biophys Acta* 1783, 601-609.
76. Stojanovski, D., Muller, J. M., Milenkovic, D., Guiard, B., Pfanner, N., and Chacinska, A. (2008) The MIA system for protein import into the mitochondrial intermembrane space, *Biochim Biophys Acta* 1783, 610-617.
77. Diekert, K., de Kroon, A. I., Ahting, U., Niggemeyer, B., Neupert, W., de Kruijff, B., and Lill, R. (2001) Apocytochrome c requires the TOM complex for translocation across the mitochondrial outer membrane, *EMBO J* 20, 5626-5635.
78. Walther, D. M., and Rapaport, D. (2009) Biogenesis of mitochondrial outer membrane proteins, *Biochim Biophys Acta* 1793, 42-51.
79. Rojo, M., Legros, F., Chateau, D., and Lombes, A. (2002) Membrane topology and mitochondrial targeting of mitofusins, ubiquitous mammalian homologs of the transmembrane GTPase Fzo, *J Cell Sci* 115, 1663-1674.
80. Fritz, S., Rapaport, D., Klanner, E., Neupert, W., and Westermann, B. (2001) Connection of the mitochondrial outer and inner membranes by Fzo1 is critical for organellar fusion, *J Cell Biol* 152, 683-692.
81. Coonrod, E. M., Karren, M. A., and Shaw, J. M. (2007) Ugo1p is a multipass transmembrane protein with a single carrier domain required for mitochondrial fusion, *Traffic* 8, 500-511.
82. Joseph-Liauzun, E., Delmas, P., Shire, D., and Ferrara, P. (1998) Topological analysis of the peripheral benzodiazepine receptor in yeast mitochondrial membranes supports a five-transmembrane structure, *J Biol Chem* 273, 2146-2152.
83. Rapaport, D. (2003) Finding the right organelle. Targeting signals in mitochondrial outer-membrane proteins, *EMBO Rep* 4, 948-952.
84. Schlossmann, J., and Neupert, W. (1995) Assembly of the preprotein receptor MOM72/MAS70 into the protein import complex of the outer membrane of mitochondria, *J Biol Chem* 270, 27116-27121.
85. Schneider, H., Sollner, T., Dietmeier, K., Eckerskorn, C., Lottspeich, F., Trulzsch, B., Neupert, W., and Pfanner, N. (1991) Targeting of the master receptor MOM19 to mitochondria, *Science* 254, 1659-1662.
86. Ahting, U., Waizenegger, T., Neupert, W., and Rapaport, D. (2005) Signal-anchored proteins follow a unique insertion pathway into the outer membrane of mitochondria, *J Biol Chem* 280, 48-53.
87. Meineke, B., Engl, G., Kemper, C., Vasiljev-Neumeyer, A., Paulitschke, H., and Rapaport, D. (2008) The outer membrane form of the mitochondrial protein Mcr1 follows a TOM-independent membrane insertion pathway, *FEBS Lett* 582, 855-860.

References

88. Rapaport, D. (2005) How does the TOM complex mediate insertion of precursor proteins into the mitochondrial outer membrane?, *J Cell Biol* 171, 419-423.
89. Popov-Celeketic, J., Waizenegger, T., and Rapaport, D. (2008) Mim1 functions in an oligomeric form to facilitate the integration of Tom20 into the mitochondrial outer membrane, *J Mol Biol* 376, 671-680.
90. Hulett, J. M., Lueder, F., Chan, N. C., Perry, A. J., Wolyneec, P., Likic, V. A., Gooley, P. R., and Lithgow, T. (2008) The transmembrane segment of Tom20 is recognized by Mim1 for docking to the mitochondrial TOM complex, *J Mol Biol* 376, 694-704.
91. Becker, T., Pfannschmidt, S., Guiard, B., Stojanovski, D., Milenkovic, D., Kutik, S., Pfanner, N., Meisinger, C., and Wiedemann, N. (2008) Biogenesis of the mitochondrial TOM complex: Mim1 promotes insertion and assembly of signal-anchored receptors, *J Biol Chem* 283, 120-127.
92. Thornton, N., Stroud, D. A., Milenkovic, D., Guiard, B., Pfanner, N., and Becker, T. (2010) Two modular forms of the mitochondrial sorting and assembly machinery are involved in biogenesis of alpha-helical outer membrane proteins, *J Mol Biol* 396, 540-549.
93. Setoguchi, K., Otera, H., and Mihara, K. (2006) Cytosolic factor- and TOM-independent import of C-tail-anchored mitochondrial outer membrane proteins, *EMBO J* 25, 5635-5647.
94. Kemper, C., Habib, S. J., Engl, G., Heckmeyer, P., Dimmer, K. S., and Rapaport, D. (2008) Integration of tail-anchored proteins into the mitochondrial outer membrane does not require any known import components, *J Cell Sci* 121, 1990-1998.
95. Stojanovski, D., Guiard, B., Kozjak-Pavlovic, V., Pfanner, N., and Meisinger, C. (2007) Alternative function for the mitochondrial SAM complex in biogenesis of alpha-helical TOM proteins, *J Cell Biol* 179, 881-893.
96. Otera, H., Taira, Y., Horie, C., Suzuki, Y., Suzuki, H., Setoguchi, K., Kato, H., Oka, T., and Mihara, K. (2007) A novel insertion pathway of mitochondrial outer membrane proteins with multiple transmembrane segments, *J Cell Biol* 179, 1355-1363.
97. Paschen, S. A., Waizenegger, T., Stan, T., Preuss, M., Cyrklaff, M., Hell, K., Rapaport, D., and Neupert, W. (2003) Evolutionary conservation of biogenesis of beta-barrel membrane proteins, *Nature* 426, 862-866.
98. Kozjak, V., Wiedemann, N., Milenkovic, D., Lohaus, C., Meyer, H. E., Guiard, B., Meisinger, C., and Pfanner, N. (2003) An essential role of Sam50 in the protein sorting and assembly machinery of the mitochondrial outer membrane, *J Biol Chem* 278, 48520-48523.
99. Rapaport, D. (2002) Biogenesis of the mitochondrial TOM complex, *Trends Biochem Sci* 27, 191-197.
100. Schleiff, E., Eichacker, L. A., Eckart, K., Becker, T., Mirus, O., Stahl, T., and Soll, J. (2003) Prediction of the plant beta-barrel proteome: a case study of the chloroplast outer envelope, *Protein Sci* 12, 748-759.
101. Schulz, G. E. (2002) The structure of bacterial outer membrane proteins, *Biochim Biophys Acta* 1565, 308-317.

102. Paschen, S. A., Neupert, W., and Rapaport, D. (2005) Biogenesis of beta-barrel membrane proteins of mitochondria, *Trends Biochem Sci* 30, 575-582.
103. Kim, S., Malinverni, J. C., Sliz, P., Silhavy, T. J., Harrison, S. C., and Kahne, D. (2007) Structure and function of an essential component of the outer membrane protein assembly machine, *Science* 317, 961-964.
104. Wiedemann, N., Kozjak, V., Chacinska, A., Schonfisch, B., Rospert, S., Ryan, M. T., Pfanner, N., and Meisinger, C. (2003) Machinery for protein sorting and assembly in the mitochondrial outer membrane, *Nature* 424, 565-571.
105. Waizenegger, T., Habib, S. J., Lech, M., Mokranjac, D., Paschen, S. A., Hell, K., Neupert, W., and Rapaport, D. (2004) Tob38, a novel essential component in the biogenesis of beta-barrel proteins of mitochondria, *EMBO Rep* 5, 704-709.
106. Ishikawa, D., Yamamoto, H., Tamura, Y., Moritoh, K., and Endo, T. (2004) Two novel proteins in the mitochondrial outer membrane mediate beta-barrel protein assembly, *J Cell Biol* 166, 621-627.
107. Milenkovic, D., Kozjak, V., Wiedemann, N., Lohaus, C., Meyer, H. E., Guiard, B., Pfanner, N., and Meisinger, C. (2004) Sam35 of the mitochondrial protein sorting and assembly machinery is a peripheral outer membrane protein essential for cell viability, *J Biol Chem* 279, 22781-22785.
108. Wideman, J. G., Go, N. E., Klein, A., Redmond, E., Lackey, S. W., Tao, T., Kalbacher, H., Rapaport, D., Neupert, W., and Nargang, F. E. (2010) Roles of the Mdm10, Tom7, Mdm12, and Mmm1 proteins in the assembly of mitochondrial outer membrane proteins in *Neurospora crassa*, *Mol Biol Cell* 21, 1725-1736.
109. Gentle, I., Gabriel, K., Beech, P., Waller, R., and Lithgow, T. (2004) The Omp85 family of proteins is essential for outer membrane biogenesis in mitochondria and bacteria, *J Cell Biol* 164, 19-24.
110. Knowles, T. J., Scott-Tucker, A., Overduin, M., and Henderson, I. R. (2009) Membrane protein architects: the role of the BAM complex in outer membrane protein assembly, *Nat Rev Microbiol* 7, 206-214.
111. Wu, T., Malinverni, J., Ruiz, N., Kim, S., Silhavy, T. J., and Kahne, D. (2005) Identification of a multicomponent complex required for outer membrane biogenesis in *Escherichia coli*, *Cell* 121, 235-245.
112. Voulhoux, R., Bos, M. P., Geurtsen, J., Mols, M., and Tommassen, J. (2003) Role of a highly conserved bacterial protein in outer membrane protein assembly, *Science* 299, 262-265.
113. Voulhoux, R., and Tommassen, J. (2004) Omp85, an evolutionarily conserved bacterial protein involved in outer-membrane-protein assembly, *Res Microbiol* 155, 129-135.
114. Habib, S. J., Waizenegger, T., Niewianda, A., Paschen, S. A., Neupert, W., and Rapaport, D. (2007) The N-terminal domain of Tob55 has a receptor-like function in the biogenesis of mitochondrial beta-barrel proteins, *J Cell Biol* 176, 77-88.

References

115. Jacob-Dubuisson, F., Villeret, V., Clantin, B., Delattre, A. S., and Saint, N. (2009) First structural insights into the TpsB/Omp85 superfamily, *Biol Chem* 390, 675-684.
116. Zeth, K. (2010) Structure and evolution of mitochondrial outer membrane proteins of beta-barrel topology, *Biochimica et biophysica acta* 1797, 1292-1299.
117. Sanchez-Pulido, L., Devos, D., Genevrois, S., Vicente, M., and Valencia, A. (2003) POTRA: a conserved domain in the FtsQ family and a class of beta-barrel outer membrane proteins, *Trends Biochem Sci* 28, 523-526.
118. Bos, M. P., Robert, V., and Tommassen, J. (2007) Functioning of outer membrane protein assembly factor Omp85 requires a single POTRA domain, *EMBO Rep* 8, 1149-1154.
119. Brachat, A., Liebundguth, N., Rebischung, C., Lemire, S., Scharer, F., Hoepfner, D., Demchyshyn, V., Howald, I., Dusterhoft, A., Mostl, D., Pohlmann, R., Kotter, P., Hall, M. N., Wach, A., and Philippsen, P. (2000) Analysis of deletion phenotypes and GFP fusions of 21 novel *Saccharomyces cerevisiae* open reading frames, *Yeast* 16, 241-253.
120. Hoppins, S. C., Go, N. E., Klein, A., Schmitt, S., Neupert, W., Rapaport, D., and Nargang, F. E. (2007) Alternative splicing gives rise to different isoforms of the *Neurospora crassa* Tob55 protein that vary in their ability to insert beta-barrel proteins into the outer mitochondrial membrane, *Genetics* 177, 137-149.
121. Clantin, B., Delattre, A. S., Rucktooa, P., Saint, N., Meli, A. C., Locht, C., Jacob-Dubuisson, F., and Villeret, V. (2007) Structure of the membrane protein FhaC: a member of the Omp85-TpsB transporter superfamily, *Science* 317, 957-961.
122. Gentle, I. E., Burri, L., and Lithgow, T. (2005) Molecular architecture and function of the Omp85 family of proteins, *Mol Microbiol* 58, 1216-1225.
123. Jacob-Dubuisson, F., Fernandez, R., and Coutte, L. (2004) Protein secretion through autotransporter and two-partner pathways, *Biochim Biophys Acta* 1694, 235-257.
124. Jacob-Dubuisson, F., Locht, C., and Antoine, R. (2001) Two-partner secretion in Gram-negative bacteria: a thrifty, specific pathway for large virulence proteins, *Mol Microbiol* 40, 306-313.
125. Armstrong, L. C., Komiya, T., Bergman, B. E., Mihara, K., and Bornstein, P. (1997) Metaxin is a component of a preprotein import complex in the outer membrane of the mammalian mitochondrion, *J Biol Chem* 272, 6510-6518.
126. Kozjak-Pavlovic, V., Ross, K., Benlasfer, N., Kimmig, S., Karlas, A., and Rudel, T. (2007) Conserved roles of Sam50 and metaxins in VDAC biogenesis, *EMBO Rep* 8, 576-582.
127. Abdul, K. M., Terada, K., Yano, M., Ryan, M. T., Streimann, I., Hoogenraad, N. J., and Mori, M. (2000) Functional analysis of human metaxin in mitochondrial protein import in cultured cells and its relationship with the Tom complex, *Biochem Biophys Res Commun* 276, 1028-1034.

128. Model, K., Meisinger, C., Prinz, T., Wiedemann, N., Truscott, K. N., Pfanner, N., and Ryan, M. T. (2001) Multistep assembly of the protein import channel of the mitochondrial outer membrane, *Nat Struct Biol* 8, 361-370.
129. Habib, S. J., Waizenegger, T., Lech, M., Neupert, W., and Rapaport, D. (2005) Assembly of the TOB complex of mitochondria, *J Biol Chem* 280, 6434-6440.
130. Hoppins, S. C., and Nargang, F. E. (2004) The Tim8-Tim13 complex of *Neurospora crassa* functions in the assembly of proteins into both mitochondrial membranes, *J Biol Chem* 279, 12396-12405.
131. Wiedemann, N., Truscott, K. N., Pfannschmidt, S., Guiard, B., Meisinger, C., and Pfanner, N. (2004) Biogenesis of the protein import channel Tom40 of the mitochondrial outer membrane: intermembrane space components are involved in an early stage of the assembly pathway, *J Biol Chem* 279, 18188-18194.
132. Chan, N. C., and Lithgow, T. (2008) The peripheral membrane subunits of the SAM complex function codependently in mitochondrial outer membrane biogenesis, *Mol Biol Cell* 19, 126-136.
133. Kutik, S., Stojanovski, D., Becker, L., Becker, T., Meinecke, M., Kruger, V., Prinz, C., Meisinger, C., Guiard, B., Wagner, R., Pfanner, N., and Wiedemann, N. (2008) Dissecting membrane insertion of mitochondrial beta-barrel proteins, *Cell* 132, 1011-1024.
134. Meisinger, C., Pfannschmidt, S., Rissler, M., Milenkovic, D., Becker, T., Stojanovski, D., Youngman, M. J., Jensen, R. E., Chacinska, A., Guiard, B., Pfanner, N., and Wiedemann, N. (2007) The morphology proteins Mdm12/Mmm1 function in the major beta-barrel assembly pathway of mitochondria, *EMBO J* 26, 2229-2239.
135. Meisinger, C., Rissler, M., Chacinska, A., Szklarz, L. K., Milenkovic, D., Kozjak, V., Schonfisch, B., Lohaus, C., Meyer, H. E., Yaffe, M. P., Guiard, B., Wiedemann, N., and Pfanner, N. (2004) The mitochondrial morphology protein Mdm10 functions in assembly of the preprotein translocase of the outer membrane, *Dev Cell* 7, 61-71.
136. Yamano, K., Tanaka-Yamano, S., and Endo, T. (2010) Mdm10 as a dynamic constituent of the TOB/SAM complex directs coordinated assembly of Tom40, *EMBO Rep* 11, 187-193.
137. Meisinger, C., Wiedemann, N., Rissler, M., Strub, A., Milenkovic, D., Schonfisch, B., Muller, H., Kozjak, V., and Pfanner, N. (2006) Mitochondrial protein sorting: differentiation of beta-barrel assembly by Tom7-mediated segregation of Mdm10, *J Biol Chem* 281, 22819-22826.
138. Waizenegger, T., Schmitt, S., Zivkovic, J., Neupert, W., and Rapaport, D. (2005) Mim1, a protein required for the assembly of the TOM complex of mitochondria, *EMBO Rep* 6, 57-62.
139. Nargang, F. E., and Rapaport, D. (2007) *Neurospora crassa* as a model organism for mitochondrial biogenesis, *Methods Mol Biol* 372, 107-123.
140. Wittig, I., Beckhaus, T., Wumaier, Z., Karas, M., and Schagger, H. (2010) Mass estimation of native proteins by blue native electrophoresis: principles and practical hints, *Mol Cell Proteomics* 9, 2149-2161.

141. Delattre, A. S., Clantin, B., Saint, N., Locht, C., Villeret, V., and Jacob-Dubuisson, F. (2010) Functional importance of a conserved sequence motif in FhaC, a prototypic member of the TpsB/Omp85 superfamily, *FEBS J* 277, 4755-4765.
142. Schagger, H., Cramer, W. A., and von Jagow, G. (1994) Analysis of molecular masses and oligomeric states of protein complexes by blue native electrophoresis and isolation of membrane protein complexes by two-dimensional native electrophoresis, *Anal Biochem* 217, 220-230.
143. Burkitt, W. I., Pritchard, C., Arsene, C., Henrion, A., Bunk, D., and O'Connor, G. (2008) Toward Systeme International d'Unite-traceable protein quantification: from amino acids to proteins, *Anal Biochem* 376, 242-251.
144. Arsene, C. G., Ohlendorf, R., Burkitt, W., Pritchard, C., Henrion, A., O'Connor, G., Bunk, D. M., and Guttler, B. (2008) Protein quantification by isotope dilution mass spectrometry of proteolytic fragments: cleavage rate and accuracy, *Anal Chem* 80, 4154-4160.
145. Heuberger, E. H., Veenhoff, L. M., Duurkens, R. H., Friesen, R. H., and Poolman, B. (2002) Oligomeric state of membrane transport proteins analyzed with blue native electrophoresis and analytical ultracentrifugation, *Journal of molecular biology* 317, 591-600.
146. Bornstein, P., McKinney, C. E., LaMarca, M. E., Winfield, S., Shingu, T., Devarayalu, S., Vos, H. L., and Ginns, E. I. (1995) Metaxin, a gene contiguous to both thrombospondin 3 and glucocerebrosidase, is required for embryonic development in the mouse: implications for Gaucher disease, *Proceedings of the National Academy of Sciences of the United States of America* 92, 4547-4551.
147. Knowles, T. J., Jeeves, M., Bobat, S., Dancea, F., McClelland, D., Palmer, T., Overduin, M., and Henderson, I. R. (2008) Fold and function of polypeptide transport-associated domains responsible for delivering unfolded proteins to membranes, *Molecular microbiology* 68, 1216-1227.
148. Ryan, M. T., Muller, H., and Pfanner, N. (1999) Functional staging of ADP/ATP carrier translocation across the outer mitochondrial membrane, *The Journal of biological chemistry* 274, 20619-20627.
149. Hodak, H., Clantin, B., Willery, E., Villeret, V., Locht, C., and Jacob-Dubuisson, F. (2006) Secretion signal of the filamentous haemagglutinin, a model two-partner secretion substrate, *Molecular microbiology* 61, 368-382.
150. Guedin, S., Willery, E., Tommassen, J., Fort, E., Drobecq, H., Locht, C., and Jacob-Dubuisson, F. (2000) Novel topological features of FhaC, the outer membrane transporter involved in the secretion of the Bordetella pertussis filamentous hemagglutinin, *The Journal of biological chemistry* 275, 30202-30210.
151. Ellis, R. J. (1996) Revisiting the Anfinsen cage, *Fold Des* 1, R9-15.
152. Ellis, R. J. (2001) Molecular chaperones: inside and outside the Anfinsen cage, *Current biology : CB* 11, R1038-1040.

153. Stegmeier, J. F., and Andersen, C. (2006) Characterization of pores formed by YaeT (Omp85) from *Escherichia coli*, *J Biochem* 140, 275-283.
154. Wimley, W. C. (2003) The versatile beta-barrel membrane protein, *Curr Opin Struct Biol* 13, 404-411.
155. Robert, V., Volokhina, E. B., Senf, F., Bos, M. P., Van Gelder, P., and Tommassen, J. (2006) Assembly factor Omp85 recognizes its outer membrane protein substrates by a species-specific C-terminal motif, *PLoS Biol* 4, e377.
156. Walther, D. M., Papic, D., Bos, M. P., Tommassen, J., and Rapaport, D. (2009) Signals in bacterial beta-barrel proteins are functional in eukaryotic cells for targeting to and assembly in mitochondria, *Proceedings of the National Academy of Sciences of the United States of America* 106, 2531-2536.
157. White, S. H., and Wimley, W. C. (1999) Membrane protein folding and stability: physical principles, *Annu Rev Biophys Biomol Struct* 28, 319-365.
158. Likic, V. A., Perry, A., Hulett, J., Derby, M., Traven, A., Waller, R. F., Keeling, P. J., Koehler, C. M., Curran, S. P., Gooley, P. R., and Lithgow, T. (2005) Patterns that define the four domains conserved in known and novel isoforms of the protein import receptor Tom20, *Journal of molecular biology* 347, 81-93.
159. Lister, R., Chew, O., Lee, M. N., Heazlewood, J. L., Clifton, R., Parker, K. L., Millar, A. H., and Whelan, J. (2004) A transcriptomic and proteomic characterization of the *Arabidopsis* mitochondrial protein import apparatus and its response to mitochondrial dysfunction, *Plant Physiol* 134, 777-789.
160. Taylor, R. D., McHale, B. J., and Nargang, F. E. (2003) Characterization of *Neurospora crassa* Tom40-deficient mutants and effect of specific mutations on Tom40 assembly, *J Biol Chem* 278, 765-775.
161. Nargang, F. E., Kunkele, K. P., Mayer, A., Ritzel, R. G., Neupert, W., and Lill, R. (1995) 'Sheltered disruption' of *Neurospora crassa* MOM22, an essential component of the mitochondrial protein import complex, *EMBO J* 14, 1099-1108.
162. Summers, W. A. T. (2010) An in vivo approach to elucidating the function of mitochondrial porin by the characterisation of *Neurospora crassa* strains deficient in porin, In *Microbiology*, Manitoba.
163. Keil, P., and Pfanner, N. (1993) Insertion of MOM22 into the mitochondrial outer membrane strictly depends on surface receptors, *FEBS Lett* 321, 197-200.
164. Kunkele, K. P., Heins, S., Dembowski, M., Nargang, F. E., Benz, R., Thieffry, M., Walz, J., Lill, R., Nussberger, S., and Neupert, W. (1998) The preprotein translocation channel of the outer membrane of mitochondria, *Cell* 93, 1009-1019.
165. Mayer, A., Lill, R., and Neupert, W. (1993) Translocation and insertion of precursor proteins into isolated outer membranes of mitochondria, *J Cell Biol* 121, 1233-1243.

References

166. Pfanner, N., Tropschug, M., and Neupert, W. (1987) Mitochondrial protein import: nucleoside triphosphates are involved in conferring import-competence to precursors, *Cell* 49, 815-823.
167. Keil, P., Weinzierl, A., Kiebler, M., Dietmeier, K., Sollner, T., and Pfanner, N. (1993) Biogenesis of the mitochondrial receptor complex. Two receptors are required for binding of MOM38 to the outer membrane surface, *J Biol Chem* 268, 19177-19180.
168. Davis, R. H., and de Serres, F. J. (1970) [4] Genetic and microbiological research techniques for *Neurospora crassa*, In *Methods in Enzymology* (Herbert Tabor, C. W. T., Ed.), pp 79-143, Academic Press.
169. Sambrook, J., Fritsch, E. F., and Maniatis, T. (1989) *Molecular cloning : a laboratory manual*, 2nd ed. ed., Cold Spring Harbor Laboratory, Cold Spring Harbor, N.Y.
170. Daum, G., Bohni, P. C., and Schatz, G. (1982) Import of proteins into mitochondria. Cytochrome b2 and cytochrome c peroxidase are located in the intermembrane space of yeast mitochondria, *The Journal of biological chemistry* 257, 13028-13033.
171. Schreiner, P. (2008) Structural investigation of two supramolecular complexes of the eukaryotic cell: the proteasome and the mitochondrial TOM complex.
172. Ahting, U., Thun, C., Hegerl, R., Typke, D., Nargang, F. E., Neupert, W., and Nussberger, S. (1999) The TOM core complex: the general protein import pore of the outer membrane of mitochondria, *The Journal of cell biology* 147, 959-968.
173. Laemmli, U. K. (1970) Cleavage of structural proteins during the assembly of the head of bacteriophage T4, *Nature* 227, 680-685.
174. Schagger, H., and von Jagow, G. (1991) Blue native electrophoresis for isolation of membrane protein complexes in enzymatically active form, *Anal Biochem* 199, 223-231.
175. Kyhse-Andersen, J. (1984) Electroblotting of multiple gels: a simple apparatus without buffer tank for rapid transfer of proteins from polyacrylamide to nitrocellulose, *J Biochem Biophys Methods* 10, 203-209.
176. Towbin, H., Staehelin, T., and Gordon, J. (1979) Electrophoretic transfer of proteins from polyacrylamide gels to nitrocellulose sheets: procedure and some applications, *Proceedings of the National Academy of Sciences of the United States of America* 76, 4350-4354.
177. Gasteiger, E., Hoogland, C., Gattiker, A., Duvaud, S. e., Wilkins, M. R., Appel, R. D., and Bairoch, A. (2005) Protein Identification and Analysis Tools on the ExPASy Server, pp 571-607.
178. Wilkins, M. R., Lindskog, I., Gasteiger, E., Bairoch, A., Sanchez, J. C., Hochstrasser, D. F., and Appel, R. D. (1997) Detailed peptide characterization using PEPTIDEMASS – a World-Wide-Web-accessible tool, *ELECTROPHORESIS* 18, 403-408.
179. Nickell, S., Forster, F., Linaroudis, A., Net, W. D., Beck, F., Hegerl, R., Baumeister, W., and Plitzko, J. M. (2005) TOM software toolbox:

- acquisition and analysis for electron tomography, *J Struct Biol* 149, 227-234.
180. Frank, J., Radermacher, M., Penczek, P., Zhu, J., Li, Y., Ladjadj, M., and Leith, A. (1996) SPIDER and WEB: processing and visualization of images in 3D electron microscopy and related fields, *J Struct Biol* 116, 190-199.
 181. Frank, J., Shimkin, B., and Dowse, H. (1981) Spider - a Modular Software System for Electron Image-Processing, *Ultramicroscopy* 6, 343-357.